

FINAL REPORT
OF THE
UGC MAJOR RESEARCH PROJECT
F.No. 42/354//2013/(SR) , dt. 01.04.2013

**SYNTHESIS, STRUCTURE AND PROPERTIES OF
NANOPARTICULATE METAL COMPLEXES AND
THEIR BIOLOGICAL ACTIVITY**

Submitted to
THE UNIVERSITY GRANTS COMMISSION
Bahadur Shah Zafar Marg,
New Delhi - 110 002

By
Dr. B. Kishore Babu
Principal Investigator

Prof. V. Veeraiah
Co-Investigator



Department of Engineering Chemistry
AU College of Engineering (A)
Andhra University, Visakhapatnam - 530 003. AP.
ACCREDITED BY NAAC WITH 'A' GRADE - ISO 9001-2015 CERTIFIED

**UNIVERSITY GRANTS COMMISSION
BAHADUR SHAH ZAFAR MARG
NEW DELHI 110 002**

FINAL REPORT OF THE WORK DONE ON MAJOR RESEARCH PROJECT

1.	Project Report No.	:	FINAL
2.	UGC Reference No.	:	File No: 42/354//2013/(SR)
3.	Period of Report	:	From 01-04-2013 to 31-03-2017
4.	Title of Research Project	:	SYNTHESIS, STRUCTURE AND PROPERTIES OF NANOPARTICULATE METAL COMPLEXES AND THEIR BIOLOGICAL ACTIVITY
5.	(a) Name of the Principal Investigator	:	Dr. B. Kishore Babu
	(a) Name of the Co-Investigator		Prof. V. Veeraiah
	(b) Department and University where work has progressed	:	Department of Engineering Chemistry, AU College of Engineering (A) Andhra University Visakhapatnam 530 003 (AP) Email: jacobkishore@gmail.com Phone: 8498933300(M)
6.	Effective date of starting of the project	:	01-04-2013
7.	Grant approved and expenditure incurred during the period of the report:		
	(a) Total amount approved	:	Rs. 10,48,300/-
	(b) Total expenditure	:	Rs. 10,28,130/-

**UNIVERSITY GRANTS COMMISSION
BAHADUR SHAH ZAFAR MARG
NEW DELHI 110 002**

**SUBMISSION OF INFORMATION AT THE TIME OF SENDING THE FINAL
REPORT OF THE WORK DONE ON THE PROJECT**

1.	Name and address of the Principal Investigator	:	Dr. B. Kishore Babu
2.	Name and address of the Institution	:	Department of Engineering Chemistry AU College of Engineering (A) Andhra University Visakhapatnam 530 003 Email: pauldouglas12@gmail.com
3.	UGC Approval No. and Date	:	File No: 42/354//2013/(SR) From 01-04-2013 to 31-03-2017
4.	Date of implementation	:	01.04.2013
5.	Tenure of the Project	:	Three years
6.	Total grant allocated	:	Rs. 10,48,300/-
7.	Total grant received	:	Rs. 10,48,300/-
8.	Final expenditure	:	Rs. 10,28,130/-
9.	Title of the Project	:	SYNTHESIS, STRUCTURE AND PROPERTIES OF NANOPARTICULATE METAL COMPLEXES AND THEIR BIOLOGICAL ACTIVITY
10.	Objectives of the Project:	:	1. To prepare various Nanoparticulate metal complexes by self assembly and hydrothermal routes. 2. To characterize metal complexes and nanoparticle with various physicochemical and spectroscopic methods 3. To Biological applications such as microbial and anti-cancer
11.	Whether objectives were achieved	:	All the objectives were achieved
12.	Achievements from the project:	:	

	<ul style="list-style-type: none"> • Preparation of a series of Biologically potent nanoparticulate metal complexes • Characterization of transition and noble metal particulates by physicochemical and spectroscopic methods such as FT-IR, XRD and Fe-SEM, • Evaluation of the Bio-active studies such as pathogenic, microbial and anti-proliferative(cancer) 		
13.	Summary of the Findings	:	

Detailed Work done: Synthesis, structural and biological properties of metal complexes has been one of the research areas of the principal investigator. In this connection, 40 complexes of Cu, Co, Ni, Sr, Cd, Pb metal possessing non-hydrocarbon ligands: pseudohalogen such as azides, thiocyanates, isocyanates, cyanides, nitrile donors and halogen in alliance bioactive nitrogen bases: imidazole, 2,2 bipyridyl, 1,10-phenanthroline 1,3,5- triazole, 4,5-diazafluoren-9-one (dafone), riboflavin, and amino acid: arginine, tyrosine and orotic acid as ligands have been synthesized using simple synthetic routes. The synthesized complexes were evaluated for their anticancer activities using an antiproliferative activity assay (MTT assay) and Flow cytometric analysis of cell cycle. Conversion of metal complexes in nano form has been underway. Some of the metal complexes obtained in the form of nano have been studied for their anticancer activity.

Anti-proliferative activity evaluation of the compounds

Complexes 1-26 were subjected to the preliminary antiproliferative activity test for their cytotoxicity against three human cancer cell lines MCF-7 (breast, ER positive), Hep G2 (human liver carcinoma cell line) and A431 (Human epithelial carcinoma cell line). IC₅₀ values (Table 1) were determined over the periods 24 h and 48 h.

Table 1.

Complexes	Cell lines					
	MCF-7		A-431		HepG-2	
	24 h	48 h	24 h	48 h	24 h	48 h
1. [Cu(arg)(N ₃)(NO ₃)(H ₂ O) ₂].2H ₂ O	70.54		80.78		149.34	
2. [(Cu) ₄ (dafone) ₄ (N ₃) ₈]	86.53		93.82		83.72	
3. [Cu(imd) ₄ (N ₃) ₂].3H ₂ O.ClO ₄	36.19		53.72		53.72	
4. [Cu(bpy)(NCO)(H ₂ O) ₃]	36.89		45.72		50.07	
5. [Cu(imd) ₂ (NCS) ₂ (H ₂ O) ₂].ClO ₄	9.13		52.59		56.66	
6. [Cu(HOr) ₂ (Br) ₂].3H ₂ O.ClO ₄	45.02		54.42		83.72	

7. [Pb(TPTZ)(N ₃)(H ₂ O)]	>500		83.72		>500	
8. [Co(imd) ₂ (N ₃) ₂ (H ₂ O) ₂].3H ₂ O	9.13		53.01		2.54	5.20
9. [Ni(H ₂ Or)(N ₃) ₂ (H ₂ O) ₂].7H ₂ O	92.42		91.01		>500	40.74
10. [Sr(bipy)(N ₃) ₂ (H ₂ O) ₂].H ₂ O	96.48		71.52		63.53	
11. [Sr(bipy)(NCS) ₂ (H ₂ O) ₂].4H ₂ O	64.23		126.77		105.6	
12. [Cd (phen)(NCO)(H ₂ O) ₃]	3.38		6.18		4.78	
13. [Cu(bpy) ₃].2ClO ₄	7.5		7.58		5.48	0.79
14. [Cu(HOr)(bpy)(H ₂ O) ₂].ClO ₄	45.02		41.38	42.08	9.27	8.43
15. [Co(HOr)(bipy)(H ₂ O) ₂].H ₂ O. SO ₄	177.11		112.89		315.92	
16. [Cd(bpy) ₂ (H ₂ O) ₂].H ₂ O	7.73		9.13		0.84	3.38
17. [Co(ribo) ₂ (H ₂ O) ₂]	>500		>500		440.01	
18. [Ni(ribo) ₂ (H ₂ O) ₂]	>500		>500		>500	
19. [Co(bpy) ₂ (H ₂ O) ₂].H ₂ O	>500	>500	482.35	362.61	>500	479.41
20. [Co(bpy)(dmg)](H ₂ O)].SO ₄	245.81	-	260.39	-	105.6	-
21. [Ni(imd) ₆]	204.87	242.87	105.06	-	415.19	213.70
22. [Ni(Tyr) ₂ (imd) ₂].2H ₂ O	>500	339.19	>500	>500	441.41	276.38
23. [Ni(Tyr)(bpy)(H ₂ O) ₂]	>500	>500	>500	-	>500	>500
24. [Ni(Tyr)(bpy) ₂].3H ₂ O.2SO ₄	410.84	-	>500	-	>500	>500
25. [Cu(Tyr)(4NP)(H ₂ O) ₂].ClO ₄	9.13	-	42.78	-	7.73	-
26. [Cu(dmg) ₂]	47.13	-	46	-	50.07	-

The studies on copper (II), zinc (II), 2-picolonic Acid, 2-Amino pyridine, 2- amino pyrimidine 2,2 bipyridine,1,10 phenanthroline pseudo halide single Crystal XRD Compounds are of great interest due to their relevance in various biological systems like antimicrobial studies, cytotoxic studies and their importance in medicinal chemistry. The thesis explores synthesis, structure and properties of various transition metal mixed ligand Crystal compounds The Entire thesis is divided into five chapters. Chapter I gives a brief introduction to geometrical patterns and literature review on biological properties of Copper (II), zinc (II), metal ions and metal complexes, chemistry of ligands viz, 2- picolonic Acid, 2-Amino pyridine, 2- amino pyrimidine 2,2 bipyridine, 1,10 phenanthroline, imidazole and their Crystal packing Diagrams ,importance of metal organic frameworks in inorganic chemistry and importance in biology. Further, it contains introduction to cancer chemotherapy, classes of metal based pharmaceuticals, new metal complexes as potential therapeutics, microbiology of metal complexes, pseudohalide chemistry and their bridging modes, and research methodologies followed. Chapter II deals with synthesis, Crystal structures, Crystal description, Crystal Packing diagrams, C-H- π & π - π Interactions, C-H-O Interactions and some organic frameworks, IR spectra, electronic spectra, Emission Spectra, P-xrd spectra, studies of [(Cu) (2-amino pyrimidine) n (OH) n ClO₄] 2-amino pyrimidine and [Cu(2-aminopyridine) 2(acetate) 2] (2) are studied for antimicrobial properties by using disc diffusion method.

Antibacterial activity of above two samples are screened against 7 human pathogenic bacteria's such as *Staphylococcus aureus* MTCC 96, *Pseudomonas aeruginosa* MTCC 3216, *Proteus mirabilis* MTCC 1429, *Vibrio cholera* MTCC 3905, *Escherichia coli* MTCC 443, *Shigella flexineri* MTCC 1457, and *Micrococcus luteus* MTCC 106. Cultures of test organisms are maintained in the inoculum suspensions of pathogenic bacterial, cultures were swabbed onto entire surfaces of Mueller-Hinton agar plates and sub cultured in petri dishes prior to testing studies. Chapter III deals with synthesis, Crystal structures, Crystal description, Crystal Packing diagrams, C-H- π & π - π Interactions, C-H-O Interactions and some organic frame works, IR spectra, electronic spectra, Emission Spectra, P-xrd spectra, studies of $[\text{Cu}(\text{2-pico})_3] \cdot \text{H}_2\text{O}$ and $[\text{Cu}(\text{2-picolonate})_2] \cdot 2\text{H}_2\text{O}$ are studied for antimicrobial properties by using disc diffusion method. Antibacterial activity of above two samples are screened against 7 human pathogenic bacteria's such as *Staphylococcus aureus* MTCC 96, *Pseudomonas aeruginosa* MTCC 3216, *Proteus mirabilis* MTCC 1429, *Vibrio cholera* MTCC 3905, *Escherichia coli* MTCC 443, *Shigella flexineri* MTCC 1457, and *Micrococcus luteus* MTCC 106. Cultures of test organisms are maintained in the inoculum suspensions of pathogenic bacterial, cultures were swabbed onto entire surfaces of Mueller-Hinton agar plates and sub cultured in petri dishes prior to testing studies. Chapter IV deals with synthesis, Crystal structures, Crystal description, Crystal Packing diagrams, C-H- π & π - π Interactions, C-H-O Interactions and some organic frame works, IR spectra, electronic spectra, Emission Spectra, P-xrd spectra, studies of $[\text{Zn}(\text{Bpy})_3] \cdot \text{Zn}(\text{NCO})_4$ and $[\text{Zn}_2(\text{Bpy})_6] \cdot \text{SO}_4 \cdot 9\text{H}_2\text{O}$ are studied for antimicrobial properties by using disc diffusion method. Antibacterial activity of above two samples are screened against 7 human pathogenic bacteria's such as *Staphylococcus aureus* MTCC 96, *Pseudomonas aeruginosa* MTCC 3216, *Proteus mirabilis* MTCC 1429, *Vibrio cholera* MTCC 3905, *Escherichia coli* MTCC 443, *Shigella flexineri* MTCC 1457, and *Micrococcus luteus* MTCC 106. Cultures of test organisms are maintained in the inoculum suspensions of pathogenic bacterial, cultures were swabbed onto entire surfaces of Mueller-Hinton agar plates and sub cultured in petri dishes prior to

testing studies. Chapter V deals with synthesis, Crystal structures, Crystal description, Crystal Packing diagrams, C-H- π & π - π Interactions, C-H-O Interactions and some organic frame works, IR spectra, electronic spectra, Emission Spectra, P-xrd spectra, studies of [Zn (Phen) 2 (NCO) 2] and [Zn (Phen) 2 (N 3) 2] are studied for antimicrobial properties by using disc diffusion method. Antibacterial activity of above two samples are screened against 7 human pathogenic bacteria's such as Staphylococcus aureus MTCC 96, Pseudomonas aeruginosa MTCC 3216, Proteus mirabilis MTCC 1429, Vibrio cholera MTCC 3905, Escherichia coli MTCC 443, Shigella flexineri MTCC 1457, and Micrococcus luteus MTCC 106. Cultures of test organisms are maintained in the inoculum suspensions of pathogenic bacterial, cultures were swabbed onto entire surfaces of Mueller-Hinton agar plates and sub cultured in petri dishes prior to testing studies.

Rational of the Study and the Research Gap

It is observed from the review of literature that there available a plethora of research being conducted all over the world to develop new pseudo halide metal complexes and Schiff bases and establish the procedures for the application at the lab level and in scaling up process. Very few of the available researches have been presented in this part.

Further, keeping in view of the advantages of nano particulate metal complex systems, many new reactions have been studied in the limited time framework of research to be completed and submitted as part of the course work. Many areas could be studied and many factors could also be considered in selecting the objectives and scope of the work, but finally keeping in view of the framework of the course, the study confined to the objectives selected.

The main aim of this research work is on the synthesis and characterisation of nano crystalline complexes and study their biological application in the synthesis of some new class of organo metallic compounds by one-pot multicomponent synthesis using greener strategies. The bioactive compounds have been prepared by self-assembly method and hydrothermal method. Phase pure nano crystalline nanoparticulate metal complexes with different compositions. The bio active compounds have been characterized and used in the research as pharmacological active compounds. This technique produced good yield and ensured complete homogeneity. Hence this process could be scaled.

The objectives of the study are:

1. To synthesize nano particulate compounds and its metal chelates by self assembly and hydrothermal methods.
2. To characterize the synthesized nano ferrites using FT-IR, XRD, SEM, EDAX, TEM and BET surface area techniques to interpret their structure, morphology and size.
3. To characterise the structure of the newly synthesized metal complexes and its nanostructures using FT-IR, ^1H NMR and MASS spectral analysis
4. To study the biological activity of the newly synthesized Metal complex compounds.

In vitro antimicrobial activity.

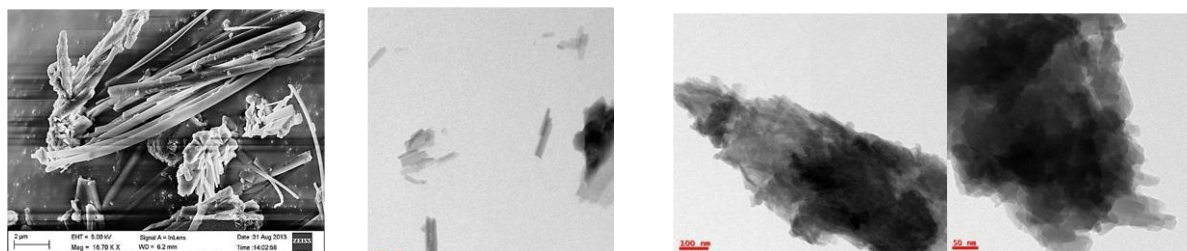
Copper complexes 1-26 were screened *in vitro* for antibacterial activity against two bacterial species; *E.coli*, *P.aeruginosa* and *S.aureus* as well as antifungal activity was determined against fungal stain *R.oligospires* and *A.niger* by disc diffusion method. The resulting activities of the complexes are summarized in the Table 2.

Table 2: Inhibition Zones for complexes 1-26 against Bacteria and Fungi.

Complexes	Bacteria			Fungi	
	S.aureus	E.coli	P.aeruginosa	R.oligospires	A.niger
1. [Cu(arg)(N ₃)(NO ₃)(H ₂ O) ₂].2H ₂ O	3	3		Nil	
2. [(Cu) ₄ (dafone) ₄ (N ₃) ₈]	3	3.5		3	
3. [Cu(imd) ₄ (N ₃) ₂].3H ₂ O.ClO ₄	4	4		Nil	
4. [Cu(bpy)(NCO)(H ₂ O) ₃]	10	7.5		Nil	
5. [Cu(imd) ₂ (NCS) ₂ (H ₂ O) ₂].ClO ₄	3.5	2		2.5	
6. [Cu(HOr) ₂ (Br) ₂].3H ₂ O.ClO ₄	3.5	4		Nil	
7. [Pb(TPTZ)(N ₃)(H ₂ O)]	3	3	-	Nil	-
8. [Co(imd) ₂ (N ₃) ₂ (H ₂ O) ₂].3H ₂ O	2	-	-	-	-
9. [Ni(H ₂ Or)(N ₃) ₂ (H ₂ O) ₂].7H ₂ O	Nil	Nil	3	3.5	3.5
10. [Sr(bipy)(N ₃) ₂ (H ₂ O) ₂].H ₂ O	4	3	-	11	Nil
11. [Sr(bipy)(NCS) ₂ (H ₂ O) ₂].4H ₂ O	3.5	3.5	3.5	Nil	-
12. [Cd(phen)(NCO)(H ₂ O) ₃]	3.5	5.5	-	Nil	-
13. [Cu(bpy) ₃].2ClO ₄	9	8		3	
14. [Cu(HOr)(bpy)(H ₂ O) ₂].ClO ₄	12.5	9.5		2	
15. [Co(HOr)(bipy)(H ₂ O) ₂].H ₂ O. SO ₄	3	3.5		Nil	
16. [Cd(bpy) ₂ (H ₂ O) ₂].H ₂ O	5	4.5		11	
17. [Co(ribo) ₂ (H ₂ O) ₂]	3.5	Nil		Nil	
18. [Ni(ribo) ₂ (H ₂ O) ₂]	3	Nil		Nil	
19. [Co(bpy) ₂ (H ₂ O) ₂].H ₂ O	3.5	Nil	2.5	Nil	
20.[Co(bpy)(dmg)](H ₂ O)].SO ₄	3.5	3	-	2	
21. [Ni(imd) ₆]	Nil	Nil	-	Nil	
22. [Ni(Tyr) ₂ (imd) ₂].2H ₂ O	3	3	3	3.5	
23. [Ni(Tyr)(bpy)(H ₂ O) ₂]	3	Nil	-	Nil	
24. [Ni(Tyr)(bpy) ₂].3H ₂ O.2SO ₄	Nil	Nil	-	3	
25. [Cu(Tyr)(4NP)(H ₂ O) ₂].ClO ₄	3	2	3	Nil	
26. [Cu(dm _g) ₂]	Nil	-	-	-	

Complexes, eg. [Ni(H₂Or)(NCO)₂(H₂O)₂].9(H₂O), [Cu(HOr)(N₃)₂(H₂O)₂].ClO₄, [Cu(HOr)(NCS)

(H₂O)₂].2ClO₄, and [Cu(HOr)(NCO)₂(H₂O)₂].2H₂O.ClO₄, were obtained in nano form rod, flower shaped morphology with average particle size of 11-153 nm (Fig.1-



4). Complexes have promising antimicrobial activity

Bio active imidazole complexes

The study of imidazole as a complexing agent has been a matter of active interest for years, mainly because imidazole is involved in important biological processes¹⁻⁵. There are two nitrogen atoms in one imidazole molecule. The deprotonated nitrogen atom is a good resource to coordinate with metal ion and a series of compounds based on imidazole and different metal ions have been reported⁶⁻¹². On the other hand, the protonated nitrogen atom in imidazole molecule is a good hydrogen bonding donor and multi-dimensional supramolecular assembly can be obtained via hydrogen bonding interaction¹³⁻²⁰. It is expected that different anions and their different geometrical configurations will have influence on extended supramolecular network. The ligand imidazole plays an important role in biological systems, since the imidazole moiety of the histidyl residue in a large number of metallo proteins forms all or part of the binding site of many transition metal ions²¹⁻²³. A large range of pharmaceutical products containing the imidazole moiety have been synthesized to test anti-microbial and anti-cancer activities. Compounds containing imidazole and other ligands are of considerable interest in view of their biological and medicinal applications²⁴⁻²⁶. Imidazole can function as a neutral monodentate, bridging bidentate or in certain cases as an anionic imidazolate ligand²⁷.

The availability of Imidazole in very pure form, its solubility in a variety of solvents, its ability to function as a ligand for metals, the importance of metal-imidazole compounds in biological applications etc. are some reasons for the study of metal-imidazole compounds. Tetrakis and pentakis imidazole complexes of copper (II) were reported earlier.²⁸⁻³⁰ Recently we have published an international paper on anticancer activity of Nickel orotic acid Imidazole complex³¹. This chapter discusses the synthesis of mixed-ligand complexes of some first row transition metal ions using Imidazole as primary ligand and pseudohalides as secondary ligands.

Bio active copper orotic acid complexes

Metal chelates of orotate anions have been prepared and structurally studied^{1,2,3,4,5-15}. The transition metal complexes of orotic acid and its co-ligand derivatives continue to attract attention because of orotic acid's multidentate functionality and its significant role in bioinorganic chemistry¹⁶. Metal orotates are also widely applied in medicine¹⁷. Orotic acid has a great importance in the field of biological activity¹⁸⁻²². The transition metal complexes such as platinum, palladium and nickel orotates with wide variety of substituents have been screened as therapeutic agents for cancer²³. Moreover, zinc(II) and cobalt(II) orotate complexes have shown antimicrobial activity²⁴. Orotic acid is also an interesting organic building block in coordination chemistry^{1,2-25}. The deprotonated

orotates are a widely used ligand for the construction of coordination compounds due to their versatile bridging modes, such as monodentate, bidentate, tridentate bridging and mixed chelating bridging were prepared and structurally studied^{1-15,25-27}. We present the results of the synthesis, characterization and antimicrobial activity studies of a series of mixed-ligand complexes involving orotate copper and pseudohalides. Recently we have published an international paper on review on coordination chemistry of orotic acid.²⁸

2.1 Experimental

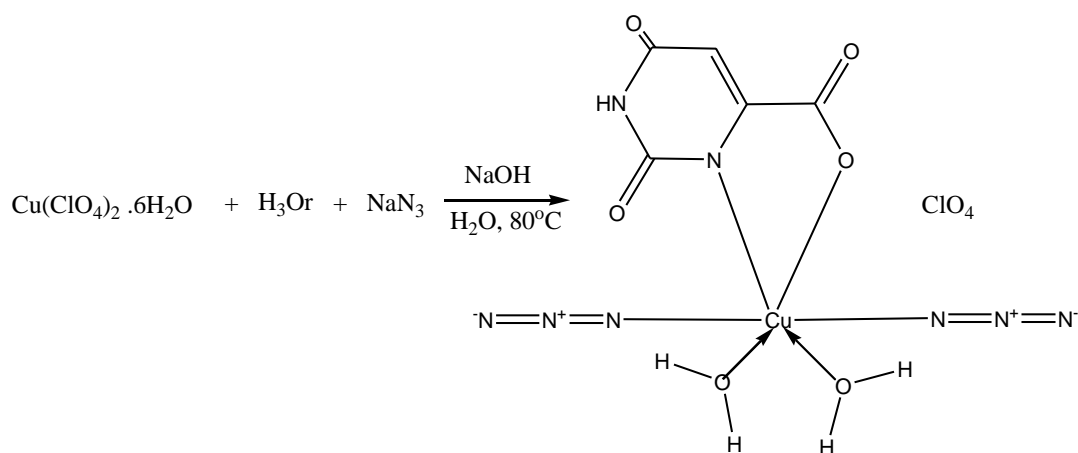
2.1.1 Reagents

Chemicals are procured from renowned companies like sigma Aldrich, molychem and used without further purification. Ethanol, methanol used for synthesis of metal complexes are A.R. grade and used as received for synthetic work. $\text{Cu}(\text{ClO}_4)_2 \cdot 6\text{H}_2\text{O}$ is procured from Alfa aesar.

Caution : Azides and perchlorates are explosive, handle with care.

2.1.2 Synthesis of $[\text{Cu}(\text{HOr})(\text{N}_3)_2(\text{H}_2\text{O})_2] \cdot \text{ClO}_4(1)$

An aqueous (5 ml) solution of copper perchlorate hexahydrate (0.37g, 1.0 mmol) is added to an sodium hydroxide solution (10ml) of orotic acid (0.156g, 1.0 mmol) under stirring conditions and the solution turned to blue colour and then aqueous solution (5 ml) of NaN_3 (0.065 g, 1.0 mmol) is added which remained as same solution but with less intensity of blue colour. After constant stirring at 80 °C temperature for 30 minutes, the solution was filtered off and the blue precipitate is collected. The precipitate is washed with methanol and toluene. Yield 0.196 g (53 %). Anal. exptl. $\text{C}_5\text{H}_6\text{N}_8\text{CuO}_{10}\text{Cl}$ (M.Wt. 437.15) C, 13.74; H, 1.38; N, 25.63. Found: C, 13.21; H, 1.18; N, 25.13. Important IR absorptions (KBr disk, cm^{-1}): 3450, 3223, 2983, 2048, 1672, 1668, 1531, 1479, 1390, 1327, 808, 763, 594, 443. Mass peaks (m/z): 305, 318, 403, 440, 641, 808.



1. Synthetic route and proposed structure of complex 1.

The title mononuclear complex, $[\text{Cu}(\text{HOr})(\text{N}_3)_2(\text{H}_2\text{O})_2]\cdot\text{ClO}_4$ (HOr is orotic acid) has been synthesized. The Cu^{II} ion in the complex has a distorted octahedral coordination geometry comprised of one deprotonated pyrimidine N atom and the adjacent carboxylate O atom of the orotate ligand, two azide N atoms and two aqua ligands in the coordination sphere and one perchlorate ion in the outersphere.

2.2 Physical Measurements

IR spectra are obtained with a Shimadzu IR Prestige 21 FT-IR spectrophotometer. UV spectra are recorded on Thermoscientific UV spectrophotometer. Elemental analysis is obtained using a FLASH EA 1112 SERIES CHNS analyser. LC-MS Spectra are recorded on AGILANT QQQ (ESI-MS) mass spectrometer. TGA Spectra are recorded using TGA Q500 V20.13. SEM and TEM are recorded on ZEISS ULTRA-55 and FEI TECNAI G² S-TWIN 200 KV respectively.

2.2.1 IR Spectrum of [Cu(HOr)(N₃)₂(H₂O)₂].ClO₄(1)

The infrared spectrum of orotic acid (Fig 2.1) showed the following:

- (1) Two bands at 3166 and 3014 cm⁻¹, which are due to $\nu(\text{NH})$ ²⁹ of the pyrimidine ring. Their low frequencies indicate that the NH groups participate in hydrogen bonding³⁰⁻³².
- (2) The C2 - O stretching vibration is observed at 1705 cm⁻¹, while the C4 - O and C_{acid} - O stretching vibrations are partially overlapping and the band at 1667 cm⁻¹ is assigned to them. This would elaborate upon our previous conclusion that, orotic acid exists in the keto form. Price et al.³³ studied the IR spectra of some barbiturates where in solution, two absorption bands are observed at 1740 and 1708 cm⁻¹ state. On passing to the solid phase, such compounds show a pronounced shift of both peaks to 1698 and 1661 cm⁻¹. This was explained on the basis that carbonyl groups participate in hydrogen bonding.
- (3) The moderate band at 2834 to 2500 cm⁻¹³⁴ may be due to $\nu(\text{OH})$ of the carboxylic group.
- (4) Bands at 1518 and 1423 cm⁻¹ are due to $\delta(\text{N1H})$ and $\delta(\text{N3H})$, respectively³⁵.

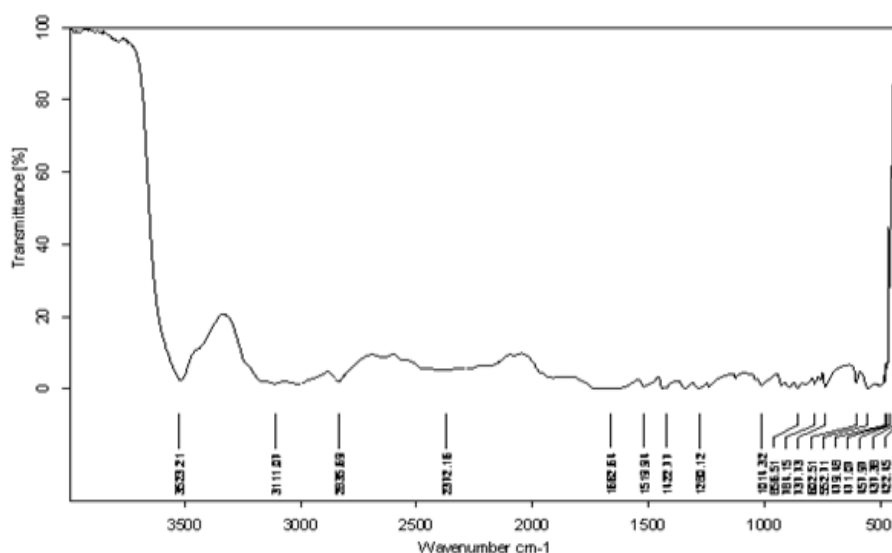


Figure 2.1 IR spectrum of free orotic acid

A comparison of the IR spectra of the ligand and the metal complexes brings out the following facts to light

- (1) The spectra of the solid complexes exhibited bands in the 3450–3300 cm⁻¹ regions, which may be attributed to $\nu(\text{OH})$ of the coordinated water³⁶ molecules.
- (2) The $\nu(\text{NH})$ bands at 3166 and 3014 cm⁻¹ show dramatic changes in the position and the intensity, which would suggest that at least one of the imino groups of the pyrimidine ring participate in bond formation with the metal ions.
- (3) The position and intensity of $\nu(\text{C}=\text{O})$ of the free ligand, changes appreciably during

complexation, while there is a little change in $\nu(\text{C4 O})$. Björling et al.³⁷ found that, C=O stretching bands situated adjacent to N-M will be greatly affected.

(4) The $\delta(\text{N1H})$ band at 1518 cm^{-1} almost disappeared in the spectra of Cu(II) and Co(II) suggesting that N1H group participate in binding with the metal ion through deprotonation. However, $\delta(\text{N3H})$ band in all the studied complexes is almost unchanged from that in the corresponding free neutral ligand, which confirms the inability of the N3H group to participate in the coordination.

(5) In the spectra of all studied complexes, the $\nu(\text{OHacid})$ band at 2500 cm^{-1} in the free ligand completely disappeared and a new carboxylate band (νCOO) appeared in the region $1496\text{--}1479 \text{ cm}^{-1}$ indicating that the carboxylic group of orotic acid participate in the coordination with the metal ions through deprotonation. From the above result, we conclude that all metal ions studied, coordinate to orotic acid via the N1 nitrogen and adjacent carboxylate group. The IR spectral data of all the complexes are listed in Table 2.17.

The IR spectrum of the complex 1 (Fig 2.2) exhibits bands in the $3450\text{--}3300 \text{ cm}^{-1}$ regions, which may be attributed to $\nu(\text{OH})$ of the coordinated water³⁶ molecules. The O-H vibration of the carboxyl group, which is observed for the free orotic acid at 2500 cm^{-1} , has disappeared and a new carboxylate band (νCOO) appeared at 1479 cm^{-1} indicating that the carboxylic group of orotic acid participate in the coordination with the metal ions through deprotonation. The N(1)H vibration bands which appear at $3170, 1431 \text{ cm}^{-1}$ for the free orotic acid are not observed in the complex which confirms the coordination through N atom. The carbonyl groups give rise to two main peaks at 1700 cm^{-1} [$\nu\text{C}=\text{O}(\text{acid}) + \nu\text{C}(2)=\text{O}$] and 1660 cm^{-1} [$\nu\text{C}(6)=\text{O} + \nu\text{C}=\text{C}$] for the free H_3Or ³⁸. The carbonyl stretching modes in the title complex are observed at 1672 and 1643 cm^{-1} . The spectrum exhibits an intense absorption at 2048 cm^{-1} which is associated with the asymmetric stretching mode of the azide ligand. The $\nu_s(\text{N}_3)$ stretching mode of the azide group is observed as a medium band at 1327 cm^{-1} . The deformation mode of the azido ligand is observed as a weak band at 763 cm^{-1} . The presence of an unsplit band at 1109 cm^{-1} corresponding to $\nu_3(\text{ClO}_4)$ and at 594 cm^{-1} assignable to $\nu_4(\text{ClO}_4)$ in above complex which suggests that the perchlorate ion is outside the coordination sphere of the complex and hence ionic in nature³⁹⁻⁴².

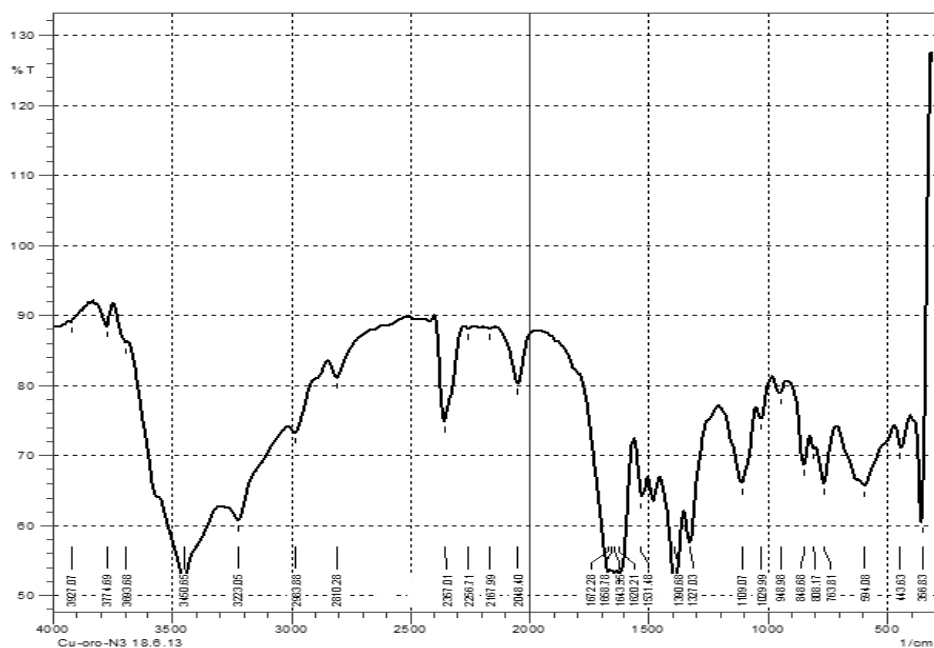


Figure 2.2. IR Spectrum of Complex 1

2.2.2 Electronic Spectrum of [Cu(HOr)(N₃)₂(H₂O)₂].ClO₄(1)

The spectra of the orotic acid complexes are taken in methanol. There are two detected absorption bands at around (210 -235 nm) and 280 nm assigned to $\pi-\pi^*$ and $n-\pi^*$ transitions, respectively, in the electronic spectrum of the ligand. These transitions also found in the spectra of the complexes, but they are shifted towards lower wavelength, confirming the coordination of the ligand to the metal ions. The first band around 210 to 235 nm is probably due to a $\pi-\pi^*$ of the exocyclic band in heterocyclic ring and also assigned to the two carbonyl groups. However, the second band around 280 nm is due to the presence of COOH group⁴³. In case of orotate complexes, the carboxylic group is blue shifted with increase in the intensity (absorbance). This result confirms the complexation of metal ions via carboxylic group. The complexes showed shoulder broad bands in the range of 300-325 nm may be assigned to the d-d transition.

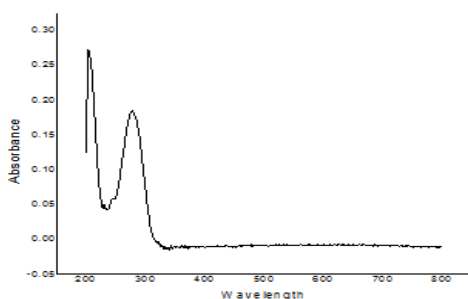


Figure 2.3. Electronic spectrum of Free Orotic Acid

The solution spectra of the ligand and all complexes are taken in methanol and presented in Table 2.18. The complex 1 has a shoulder broad band at 321 nm may be assigned to the d-d

transition. This result confirms the complexation of metal ion via carboxylic group.

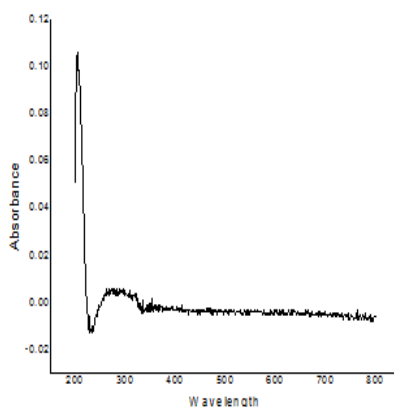


Figure 2.4 Electronic Spectrum of complex 1

2.2.3 LC-MS Spectrum of $[\text{Cu}(\text{HOr})(\text{N}_3)_2(\text{H}_2\text{O})_2] \cdot \text{ClO}_4(1)$

The LC/MS studies are performed in search of the molecular weights of the complexes. LC-ESI/MS technique is a good method to analyze the complexes. The peak at 305(m/z) is complex bound to one orotic acid, two azide molecules, $[\text{Cu}(\text{HOr})(\text{N}_3)_2]$ and the peak at 318(m/z) is complex bound to orotic acid, one water molecule and two azide molecules present in 1:1:2 ratio, $[\text{Cu}(\text{HOr})(\text{H}_2\text{O})(\text{N}_3)_2]$. The peaks around 403(m/z) and 440(m/z) refer to the $[\text{Cu}(\text{HOr})(\text{N}_3)_2] \cdot \text{ClO}_4$ and $[\text{Cu}(\text{HOr})(\text{N}_3)_2(\text{H}_2\text{O})_2] \cdot \text{ClO}_4$ complexes respectively. The peak at 641(m/z) corresponds to dimer of $[\text{Cu}(\text{HOr})(\text{N}_3)_2(\text{H}_2\text{O})]$ and 808(m/z) corresponds to dimer of $[\text{Cu}(\text{HOr})(\text{N}_3)_2] \cdot \text{ClO}_4$.

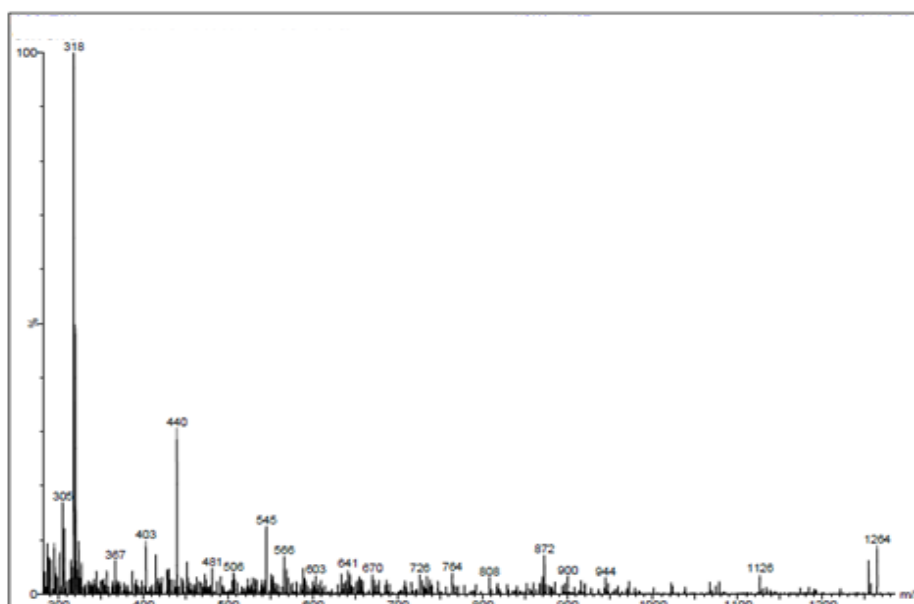


Figure 2.5 LC-MS Spectrum of complex 1

2.2.4 Thermal Gravimetric Analysis of $[\text{Cu}(\text{HOr})(\text{N}_3)_2(\text{H}_2\text{O})_2]\cdot\text{ClO}_4(1)$

The thermal behavior of metal complexes shows that the hydrated complexes lose molecules of hydration first; followed by decomposition of ligand molecules in the subsequent steps. The thermal degradation behaviour of the copper(II) complex of orotic acid is studied by thermogravimetric analysis. Thermal stabilities of all the complexes are studied by TG-DTA technique. The thermal behavior shows that the dissociation occurs in regular sequence and thermal stabilities do not differ significantly from one another. It is concluded that the same trend in decomposition pattern indicates no difference in their geometries. In all the complexes, the mode of disintegration is such that the ligand decomposes before its vaporization as a complete moiety, showing the stability of coordination moiety. Later on, the remaining component of the ligand vaporizes in the temperature range of 250–400°C, leaving the corresponding metal halide behind that which combines with atmospheric oxygen to yield metal oxide at high temperature. The thermogravimetric studies of the complex 1 is carried out in the temperature range of 24.4–500°C with a sample heating rate 10°C/min in air atmosphere.

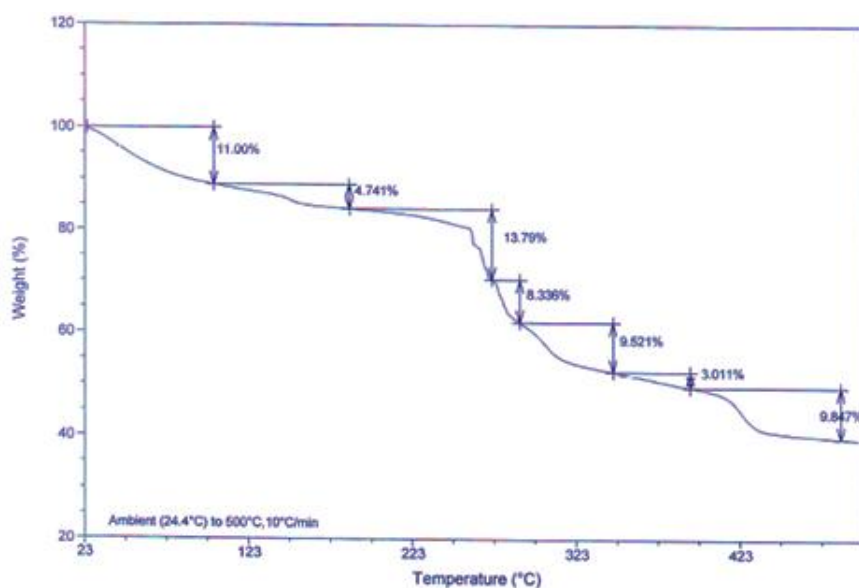


Figure 2.6 TG-DTA Spectrum of complex 1

The thermal decomposition of the title complex, $[\text{Cu}(\text{HOr})(\text{N}_3)_2(\text{H}_2\text{O})_2]\cdot\text{ClO}_4(1)$, presented in Fig. 2.6 is well defined, consisting of two stages. In the first step, dehydration of the complex occurs in the temperature interval of 40 – 170°C corresponding to elimination of two coordinated water molecules (Remaining Wt.%, Obs./Calcd., 92.35/91.50). After this temperature, a loss in weight is observed in general up to 400°C corresponding to the loss of partially decomposed ligand part from the complex (Remaining Wt.%, Obs./Calcd., 56.53/55.81). Above this temperature, a weight loss has

been occurred upto 500°C. This corresponds to metal oxide as an ultimate pyrolysis product(Remaining Wt.%, Obs./Calcd., 13.93/13.72). The thermal analysis evaluates the thermal stability of the metal complexes, this study also helped to characterize the metal complexes.

2.2.5 Powder X-Ray Diffractogram of [Cu(HOr)(N₃)₂(H₂O)₂].ClO₄(1)

Although single crystal X-ray crystallographic investigation is the most precise source of information regarding the structure of a complex, the difficulty of obtaining crystalline complexes renders this method unsuitable for such a study. However, a variety of other spectroscopic techniques could be used with good effect for characterizing the metal complexes as X-ray powder diffraction. So, X-ray powder diffraction (XRD) measurement of the complex 1 is performed. The diffractogram obtained for complex 1 is given in Fig.2.7 and with the help of the data obtained from the powder XRD, the crystallite size calculations are performed using Scherrer equation^{44,45}. By the comparison of bulk and nano diffractograms, it is observed that in both complexes phase formation is same. The 2θ values and FWHM values are having small differences and according to the spectral comparisons no structural diversity is seen.

Complex no.	2θ	FWHM	Crystallite size
1.	11.213	0.613°	2.524 Å
1 (nano).	28.558	2.144	0.741 Å

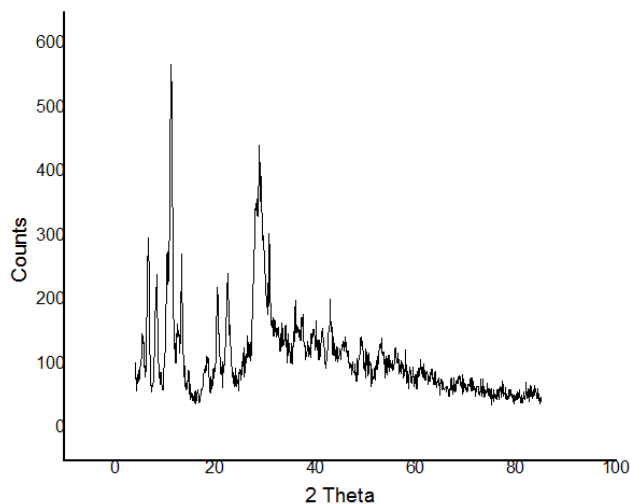


Figure 2.7 Powder XRD diffractogram of complex 1

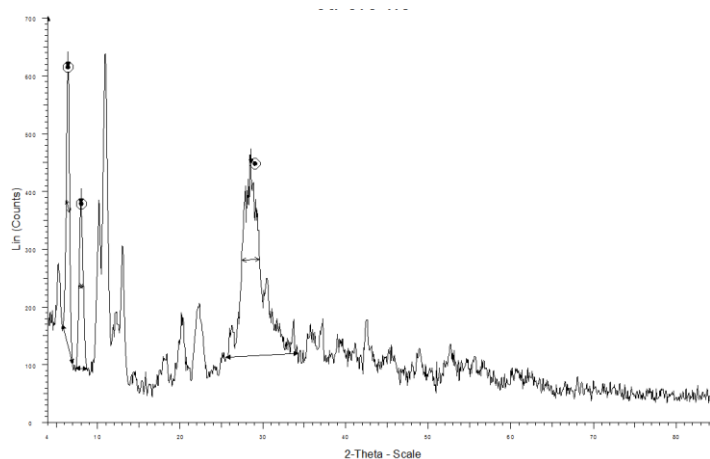


Figure 2.8 Powder XRD diffractogram of complex 1 (nano)

Crystallite size is obtained using Scherrer's equation, $D = K\lambda/(\beta\cos\theta)$, where D is the particle size in nm of the crystal grain has been calculated using maximum intensity peak; K is the Scherrer's constant; λ is the wavelength of target used; β is the full width at half maximum reflection height in terms of radian and θ is the Bragg diffraction angle at peak position in degree.

2.2.6 (a) FE-SEM of $[\text{Cu}(\text{HOr})(\text{N}_3)_2(\text{H}_2\text{O})_2]\cdot\text{ClO}_4(1)$

FE-SEM is used to evaluate morphology and particle size of the metal complexes. FE-SEM photographs of the synthesized complex 1 are illustrated in Fig 2.10. From the FE-SEM photographs, we noted that there is a uniform matrix of the synthesized complexes, i.e., the complexes are of homogeneous phase material. The scanning electron micrograph (SEM) is used to evaluate the surface morphology of the free ligand and their metal complexes. FE-SEM images of orotic acid ligand (Fig 2.9) differ significantly from that of the complex 1 (Fig 2.10) due to the coordination of the metal ions to the donor sites of the ligands. FE-SEM images of free orotic acid differs widely from the metal complexes in terms of morphology.

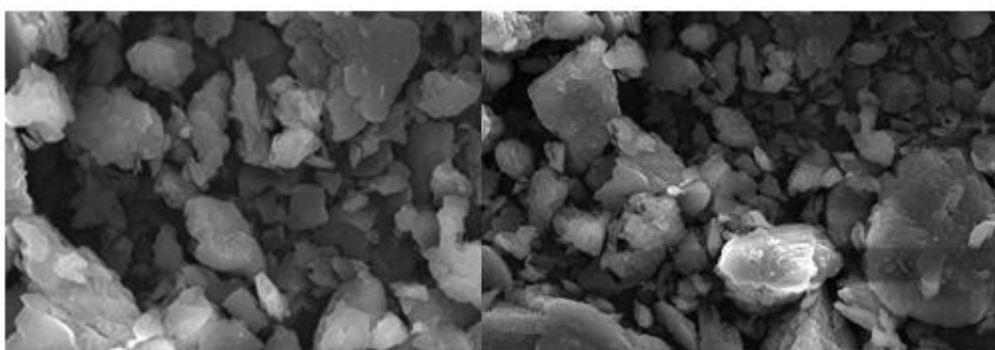


Fig 2.9 FE-SEM images of Free orotic acid

Complex 1 is made nano by using High energy ball milling method and is confirmed by HR-TEM. Complex 1 is having rod shaped morphology with $2\mu\text{m}$ particle size. In general, the FE-SEM

photographs of complex 1 show single phase formation with well-defined shape and particle size in the range of 2–3 μm.

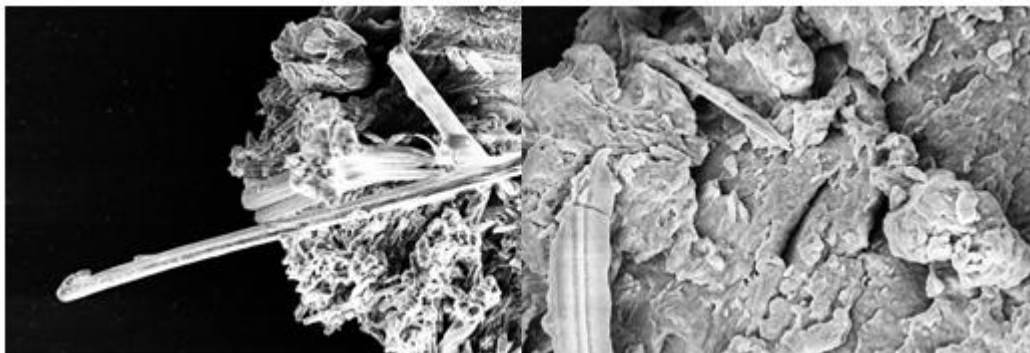


Fig 2.10FE-SEM images of complex 1

2.2.6 (b) EDX Spectrum of [Cu(HOr)(N₃)₂(H₂O)₂].ClO₄(1)

It is an analytical technique used for the elemental analysis or chemical characterization of a sample. It relies on the investigation of an interaction of some source of X-ray excitation and a sample. Its characterization capabilities are due in large part to the fundamental principle that each element has a unique atomic structure allowing unique set of peaks on its X-ray spectrum. To stimulate the emission of characteristic X-rays from specimen, a high energy beam of charged particles such as electrons and protons or a beam of X-rays, is focused into the sample being studied. At rest, an atom within the sample contains ground state (or unexcited) electrons in the discrete energy levels or electron shells bound to the nucleus. The incident beam may excite an electron in an inner shell, ejecting it from the shell while creating an electron hole where the electron was. An electron from an outer, higher-energy shell then fills the hole, and the difference in energy between the higher-energy shell and the lower energy shell may be released in the form of an X-ray. The number and the energy of the X-ray emitted from a specimen can be measured by an energy-dispersive spectrometer. As the energy of the x-rays are characteristic of the difference in the energy between the two shells, and of the atomic structure of the element from which they were emitted, this allows the elemental composition of the specimen to be measured.

Element	Weight%	Atomic%
C K	18.81	26.66
N K	18.93	23.01
O K	34.91	37.15
Na K	10.96	8.11
Cl K	3.18	1.53
Cu K	13.20	3.54
Totals	100.00	

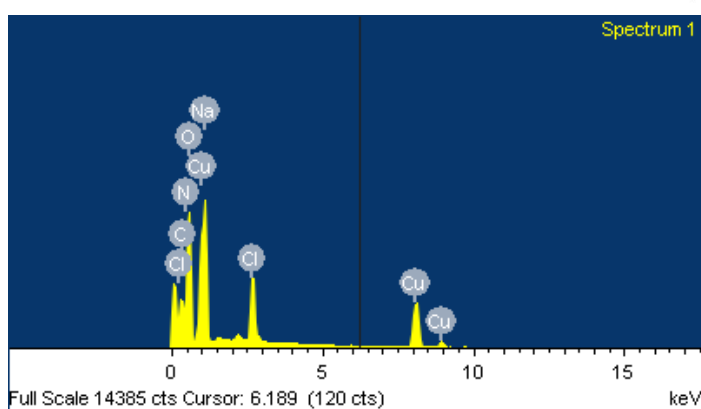
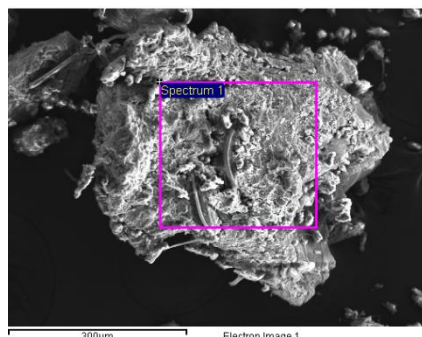


Fig 2.11 EDX Spectrum of complex 1

In the presented complex 1, the elements such as carbon, nitrogen, oxygen, sodium (sodium orotate), chlorine (copper perchlorate) and copper are identified.

2.2.7HR-TEM of $[\text{Cu}(\text{HOr})(\text{N}_3)_2(\text{H}_2\text{O})_2]\cdot\text{ClO}_4(1)$

It is a microscopy technique in which a beam of electrons is transmitted through an ultra-thin specimen, interacting with the specimen as it passes through. An image is formed from the interaction of the electrons transmitted through the specimen; the image is magnified and focused onto an imaging device, such as a fluorescent screen, on a layer of photographic film, or to be detected by a sensor such as a CCD camera. By adjusting the magnetic lenses such that the back focal plane of the lens rather than the imaging plane is placed on the imaging apparatus a diffraction pattern can be generated. For thin crystalline samples, this produces an image that consists of a pattern of dots in the case of a single crystal, or a series of rings in the case of a polycrystalline material. HR-TEM images gives information about the crystalline nature, morphology and orientation of the complex 1 and are illustrated in fig. 2.12. The size of the particles is 50-100 nm.

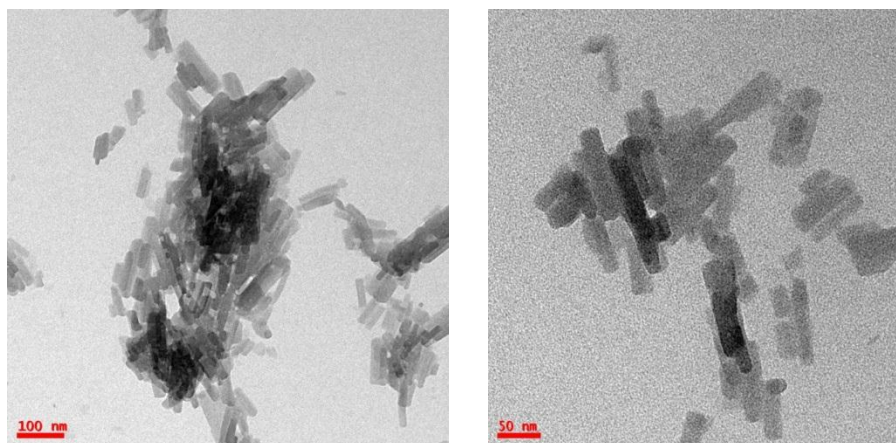


Fig 2.12.HR-TEM images of complex 1 at 50 nm and 100 nm.

Diffraction pattern consists of a pattern of a series of rings which suggests that the complex 1 is a polycrystalline material.

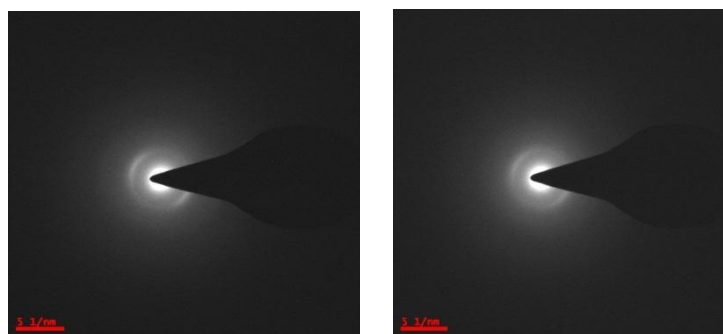


Fig 2.13Nano beam electron diffraction pattern of Complex 1.

2.2.8Antimicrobial Screening of $[\text{Cu}(\text{HOR})(\text{N}_3)_2(\text{H}_2\text{O})_2]\cdot\text{ClO}_4(1)$

The complex 1 is screened *invitro* for antibacterial activity against *E.coli*, *S.aureus* and *K. pneumoniae* and antifungal activity against *R.oligospores* and *A.niger* by disc diffusion method. The antibacterial and antifungal activities of complex 1 are listed in table 2.1.



Fig 2.14Inhibition zones for complex 1 (15) against E.coli and S.aureus

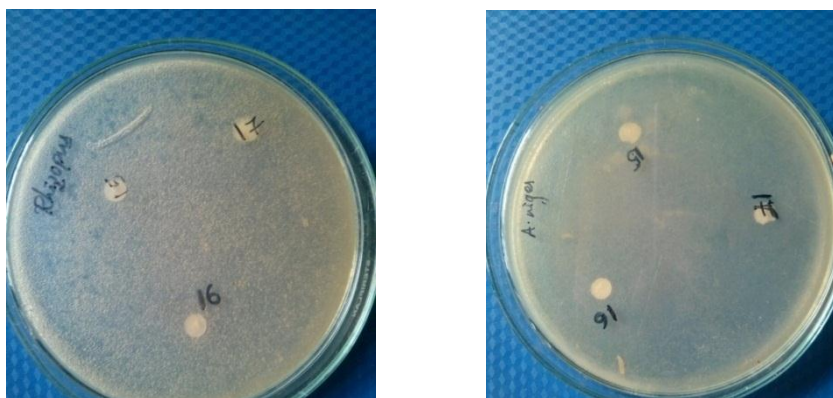


Fig 2.15 Inhibition zones for complex 1(15) against *R. oligosporus* and *A. niger*

Table 2.1 Inhibition zones for complex 1 (15)

Bacteria	Inhibition zone (mm)
E.coli	7.5
S.aureus	7
Fungi	Inhibition zone (mm)
<i>R. oligosporus</i>	Nil
<i>A. niger</i>	Nil

The complex 1 showed good antibacterial activity against *E. coli* and *S. aureus* but didn't show any activity against fungal organisms.

New polymeric copper 2-picolonic Acid Crystal Structures and its Biology

3.1 Introduction

In modern years, chemists have tended to plan and synthesis metal-organic frameworks, which are undergoing accelerated and continuous growth because of their fascinating structures, and potential applications, such as molecular adsorption, catalysis, gas storage, multifunctional materials, and chemical separation [1–10]. The transition metal carboxylates have the diversity of coordination modes, which leads to an affinity to form cluster or polymer structures [11]. It is known that 2-picolonic acids terminal tryptophan metabolite, the pyridine nitrogen atom and the carboxylate oxygenates are access to coordinate with different metal ions. Besides, 2-picolonic acid is not only a potential proton acceptor but also proton donor depending on deprotonated groups [12]. To the

best of our understanding, the crystal structures of 2-picolinic acid with Ni(II), Zn(II), Co(III), and Cu(II) derivations have been reported [11–14]. The method of room temperature solid-solid synthesis is a simple and suitable method for the preparation of metal complexes, and many complexes have been synthesized by this method [15–17]. Advantages of the solid-solid synthesis method are much higher yield, being inexpensive, faster reaction rate, easier operating, energy saving and environmental friendly [18], and it is in unity with the requirements of green chemistry. Copper and cobalt is important trace elements for human and all animals, and its complexes have been used in the fields of medicine, bioinorganic chemistry, functional materials, and so forth [19–24]. At the same time, the cobalt compounds are often used in chemical reactions as oxidation catalysts, such as assembly *calc.* catalysts that are the cobalt carboxylates, which are also used in paints, varnishes, and pigments industry [25].

1-D Polymers are among the most explored and greatest investigated supramolecular architectures [26–28]. As hydrogen bonds and other non-covalent interactions are the main driving forces, supramolecular chemistry is characterizing and understanding various hydrogen bonded water clusters in metal-organic hosts in the form of tetramers [29], hexamers [30], octamers [31], decamers [32], and 1-D infinite water chains [33, 34] in various organic and metal-organic crystal hosts. Zeolite like 3-D network structures with chiral channels filled with highly ordered water molecules are well known [35]. 1-D water chains attract attention because of their vital role in biological transport of water, protons, and ions [36]. Transport of water or protons across the cell involves assembly of extremely mobile hydrogen-bonded water molecules into a single chain at the positively charged slight pore of the membrane-channel protein aquaporin-1 [37]. While 1-D water chains play crucial roles in stabilizing the native conformation of biopolymers, helical water chains are extremely rare in synthetic crystal hosts [33, 34]. Here, we report an interesting 1-D coordination polymeric architecture of a copper (II)-picolinate complex that hosts a 1-D zigzag chain of lattice water molecules through hydrogen bonding. As a part of our ongoing research on

molecular self-assembly through in-built peripheral hydrogen bonding group into higher dimensionality [38,39] and trapping of water in host lattices [29, 30]

Pyridine-2-carboxaldehyde into 2-picolinic acid (scheme 1). Lattice water molecules from the metal salt are trapped in the Cu-picolinate network lattice forming a 1-D water chain and playing a major role in formation of the H-bonded coordination network in this chapter crystal engineering of copper picolinate complex formed by in situ oxidation of pyridine-2-carboxaldehyde with copper(II) perchlorate is discussed. The carboxylate ions not only take part in coordination to metal but also provide hydrogen bond acceptor sites for lattice water. The synthesis, single-crystal X-ray structure, FTIR, luminescence and Biology of a new Cu (II)-picolinate coordination complex is reported.

3.2. Experimental

3.2.1 Reagents

All chemicals are purchased from companies like Coastal Chemicals, Sigma Aldrich Chemicals and used without further purification. Ethanol, methanol solvents are purchased as A.R. grade and used as received for synthetic work.

3.2.2 SYNTHESIS OF [Cu (2-pico)₃].H₂O

To the 5 mL solution of copper perchlorate hexahydrate (0.370g, 1.0 m.mol) in water, is added 5 mL aqua solution of 2- picolinic acid (0.123g, 1.0 m.mol), entire solution is stirred at 60⁰C with a color change from water shoot to lemon soufflé. After 20 min further stirring, sodium azide in 5 ml aqua solution (0.065g, 1.0 m mole) is added to the mixture solution, and left it for stirring until the color observation from lemon soufflé to coffee color. The small amount of precipitate is formed, filtered and wash with distilled water, and methanol. The filtrate solution is left at room temperature, and by the slow evaporation process finally we observed green color shiny crystals.

These crystals are suitable for single crystal X-ray diffraction method, and calculated amount of yield is 46%. Anal calcd for $C_{12}H_{12}CuN_2O_6$ (Mol.wt: 343.79): C, 41.92; H, 3.52; Cu, 8.48; N, 8.15; O, 27.19; Found: C, 49.18; H, 3.65; Cu, 13.70; N, 9.01; O, 24.20 IR absorptions (KBr disk, cm^{-1}) 3438, 3076, 1641, 1473, 1348, 776, 694, 457.

3.3. Physical Measurements

IR spectra are obtained with a Shimadzu FT-IR 8000 spectrometer. Elemental analysis is obtained using a FLASH EA 1112 SERIES CHNS analyzer. UV spectra are recorded on thermo scientific UV Spectrophotometer. Fluorescent spectral data are collected on Fluoromax-4C-1140D-2413-FM spectrophotometer.

3.3.1 X-ray Crystallographic data collection and structure determination

A single crystal of approximate dimensions 0.12 x 0.8 x 0.4 mm was mounted. The data collection was done on an Enraf Nonius CAD-4 diffract meter using Mo $K\alpha$ radiation. The data were corrected for absorption but not for extinction. The structure was solved by a combination of heavy atom and direct methods with SHELX-86 and refined with SHELXL-93 / SHELXL-97 [40-41]. Crystal data are in Table 3.1-4 and important interatomic distances and angles in Table 3.3

Table 3.1 Crystal data and structure refinement for $[Cu(2\text{-pico})_3]\cdot H_2O$	
Identification code	bmr-3
Empirical formula	$C_{12}H_{12}CuN_2O_6$
Formula weight	343.79
Temperature	293(2) K
Wavelength	0.71073 Å
Crystal system	Triclinic
Space group	P-1
Unit cell dimensions	a = 5.1325(4) Å
	b = 7.6402(8) Å
	c = 9.2404(9) Å
	$\alpha = 74.933(9)^\circ$.

	$\beta = 84.370(7)^\circ$
	$\gamma = 71.494(8)^\circ$
Volume	331.75(5) Å ³
Z	2
Density (calculated)	1.721 Mg/m ³
Absorption coefficient	1.676 mm ⁻¹
F(000)	175
Crystal size	0.60 x 0.22 x 0.20 mm ³
Theta range for data collection	3.23 to 26.37°
Index ranges	-4 ≤ h ≤ 6, -8 ≤ k ≤ 9, -11 ≤ l ≤ 11
Reflections collected	2166
Independent reflections	1365 [R(int) = 0.0223]
Completeness to theta = 26.37°	99.6 %
Absorption correction	Semi-empirical from equivalents
Max. and min. transmission	1.000 and 0.76854
Refinement method	Full-matrix least-squares on F ²
Data / restraints / parameters	1365 / 1 / 108
Goodness-of-fit on F ²	1.105
Final R indices [I > 2σ(I)]	R1 = 0.0310, wR2 = 0.0791
R indices (all data)	R1 = 0.0314, wR2 = 0.0795
Largest diff. peak and hole	0.288 and -0.385 e.Å ⁻³

Table 3.2 Atomic coordinates ($\times 10^4$) and equivalent isotropic displacement parameters ($\text{\AA}^2 \times 10^3$)

For $[\text{Cu}(\text{2-pico})_3] \cdot \text{H}_2\text{O}$, $U(\text{eq})$ is defined as one third of the trace of the orthogonalized U_{ij} tensor.

x	y	z	U(eq)	
Cu(1)	5000	0	10000	28(1)
O(1)	1698(3)	406(2)	11255(2)	31(1)
O(3)	2638(7)	9553(7)	5589(4)	90(1)
N(2)	2810(4)	2306(3)	8610(2)	26(1)
O(2)	-2715(3)	2142(3)	11166(2)	37(1)
C(3)	-707(6)	5682(4)	7069(3)	40(1)
C(4)	-1556(5)	4685(3)	8420(3)	34(1)
C(5)	278(4)	3003(3)	9158(3)	26(1)
C(1)	3600(5)	3244(4)	7290(3)	34(1)
C(2)	1878(6)	4949(4)	6501(3)	41(1)
C(6)	-359(4)	1789(3)	10646(3)	26(1)

Table 3.3 Bond lengths [\AA] and angles [$^\circ$] for $[\text{Cu}(\text{2-pico})_3] \cdot \text{H}_2\text{O}$

Cu(1)-O(1)	1.9447(16)	Cu(1)-O(1)#1	1.9447(16)
Cu(1)-N(2)#1	1.9664(18)	Cu(1)-N(2)	1.9664(18)
O(1)-C(6)	1.283(3)	N(2)-C(1)	1.342(3)
N(2)-C(5)	1.342(3)	O(2)-C(6)	1.230(3)
C(3)-C(2)	1.376(4)	C(3)-C(4)	1.392(4)
C(4)-C(5)	1.380(3)	C(5)-C(6)	1.516(3)
C(1)-C(2)	1.382(4)		
O(1)-Cu(1)-O(1)#1	180.0	O(1)-Cu(1)-N(2)#1	96.28(7)
O(1)#1-Cu(1)-N(2)#1	83.72(7)	O(1)-Cu(1)-N(2)	83.72(7)
O(1)#1-Cu(1)-N(2)	96.28(7)	N(2)#1-Cu(1)-N(2)	180.0
C(6)-O(1)-Cu(1)	114.61(15)	C(1)-N(2)-C(5)	119.6(2)

C(1)-N(2)-Cu(1)	128.16(16)	C(5)-N(2)-Cu(1)	112.14(15)
C(2)-C(3)-C(4)	119.5(2)	C(5)-C(4)-C(3)	118.1(2)
N(2)-C(5)-C(4)	122.2(2)	N(2)-C(5)-C(6)	114.11(18)
C(4)-C(5)-C(6)	123.7(2)	N(2)-C(1)-C(2)	121.1(2)
C(3)-C(2)-C(1)	119.4(2)	O(2)-C(6)-O(1)	125.0(2)
O(2)-C(6)-C(5)	120.13(19)	O(1)-C(6)-C(5)	114.86(19)

Symmetry transformations used to generate equivalent atoms: #1 -x+1,-y,-z+2

table3.4. Anisotropic displacement parameters ($\text{\AA}^2 \times 10^3$) for $[\text{Cu}(\text{2-pico})_3] \cdot \text{H}_2\text{O}$. The anisotropic displacement factor exponent takes the form: $-2\pi^2 [h^2 a^*^2 U^{11} + \dots + 2 h k a^* b^* U^{12}]$

U¹¹ U²² U³³ U²³ U¹³ U¹²

Cu(1)	17(1)	28(1)	29(1)	-1(1)	2(1)	0(1)
O(1)	22(1)	32(1)	30(1)	-2(1)	3(1)	-1(1)
O(3)	81(2)	133(3)	46(2)	14(2)	0(2)	-48(2)
N(2)	20(1)	28(1)	29(1)	-6(1)	0(1)	-5(1)
O(2)	20(1)	42(1)	42(1)	-10(1)	9(1)	0(1)
C(3)	42(2)	30(1)	39(1)	1(1)	-13(1)	-2(1)
C(4)	25(1)	31(1)	41(1)	-12(1)	-5(1)	1(1)
C(5)	22(1)	26(1)	29(1)	-9(1)	-2(1)	-5(1)
C(1)	28(1)	40(1)	30(1)	-4(1)	3(1)	-9(1)
C(2)	43(2)	42(1)	32(1)	3(1)	-2(1)	-14(1)
C(6)	23(1)	27(1)	30(1)	-11(1)	2(1)	-5(1)

3.4 Crystal structure

3.4.1 Crystal structure of [Cu (2-pico)₃].H₂O

Dark blue crystals of the compound [Cu (2-pico)₃].H₂O are crystallized in triclinic space group *P*-1. Thermal ellipsoidal diagram of the compound is [Cu (2-pico)₃].H₂O shown in Figure 3.1, in which the relevant asymmetric unit contains half of the molecule represented by labeled atoms. The corresponding bond angles and bond lengths are given in the Table 3.3. The copper sites exhibit distorted octahedral geometry, in which apical positions are occupied by two oxygen atoms (linked through the acetate from the picolate moiety), and the four bonds (oxygen, and nitrogen) are ascribed from the two molecules of the carboxylate picolate molecule. Bond lengths (O1---Cu---O1 and N2---Cu---N2) in the square part of copper are 1.944 Å, and 1.966 Å respectively. The apical bond length is (O2---Cu---O2) 2.756 Å. This data clearly indicates that the two apical oxygen atoms are far in distance, because the link-up of oxygen atoms are available with two other picolate molecules. The bond angle (N2-Cu1-O1) in the five-member chelate ring (Cu1N2C5C6O1) is 83.74° figure 3.2, the two planes of these chelate rings are in same plane, and hence the bond angle is zero, whereas the two picolate moieties are slightly deviates from the respective plane of the chelate ring. Packing of the crystal lattice showing 1-D layered polymeric architecture along the “c” axis, in the Figure 3.3. View of the crystal lattice showing of the 3-D H-bonded metal-organic framework along the “a” axis in the Figure 3.4. Coming to the crystal lattice showing 2-D H-bonded coordination polymer forms supra molecular synthon of Cu(II)-Picolate Figure 3.5. View of the crystal packing showing: (a) 1-D zig-zag water chain between the host networks with C-H...O Interactions Figure 3.6. View of the crystal packing showing 2 fold water bridged chain between the host networks with C-H...O Interactions Figure 3.7. View of the crystal packing showing ball sticking model of 2 fold water bridged chain between the host networks with C-H...O Interactions in the Figure 3.8. View of the crystal packing showing ball sticking model of

3 fold water rectangular chain between the host network with C-H...O Interactions Figure 3.9. View of the crystal lattice showing two fold zig-zag water chain between the host network with C6-H3...O1 Interactions (2.271-2.940 Å) Figure 3.10.

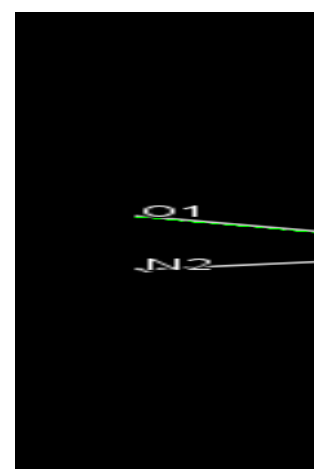
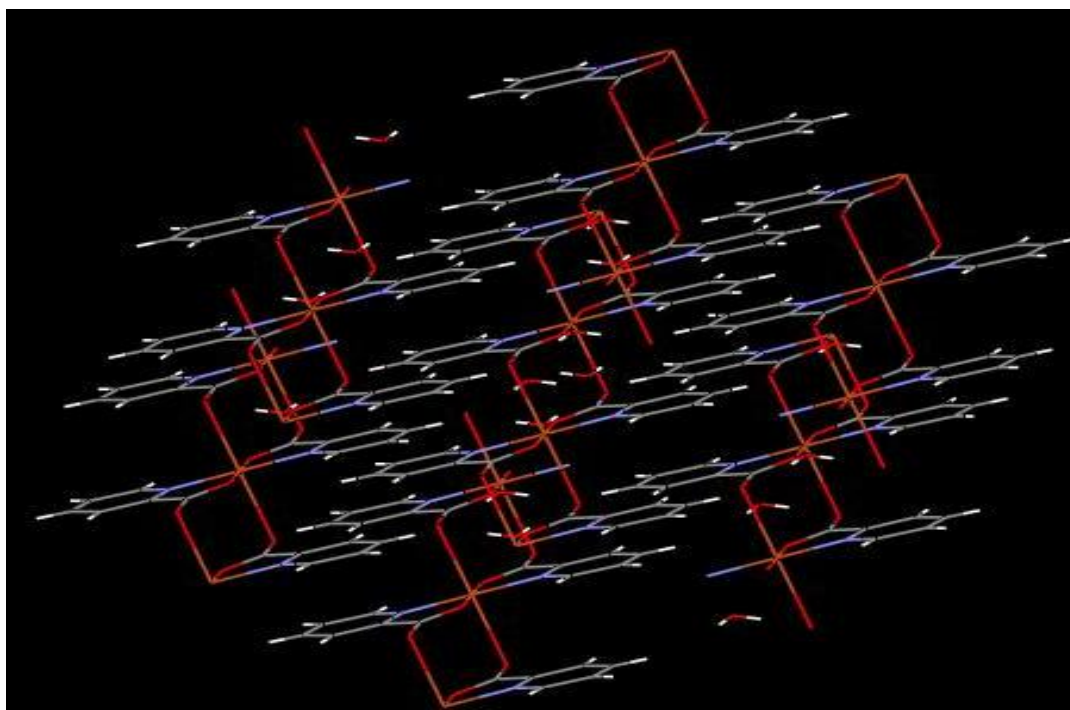
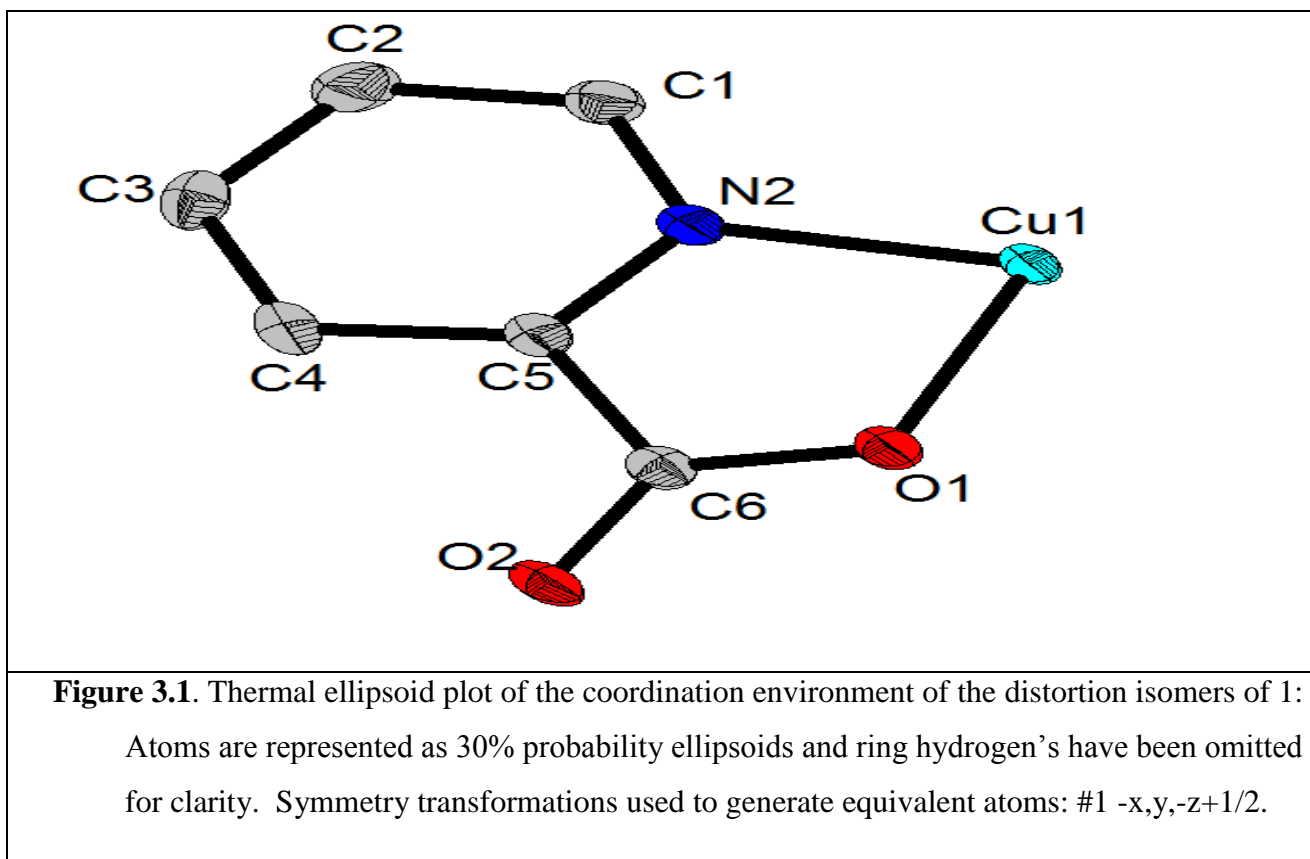


Fig 3.2

Coordination environment of the Copper(II) ion

Figure 3.3 View of the crystal lattice showing 1-D layered polymeric architecture along the “c” axis.

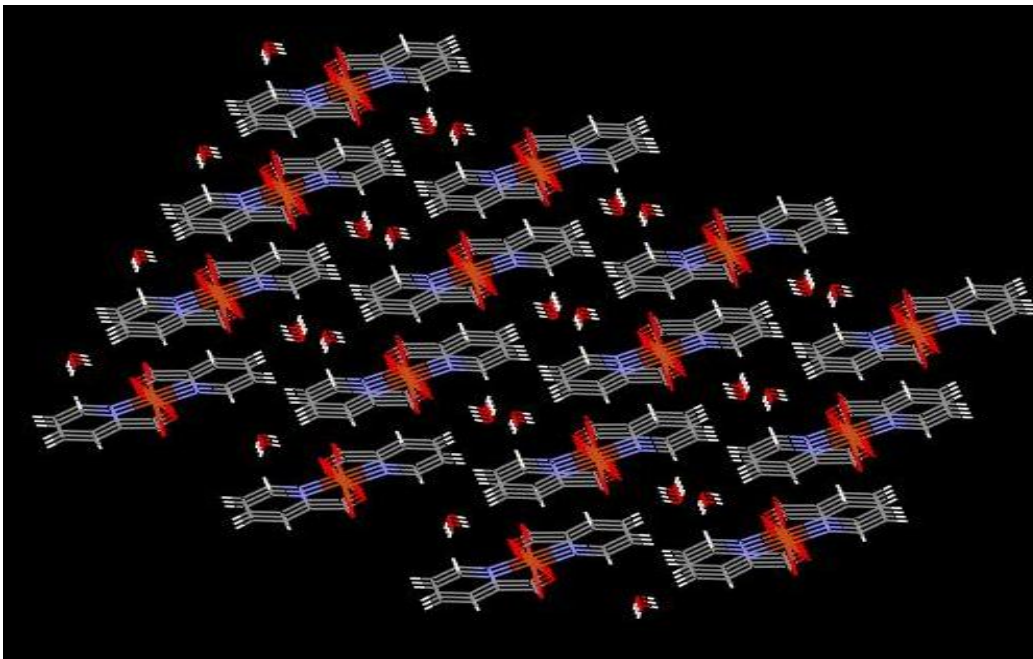


Fig 3.4 View of the crystal lattice showing of the 3-D H-bonded metal-organic axis metal-organic framework along the “a” axis

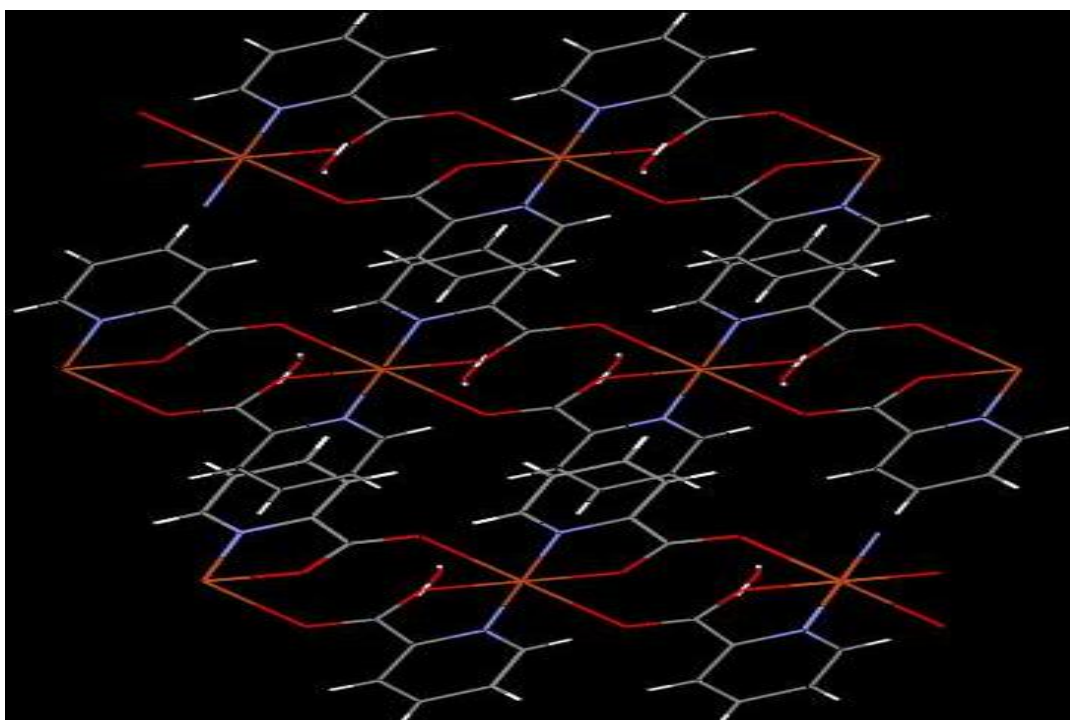


Fig 3.5 View of the crystal lattice showing 2-D H-bonded coordination polymer forms supra

molecular synthon of Cu(II)-Picolinate.

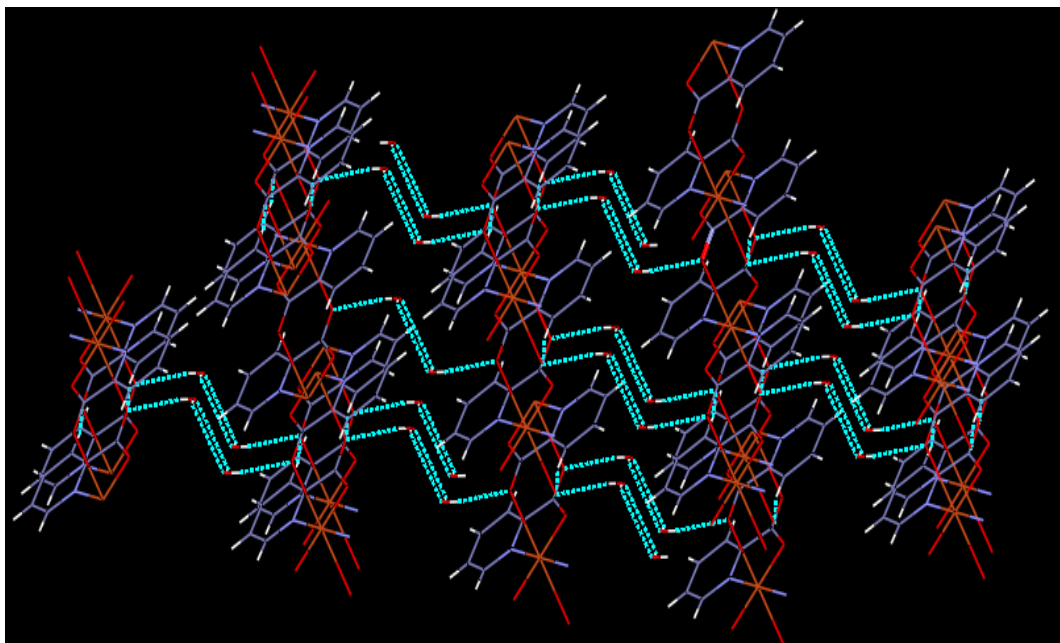


Fig 3.6 View of the crystal lattice showing: (a) 1-D zig-zag water chain between the host networks with C-H....O Interactions

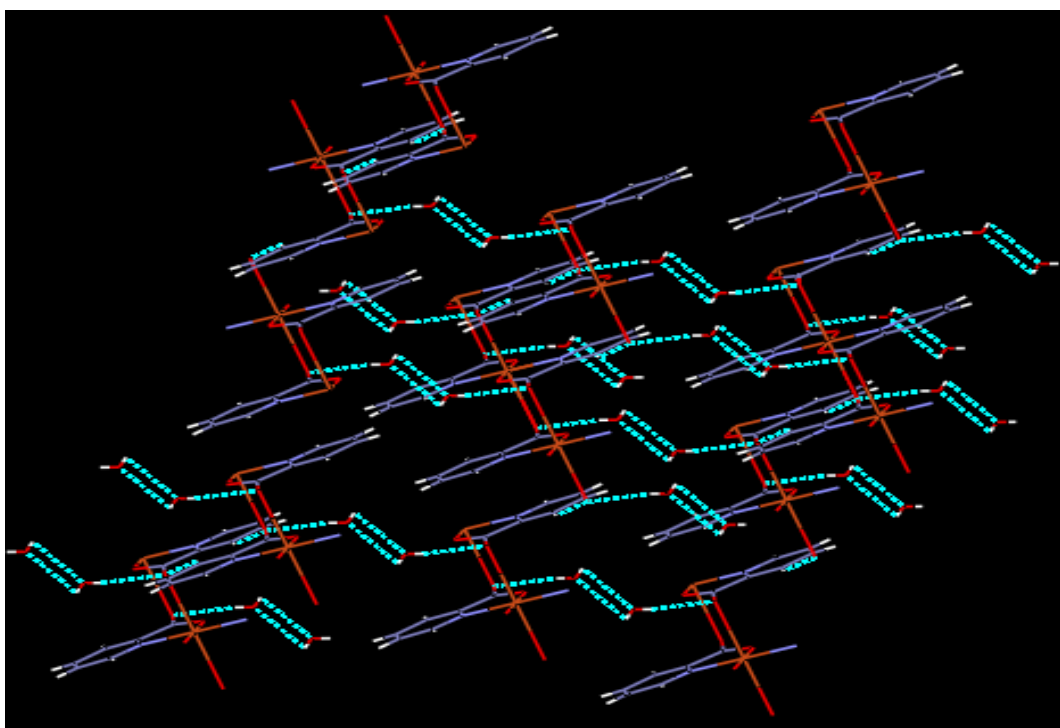


Fig 3.7 View of the crystal packing showing 2 fold water bridged chain between the host networks with C-H....O Interactions

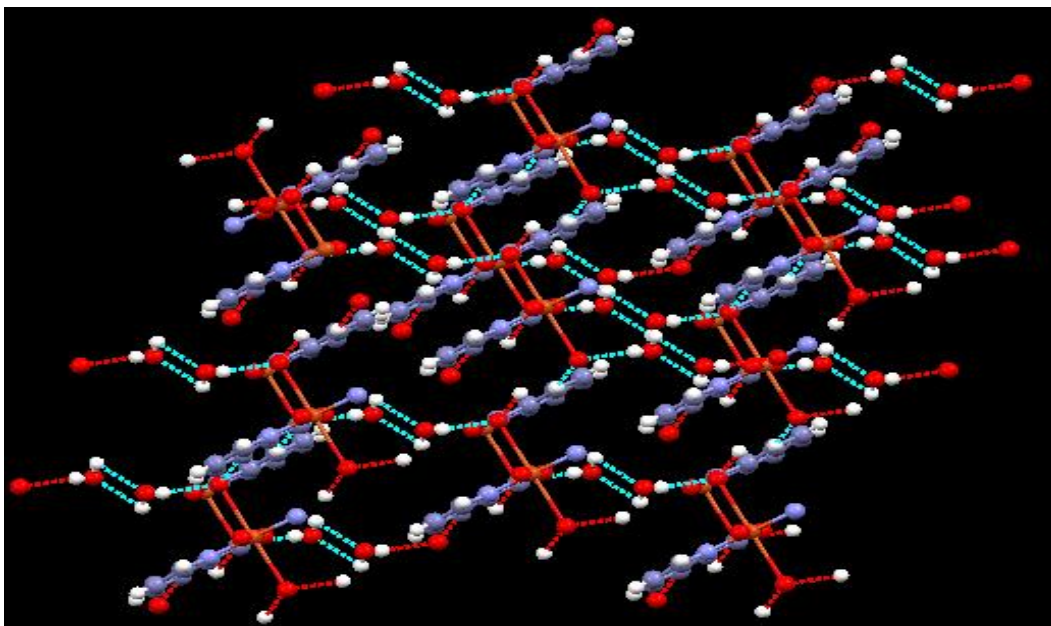


Fig 3.8 View of the crystal packing showing ball sticking model of 2 fold water bridged chain between the host networks with C-H....O Interactions

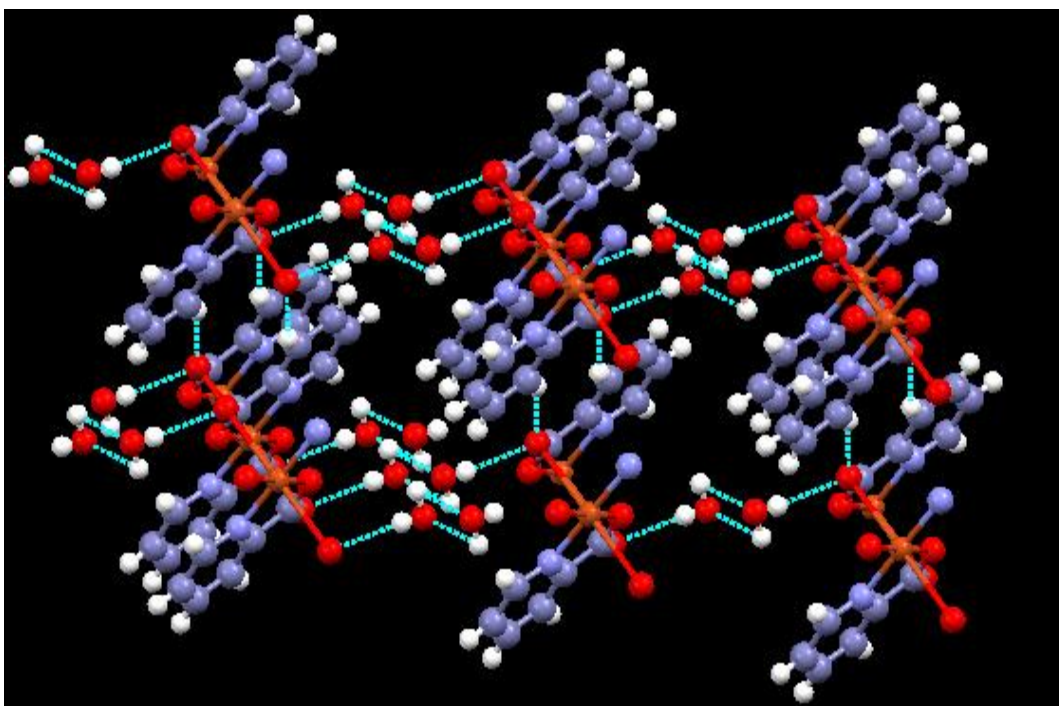


Fig 3.9 View of the crystal packing showing ball sticking model of 3 fold water rectangular chain between the host networks with C-H....O Interactions

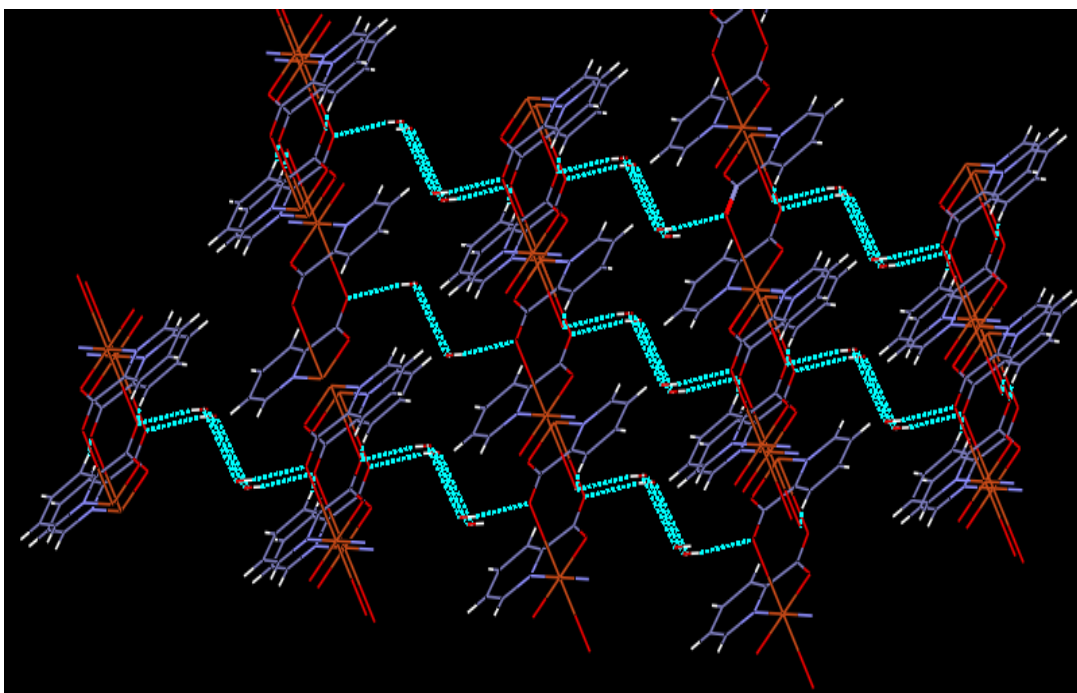


Fig 3.10 View of the crystal lattice showing two fold zig-zag water chain between the host network with C-H...O Interactions

3.4.2 IR- spectrum of [Cu (2-picO)₃]. H₂O

The FT-IR spectrum of 2-picolinic acid complex is given in Figure 3.11 IR spectra of the free ligand reveals that extensive changes in frequencies have occurred which can conclude the coordination sites in chelation. A large intense absorption band around 3438 cm^{-1} can be assigned to stretching vibration of hydroxyl from the uncoordinated water molecules. The bands related to the stretching vibration of the C-H and C=N are situated at 3076 cm^{-1} and 1641 cm^{-1} , respectively. The vibration peak originate in the 1473 cm^{-1} region is assigned to the stretching vibration of the C=C-C=C bond. The dissimilarity value of 254 cm^{-1} between the asymmetric (1602 cm^{-1}) and symmetric (1348 cm^{-1}) stretching vibration of the carboxylate group is in line with a mono dentate type of coordination [44-46]. The band consequent to the stretching vibration of the C=O group of the Hpic monomer is situated at $1700\text{--}1769\text{ cm}^{-1}$ and disappears in the complex. The IR spectra of picolinic acid contain broad absorption bands at 2607 cm^{-1} and 2152 cm^{-1} and specify the existence of O-H...N type of intermolecular hydrogen bonding, but it disappears in the complex whose recognizable fact

confirms that the nitrogen atom is coordinated to the Copper ion. The absorption peaks at 776 cm^{-1} and 694 cm^{-1} for the complex are assigned to deformation vibration of the pyridine ring which confirms that the pyridyl N atom and carboxyl O atom are coordinated with the center Copper(II) ion. The absorption peak found in the 457 cm^{-1} region is assigned to the Cu–N bond and in the 404 cm^{-1} region is assigned to the Cu–O bond [47]

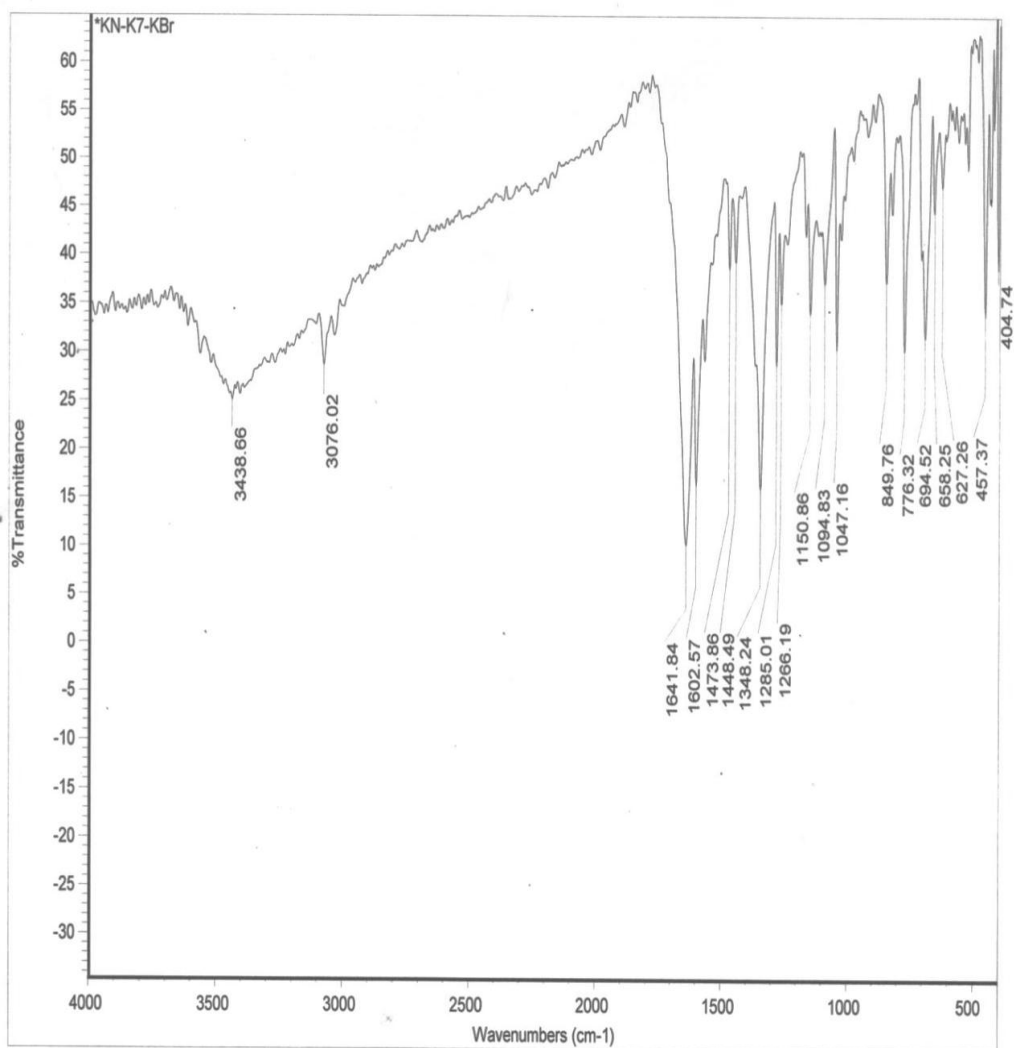


Fig 3.11 IR-spectrum of [Cu (2-pico)₃]. H₂O

3.4.3 Electronic spectrum of [Cu (2-pico)₃]. H₂O

The complex has a shoulder broad band at 240 and 280 nm may be assigned to the following charge transfer from metal to ligand. This result confirms the complexation of metal ions via carboxylate group. The electronic configuration of copper (II) complex was d^9 which confirms the

absence of any d-d electronic transitions. Nevertheless, the absorption bands in their spectra were suffered from red and blue shift with hyper chromic effects [42-43].

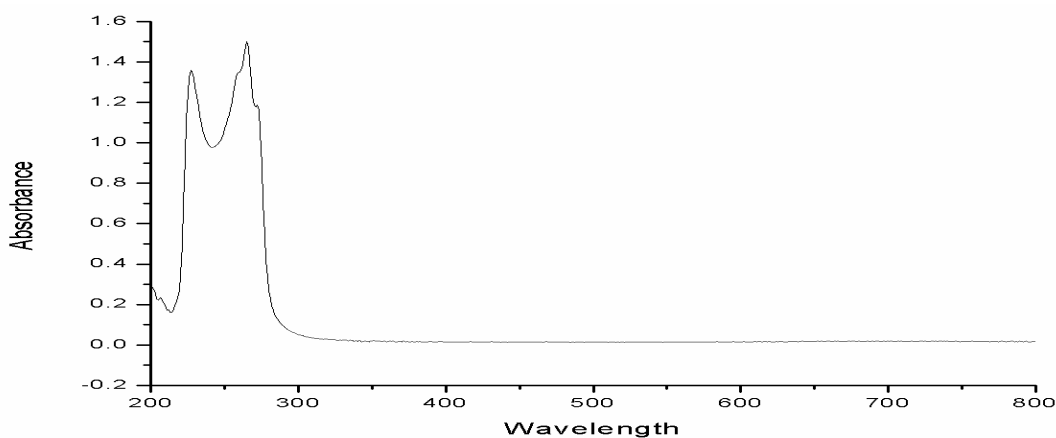


Fig 3.12 Electronic spectrum of [Cu (2-pico)₃]. H₂O

3.4.4 Fluorescent emission spectrum of [Cu (2-pico)₃].H₂O

Even more significant fluorescence enhancement has been observed for Copper. The emission spectra of bare copper-picolinic acid complex are shown in Figure 3.12 respectively. The intensity of main visible emission lines of Copper picolonic acid observed, at 530 nm increased in the presence of picolonic acid. Transition showed hyper sensitivity, which is in agreement with previous observations of copper complexes, exhibited enhanced fluorescence when complexes with picolonic acid. The emission spectrum of copper complexes were recorded at the excitation wavelength of 280 nm. No measureable fluorescence is observed for free picolonic acid bands observed at 211 and 264 nm is on excitation at this wavelength.

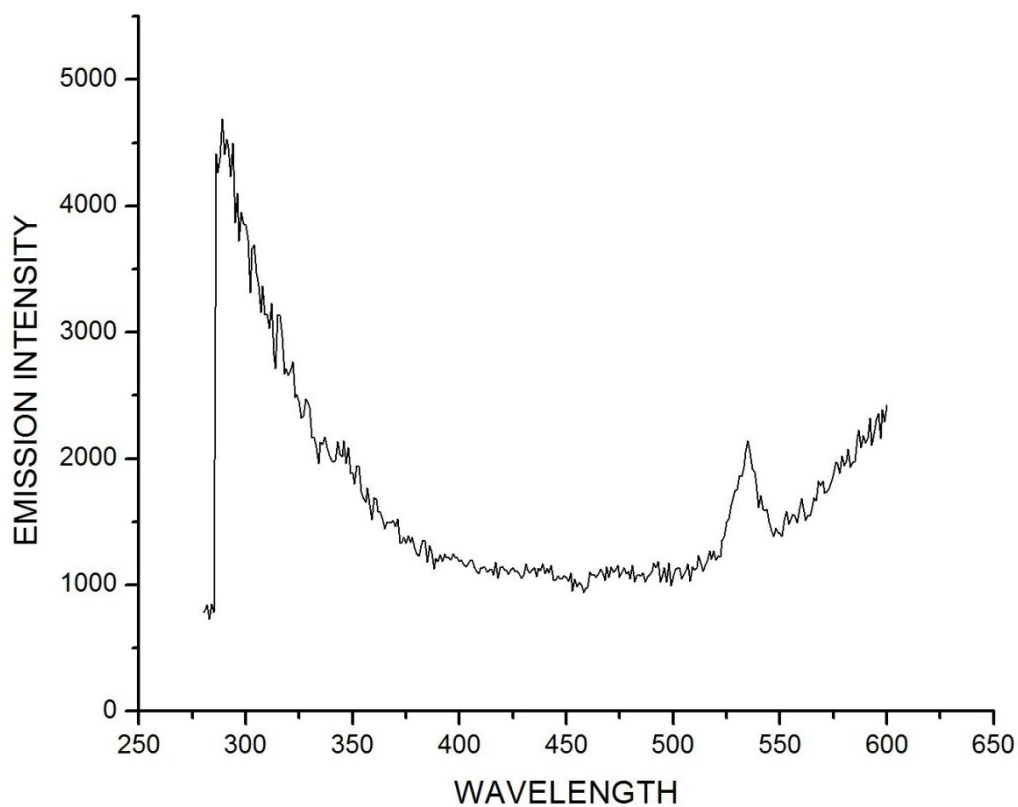


Fig 3.13 Fluorescent emission spectrum of [Cu (2-pico)₃]. H₂O

3.4.5 Powder X-Ray Diffractogram of [Cu (2-pico)₃].H₂O

The X-ray powder diffraction (XRD) measurement of the complex [Cu(2-pico)₃] H₂O is performed. The diffractogram obtained for complex is given in Fig. 3.14. From this data we calculated crystalline size and phase.

[Cu (2-pico) ₃ .H ₂ O] n]	2θ	FWHM	Crystallite size
9.902	0.102 ⁰	97.21nm	

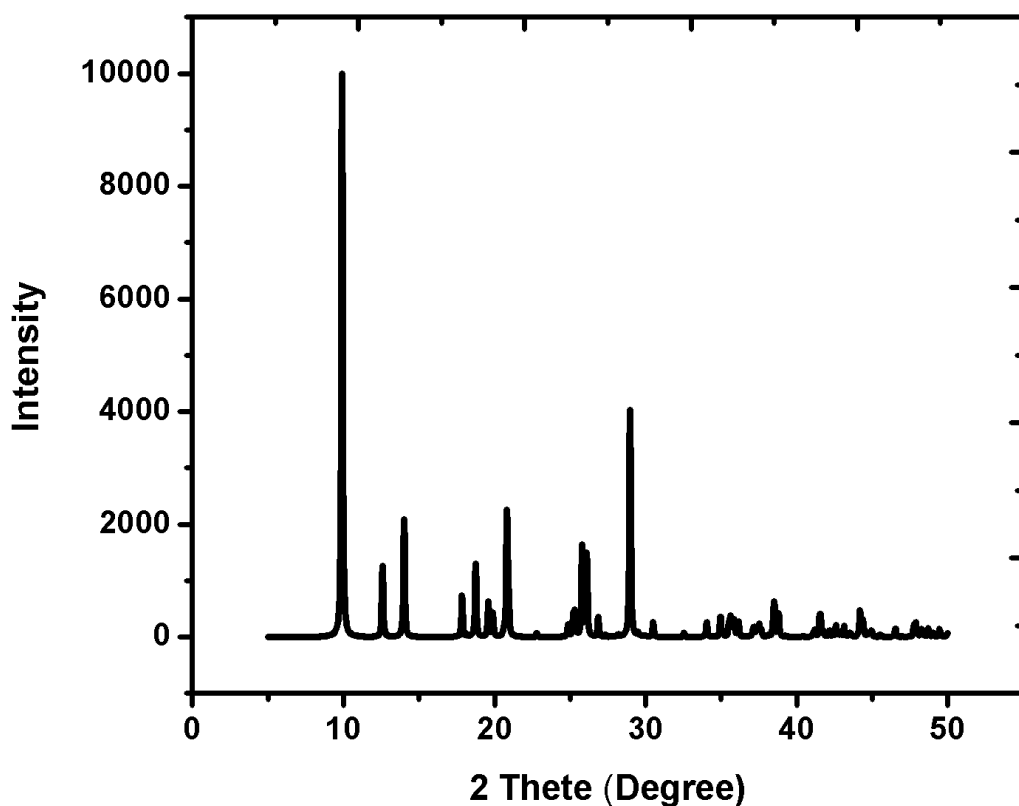
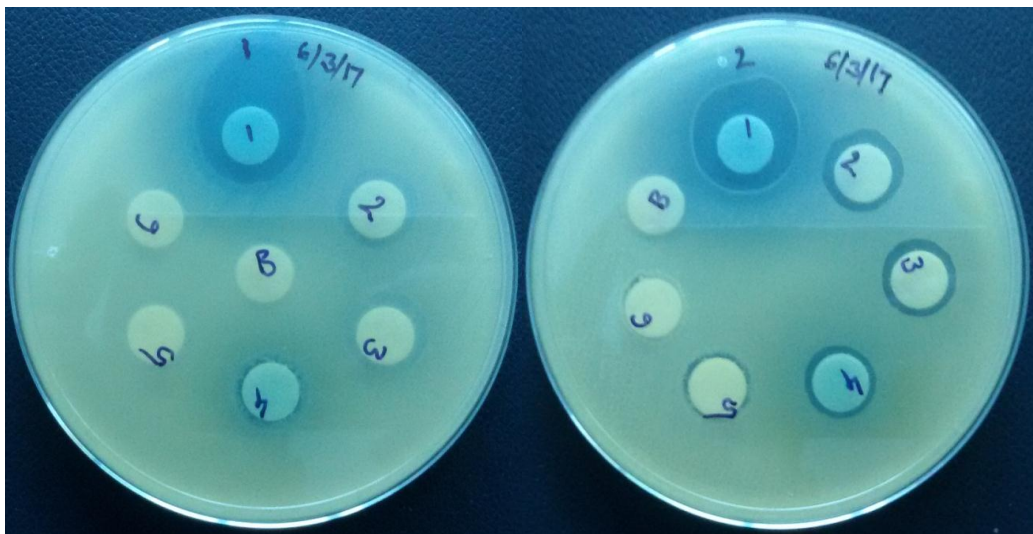


Fig 3.14The Powder X-Ray Diffractogram of [Cu (2-pico)₃]. H₂O

3.4.6 ANTI PATHOGENIC IN VITRO STUDIES OF [Cu (2-pico)₃.H₂O] n]

Antibacterial activity of sample [Cu(2-pico)₃.H₂O] n] is screened against 7 human pathogenic bacteria's such as Staphylococcus aureus MTCC 96, Pseudomonas aeruginosa MTCC 3216, Proteus mirabilis MTCC 1429, Vibrio cholera MTCC 3905, Escherichia coli MTCC 443, Shigella flexneri MTCC 1457 and Micrococcus luteus MTCC 106. The Anti Pathogenic screening data of crystal structure is summarized in the Table 3.5.

Human Pathogens	Staphylococcus aureus	Pseudomonas aeruginosa	Proteus mirabilis	Vibrio cholerae	Escherichia coli	Shigella flexneri	Micrococcus luteus
Inhibition Zone (mm)	1	12	12	12	14	12	14



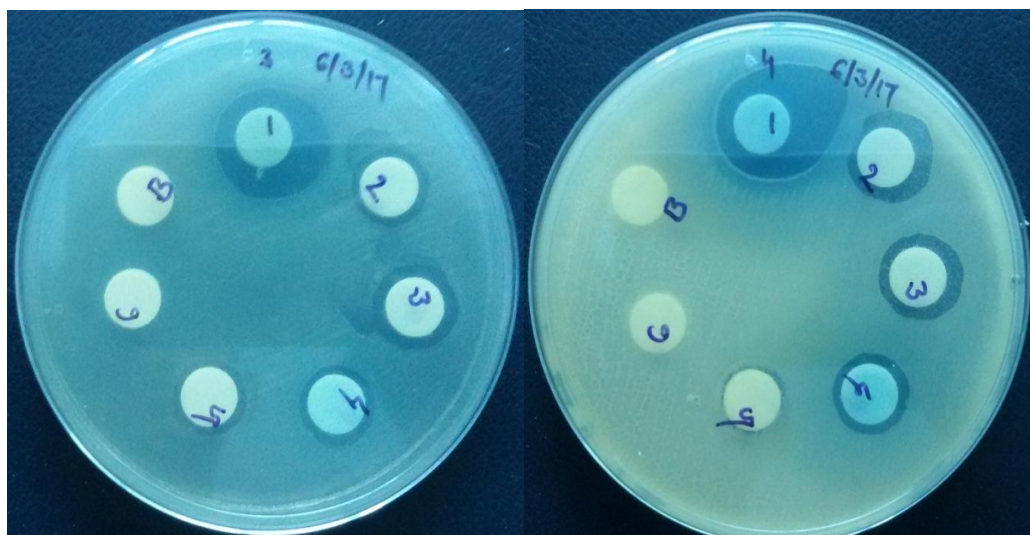


Fig 3.15 Inhibition zones for $[\text{Cu}(2\text{-pico})_3] \cdot \text{H}_2\text{O}(4)$ against *Staphylococcus aureus*, *Pseudomonas aeruginosa*, *Proteus mirabilis* and *Vibrio cholera*.

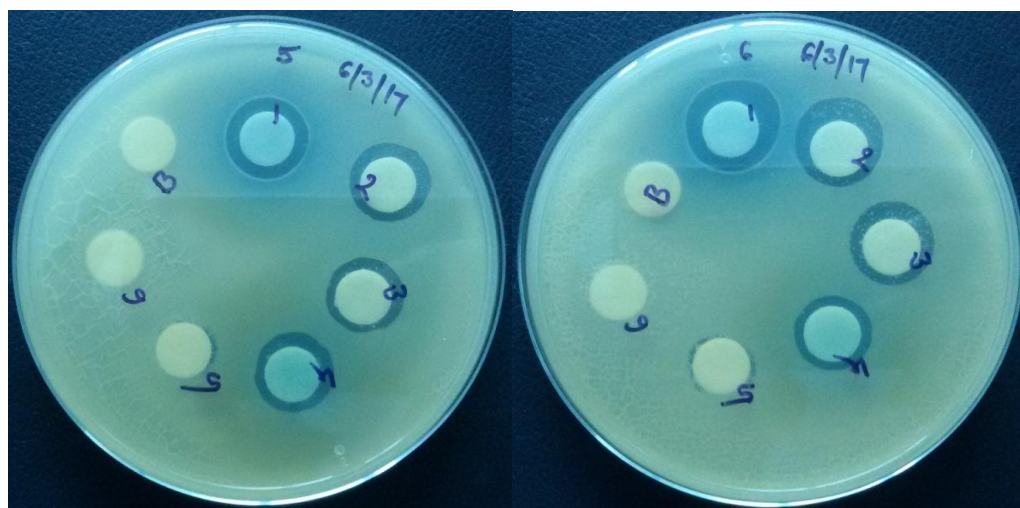


Fig3.16 Inhibition zones for [Cu (2-pico)₃].H₂O(4) against Escherichia coli, ShigellaFlexineri and Micrococcusluteus.

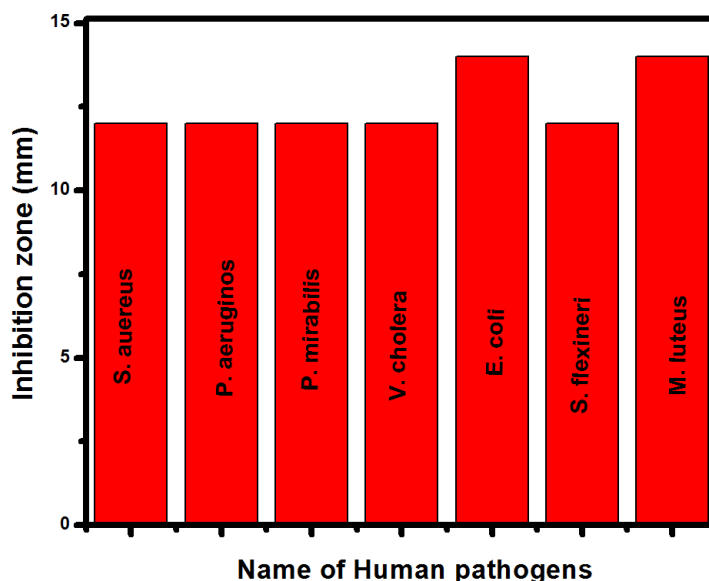


Fig 3.17 Bar chart of Anti-pathogenic activities

From the above bar chart we explained that, the Anti-pathogenic activity is good for the tested microorganisms such as Escherichia coli and Micrococcusluteus, the obtained inhibition zones are 14 mm and 14 mm. The five organisms showed low activity they are Staphylococcus aureus, Pseudomonas aeruginosa, Proteus mirabilis, Vibrio cholera and Shigella flexineri. The obtained inhibition zones are 12 mm, 12 mm, 12 mm, 12 mm and 12 mm. Based on this data, the particular sample is showed moderate activity towards the above mentioned antipathogens.

3.5 SYNTHESIS OF [Cu (2-picolonate)₂ H₂O]

An 5 mL methanol solution of Copper per chlorate hex hydrate (0.370g, 1.0 m mole) prepared in a beaker to this added 10 mL methanol solution of 2,2 Bipyridine (0.156g, 1.0 m mole) with stirring condition the colour change from water shoot to blue lagoon. Then stirring continuo's to 20 min after added 2-picolinic acid of 5 ml aqua solution (0.123g, 1.0 m mole) to above mixture solution, the stirring continuous up to 30 min the colour change blue lagoon to mogul green colour obtained. The precipitated is formed; Wash the precipitate with distilled water and methanol. The filtrate solution was left out at room temperature in the slow evaporation process we got a green coloured

crystals. These crystals are suitable for single crystal X-rd. Calculated amount of yield is 70%. Anal calcd for $C_{13}H_{13}CuN_2O_5$ (Mol.wt: 340.8): C, 45.82; H, 3.84; Cu, 18.65; N, 8.22; O, 23.47 Found: C, 45.50; H, 3.87; Cu, 18.55; N, 8.22; O, 23.40 IR absorptions (KBr disk, cm^{-1}) 3398, 3073, 1631, 1475, 1352, 771, 698, 455, 425.

3.5.1 X-ray Crystallographic data collection and structure determination

A single crystal of approximate dimensions 0.12 x 0.8 x 0.4 mm was mounted. The data collection was done on an EnrafNonius CAD-4 diffract meter using Mo $K\alpha$ radiation. The data were corrected for absorption but not for extinction. The structures were solved by a combination of heavy atom and direct methods with SHELX-86 and refined with SHELXL-93 / SHELXL-97 [40-41]. Crystal data are in Table 3.6-9 and important interatomic distances and angles in Table 3.8

Table 3.6 Crystal data and structure refinement for $[Cu(2\text{-picolonate})_2 \cdot H_2O]$	
Identification code	databkb1
Empirical formula	$C_{12}H_{10}CuN_2O_5$
Formula weight	325.76
Temperature	446(2) K
Wavelength	0.71073 Å
Crystal system	Orthorhombic
Space group	Pbca
Unit cell dimensions	a = 12.778(9) Å
	b = 12.926(10) Å
	c = 14.938(11) Å
	$\alpha = 90^\circ$.
	$\beta = 90^\circ$.
	$\gamma = 90^\circ$.
Volume	2467(3) Å ³
Z	8
Density (calculated)	1.754 Mg/m ³
Absorption coefficient	1.792 mm ⁻¹

F(000)	1320
Crystal size	0.30 x 0.28 x 0.25 mm ³
Theta range for data collection	2.73 to 26.37°.
Index ranges	-15<=h<=15, -16<=k<=16, -18<=l<=18
Reflections collected	21993
Independent reflections	2523 [R(int) = 0.0920]
Completeness to theta = 26.37°	99.9 %
Absorption correction	Semi-empirical from equivalents
Max. and min. transmission	0.6629 and 0.6155
Refinement method	Full-matrix least-squares on F ²
Data / restraints / parameters	2523 / 0 / 189
Goodness-of-fit on F ²	1.231
Final R indices [I>2sigma(I)]	R1 = 0.0471, wR2 = 0.1352
R indices (all data)	R1 = 0.0506, wR2 = 0.1379
Largest diff. peak and hole	0.400 and -0.731 e.Å ⁻³

Table 3.7 Atomic coordinates ($\times 10^4$) and equivalent isotropic displacement parameters ($\text{\AA}^2 \times 10^3$) For[Cu(2-picolonate)₂ H₂O]. U(eq) is defined as one third of the trace of the orthogonalized U^{ij} tensor.

x	y	z	U(eq)
---	---	---	-------

Cu(1)	8522(1)	6405(1)	5018(1)	30(1)
C(7)	6387(3)	6166(3)	4891(2)	34(1)
O(3)	7178(2)	6369(2)	4395(2)	38(1)
N(2)	7657(2)	6093(2)	6087(2)	30(1)
O(1)	9872(2)	6123(2)	5595(1)	34(1)
C(1)	10665(3)	6110(3)	5059(2)	28(1)
N(1)	9394(2)	6563(2)	3929(2)	29(1)
C(3)	11161(3)	6431(3)	3415(2)	34(1)
C(12)	7956(3)	5975(3)	6944(2)	38(1)
C(4)	10836(3)	6661(3)	2550(2)	39(1)

C(5)	9784(3)	6853(3)	2387(2)	39(1)
C(11)	7248(3)	5780(3)	7625(2)	43(1)
C(6)	9086(3)	6801(3)	3095(2)	36(1)
C(10)	6203(3)	5678(3)	7410(2)	44(1)
C(9)	5885(3)	5774(3)	6524(2)	40(1)
C(8)	6634(2)	5997(2)	5876(2)	30(1)
O(4)	5476(2)	6120(3)	4628(2)	56(1)
O(2)	11571(2)	5874(2)	5274(2)	42(1)
O(5)	8447(2)	8181(2)	5289(2)	51(1)
C(2)	10419(2)	6385(2)	4092(2)	27(1)

Table 3.8 Bond lengths [Å] and angles [°] for [Cu (2-picolonate)₂ H₂O].

		Cu(1)-O(3)	1.954(3)
Cu(1)-O(1)	1.963(2)	Cu(1)-N(1)	1.983(3)
Cu(1)-N(2)	1.983(3)	Cu(1)-O(5)	2.333(4)
C(7)-O(4)	1.230(4)	C(7)-O(3)	1.281(4)
C(7)-C(8)	1.519(5)	N(2)-C(12)	1.345(4)
N(2)-C(8)	1.351(4)	O(1)-C(1)	1.291(4)
C(1)-O(2)	1.239(4)	C(1)-C(2)	1.521(4)
N(1)-C(6)	1.342(4)	N(1)-C(2)	1.351(4)
C(3)-C(2)	1.388(5)	C(3)-C(4)	1.390(5)
C(3)-H(3)	0.9300	C(12)-C(11)	1.384(5)
C(12)-H(12)	0.9300	C(4)-C(5)	1.389(5)
C(4)-H(4)	0.9300	C(5)-C(6)	1.385(5)
C(5)-H(5)	0.9300	C(11)-C(10)	1.380(6)
C(11)-H(11)	0.9300	C(6)-H(6)	0.9300
C(10)-C(9)	1.389(5)	C(10)-H(10)	0.9300
C(9)-C(8)	1.392(5)	C(9)-H(9)	0.9300
O(5)-H(5A)	1.00(6)	O(5)-H(5B)	0.87(6)
O(3)-Cu(1)-O(1)	167.75(11)		
O(3)-Cu(1)-N(1)	96.05(11)	O(1)-Cu(1)-N(1)	83.42(11)

O(3)-Cu(1)-N(2)	83.62(11)	O(1)-Cu(1)-N(2)	95.66(11)
N(1)-Cu(1)-N(2)	174.16(10)	O(3)-Cu(1)-O(5)	94.05(10)
O(1)-Cu(1)-O(5)	98.21(10)	N(1)-Cu(1)-O(5)	93.68(12)
N(2)-Cu(1)-O(5)	92.16(12)	O(4)-C(7)-O(3)	124.9(3)
O(4)-C(7)-C(8)	119.9(3)	O(3)-C(7)-C(8)	115.2(3)
C(7)-O(3)-Cu(1)	115.0(2)	C(12)-N(2)-C(8)	119.2(3)
C(12)-N(2)-Cu(1)	129.1(2)	C(8)-N(2)-Cu(1)	111.7(2)
C(1)-O(1)-Cu(1)	114.81(19)	O(2)-C(1)-O(1)	125.1(3)
O(2)-C(1)-C(2)	119.8(3)	O(1)-C(1)-C(2)	115.1(3)
C(6)-N(1)-C(2)	119.4(3)	C(6)-N(1)-Cu(1)	128.4(2)
C(2)-N(1)-Cu(1)	112.3(2)	C(2)-C(3)-C(4)	118.8(3)
C(2)-C(3)-H(3)	120.6	C(4)-C(3)-H(3)	120.6
N(2)-C(12)-C(11)	122.3(3)	N(2)-C(12)-H(12)	118.9
C(11)-C(12)-H(12)	118.9	C(5)-C(4)-C(3)	119.4(3)
C(5)-C(4)-H(4)	120.3	C(3)-C(4)-H(4)	120.3
C(6)-C(5)-C(4)	118.8(3)	C(6)-C(5)-H(5)	120.6
C(4)-C(5)-H(5)	120.6	C(10)-C(11)-C(12)	118.6(3)
C(10)-C(11)-H(11)	120.7	C(12)-C(11)-H(11)	120.7
N(1)-C(6)-C(5)	122.1(3)	N(1)-C(6)-H(6)	119.0
C(5)-C(6)-H(6)	119.0	C(11)-C(10)-C(9)	119.7(3)
C(11)-C(10)-H(10)	120.2	C(9)-C(10)-H(10)	120.2
C(10)-C(9)-C(8)	118.7(3)	C(10)-C(9)-H(9)	120.6
C(8)-C(9)-H(9)	120.6	N(2)-C(8)-C(9)	121.4(3)
N(2)-C(8)-C(7)	114.4(3)	C(9)-C(8)-C(7)	124.1(3)
Cu(1)-O(5)-H(5A)	115(3)	Cu(1)-O(5)-H(5B)	114(3)
H(5A)-O(5)-H(5B)	105(5)	N(1)-C(2)-C(3)	121.6(3)
N(1)-C(2)-C(1)	114.3(3)	C(3)-C(2)-C(1)	124.1(3)

Symmetry transformations used to generate equivalent atoms:

Table 3.9 Anisotropic displacement parameters ($\text{\AA}^2 \times 10^3$) for $[\text{Cu}(\text{2-picolonate})_2 \cdot \text{H}_2\text{O}]$. The anisotropic

displacement factor exponent takes the form: $-2\pi^2 [h^2 a^{*2} U^{11} + \dots + 2 h k a^* b^* U^{12}]$

	U11	U22	U33	U23	U13	U12
Cu(1)	17(1)	52(1)	22(1)	3(1)	1(1)	2(1)
C(7)	25(2)	41(2)	34(2)	1(1)	1(1)	0(1)
O(3)	23(1)	64(2)	28(1)	6(1)	-2(1)	1(1)
N(2)	24(1)	40(1)	25(1)	0(1)	1(1)	1(1)
O(1)	21(1)	57(1)	25(1)	4(1)	-2(1)	0(1)
C(1)	19(2)	39(2)	27(2)	2(1)	-2(1)	-1(1)
N(1)	21(1)	40(1)	26(1)	2(1)	1(1)	3(1)
C(3)	26(2)	45(2)	32(2)	-1(1)	5(1)	0(1)
C(12)	31(2)	54(2)	29(2)	-1(1)	-1(1)	-1(1)
C(4)	36(2)	51(2)	29(2)	-1(1)	8(1)	-4(2)
C(5)	41(2)	51(2)	25(2)	3(1)	-2(1)	1(2)
C(11)	48(2)	56(2)	26(2)	1(1)	2(1)	2(2)
C(6)	28(2)	50(2)	28(2)	3(1)	-3(1)	3(1)
C(10)	42(2)	51(2)	37(2)	1(2)	16(2)	-3(2)
C(9)	28(2)	47(2)	43(2)	0(2)	8(1)	-4(1)
C(8)	23(1)	34(2)	32(2)	-2(1)	2(1)	0(1)
O(4)	25(1)	95(2)	48(2)	12(2)	-7(1)	-6(1)
O(2)	22(1)	66(2)	39(1)	9(1)	-3(1)	-1(1)
O(5)	26(1)	50(2)	77(2)	0(2)	-6(1)	2(1)
C(2)	22(1)	33(2)	27(1)	2(1)	-1(1)	-1(1)

3.6 Crystal structure

3.6.1 Crystal structure of [Cu (2-pico)₂ H₂O]

Dark blue crystals of the compound [Cu (2-picolonate)₂ H₂O] is crystallized in orthorhombic space group *Pbca*. Thermal ellipsoidal diagram of the compound is shown in Figure 3.18. The relevant asymmetric unit contains the full molecule represented by labeled atoms. The corresponding bond angles and bond lengths are given in the Table 3.8. Copper metal forms bond with two picolinate moieties and with one water molecule, leads to the five coordination around the copper metal. The bond lengths of the Cu–O₃, Cu–N₂, Cu–O₁, and Cu–N₁ (from the two chelate rings Cu₁N₁C₂C₁O₁, and Cu₁N₂C₈C₇O₃) are 1.954, 1.983, 1.963, and 1.983 Å respectively. Indicates, that the Cu–O bond is shorter than the Cu–N bond length, whereas in the apical link the bond length of Cu–O₅ is 2.333 Å which is higher than the above discussed bond length parameters. The angle between the two chelate rings (Cu₁N₁C₂C₁O₁, and Cu₁N₂C₈C₇O₃) is 14.63° in Figure 3.19, indicates these are deviated from the planar geometry. The bond angles in O₅–Cu–O₃, and O₅–Cu–O₁ are 94.04°, 98.21°, it gives an additional information that the two chelate rings are not in the same plane; hence the total angle is 192.25° rather than the angle 180°. C_g...C_g interactions are present with a distance of 3.981 Å. The relevant π-interactions have been shown in the Figure 3.20. A view of the supra molecular C₅-H₅...O₄ interactions (2.501-2.715 Å) synthon R₄⁴(32) of the [Cu(2-picolonate)₂ H₂O] in Figure 3.21. Down the c axis view of the two-dimensional networks of [Cu (2-picolonate)₂ H₂O] it is formed by C₁₁-H₁₁...O₂ (2.544-2.657) interactions in Figure 3.22. Coming to the Crystal packing 3-Dimensional DNA Helical Model showed in the Fig 3.23. The supercell interaction of this compound [Cu(2-picolonate)₂ H₂O] has been shown in the Figure 3.24.

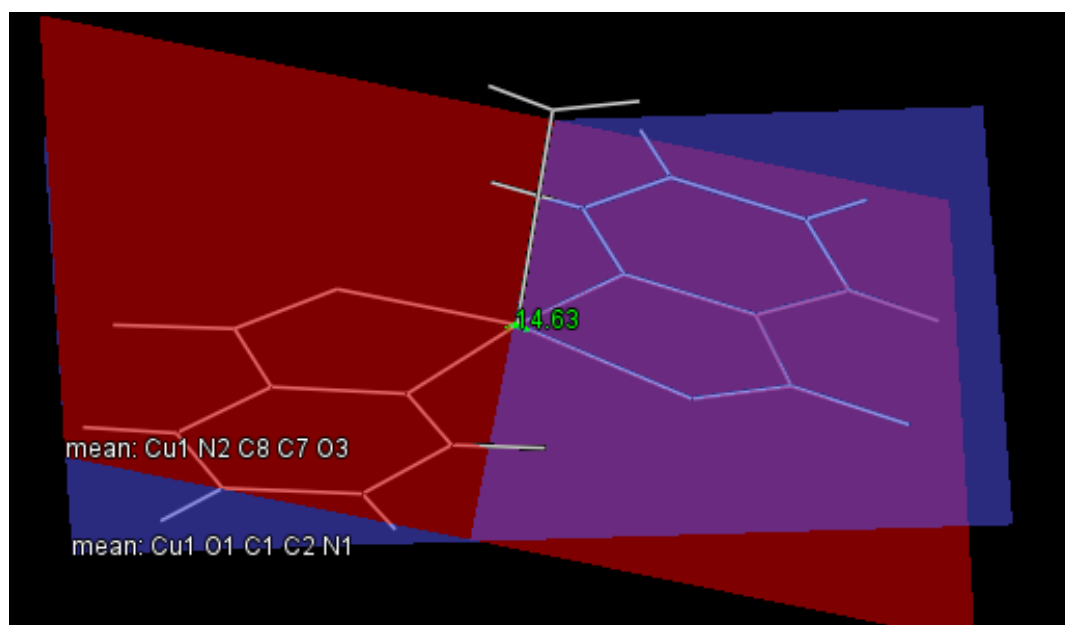
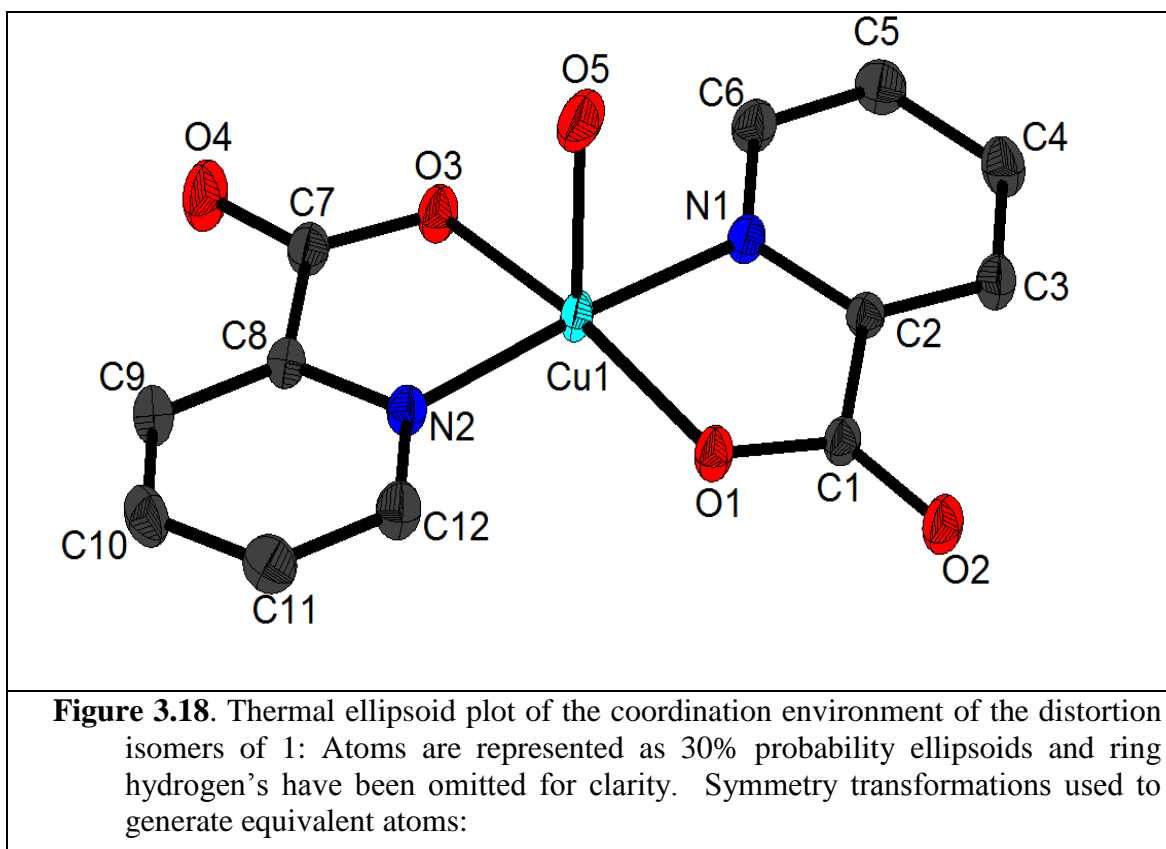


Fig 3.19 the angle between the two chelate rings (Cu1N1C2C1O1, and Cu1N2C8C7O3) is 14.63°

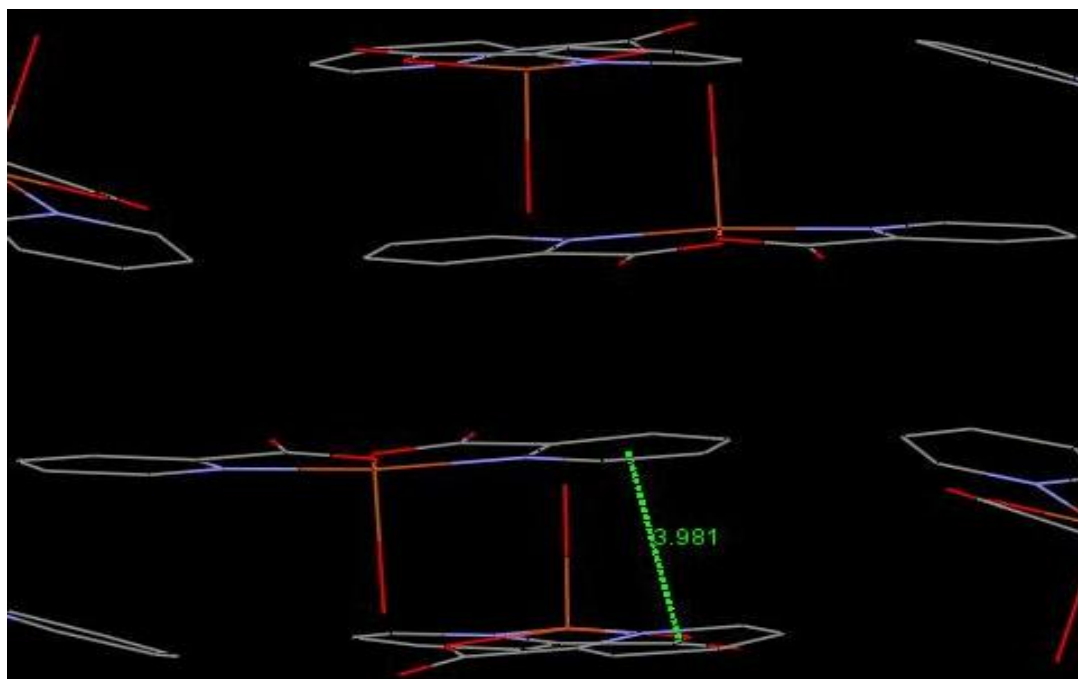


Figure 3.20 Weak spatial π - π stacking interactions of the title complex.

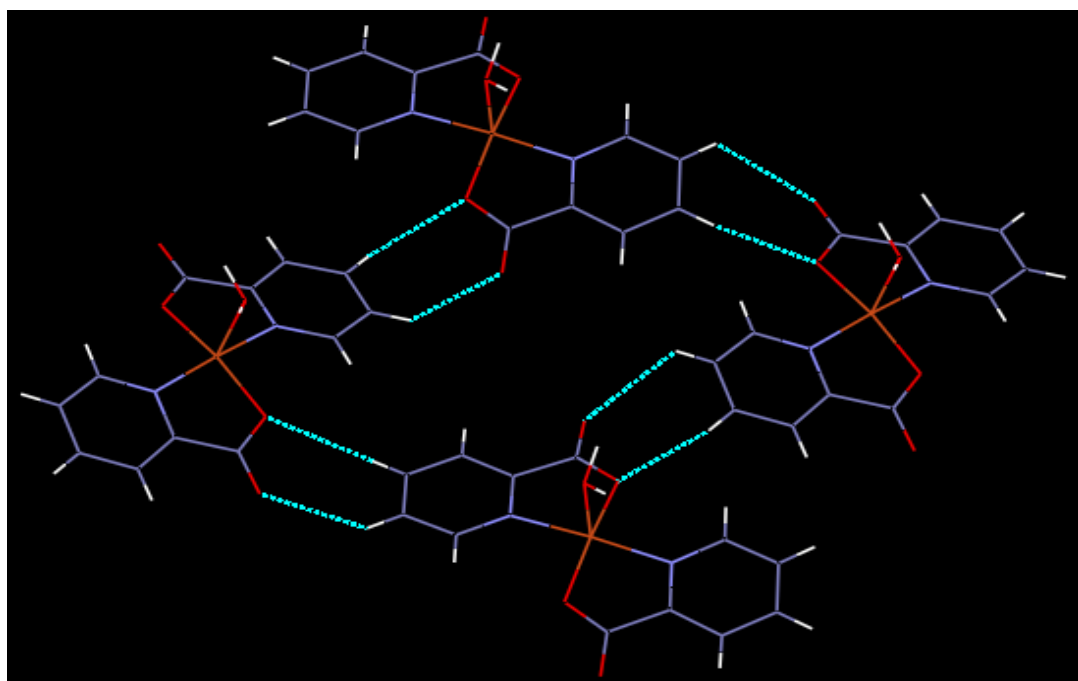


Figure 3.21A view of the supramolecular synthon $R_4^4(32)$ of the $[\text{Cu}(2\text{-picolonate})_2 \text{H}_2\text{O}]$.

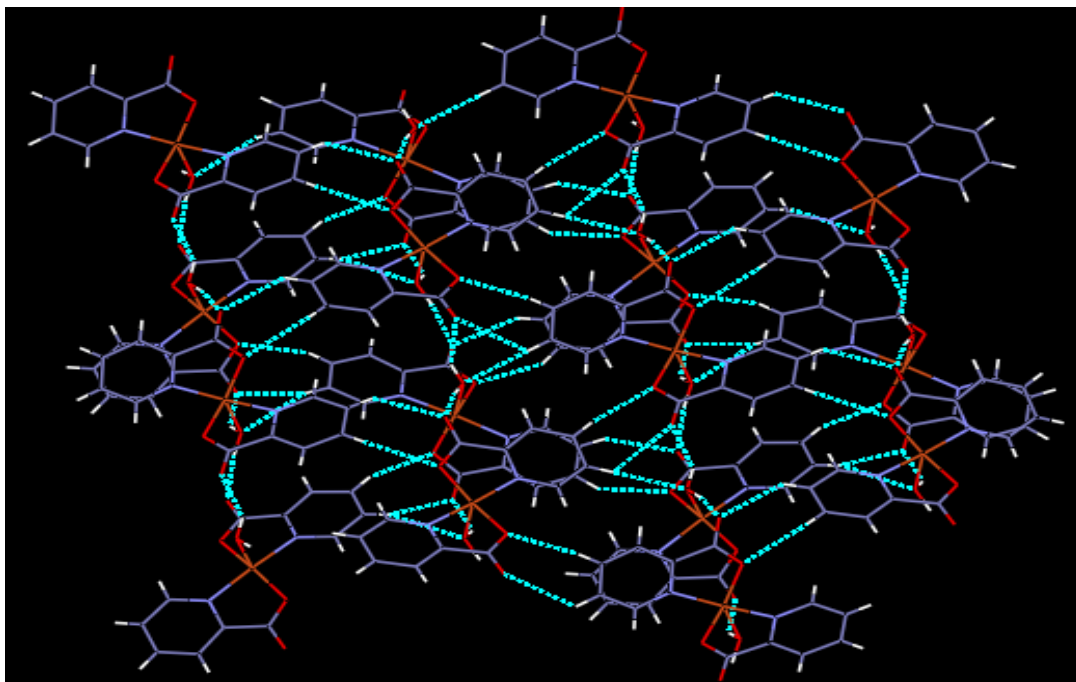


Figure 3.22 Down the *c* axis view of the two-dimensional networks of $[\text{Cu}(\text{2-picolonate})_2 \text{H}_2\text{O}]$ it was formed by C-H...O interactions.

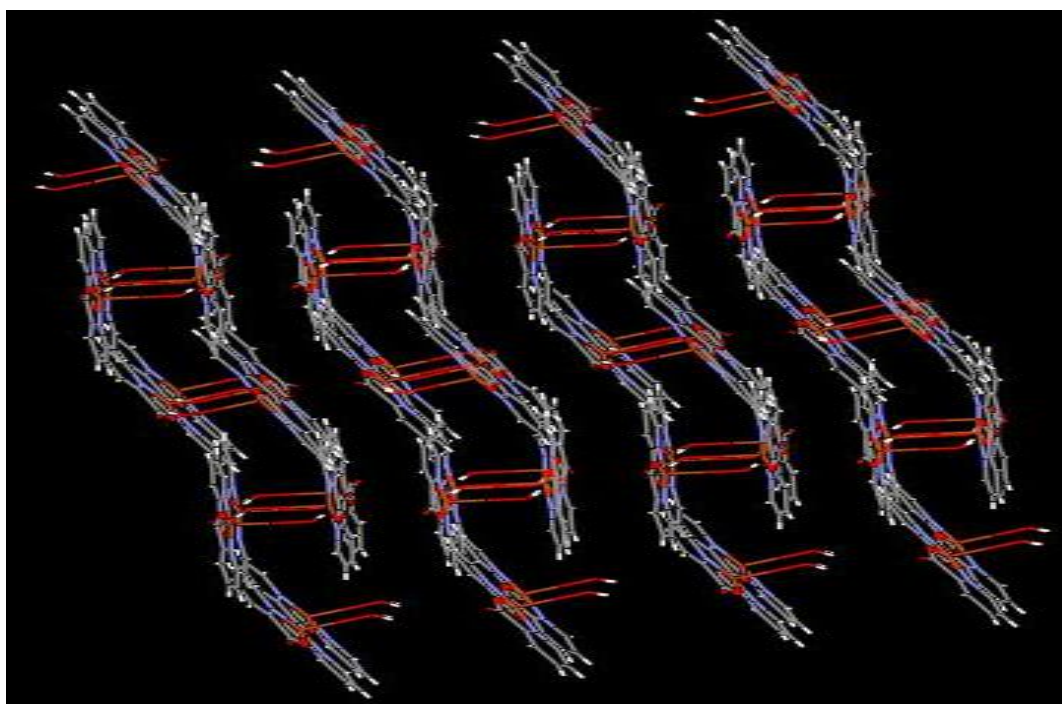


Fig 3.23 View of Crystal packing in 3-Dimensional DNA Helical Model.

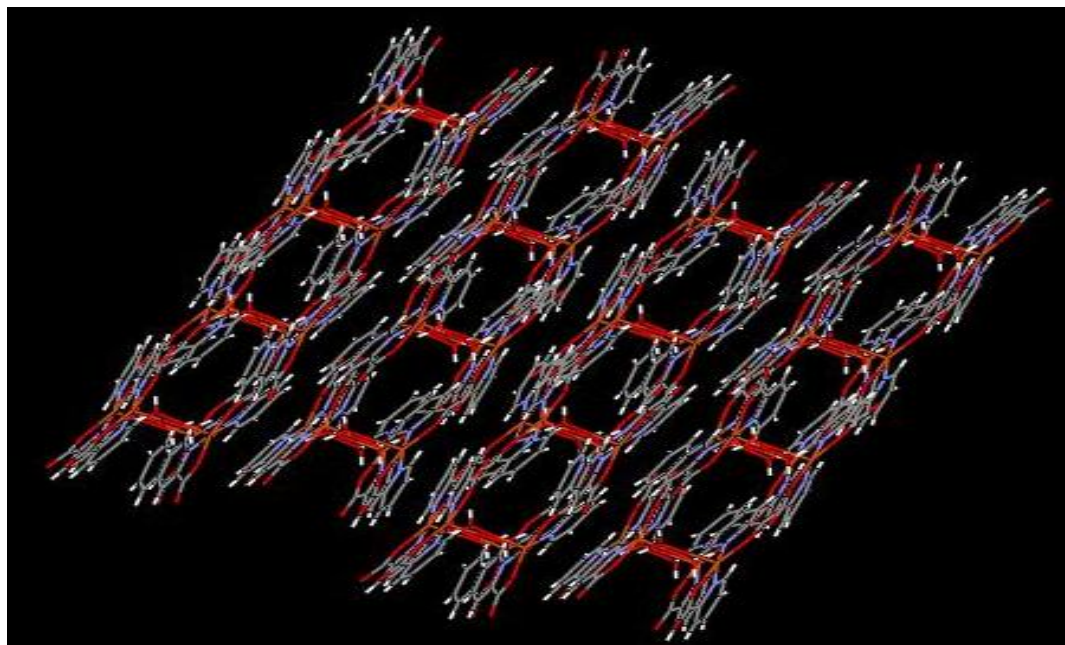


Fig 3.24 View of the crystal packing showing three fold water bridged chain between the host networks with C-H...O Interactions.

3.6.2 IR- spectrum of [Cu (2-pico)₂. H₂O]

The FT-IR spectra of 2-picolinic acid complex are given in Figure 3.25 IR spectra of the free ligand reveals that considerable changes in frequencies have occurred which can conclude the coordination sites in chelation. A broad intense absorption band around 3398 cm^{-1} can be assigned to stretching vibration of hydroxyl from the water molecules. The bands corresponding to the stretching vibration of the C–H and C=N are situated at 3073 cm^{-1} and 1631 cm^{-1} , respectively. The vibration peak originate in the 1475 cm^{-1} region is assigned to the stretching vibration of the C=C–C=C bond. The difference value of 122 cm^{-1} between the asymmetric (1474 cm^{-1}) and symmetric (1352 cm^{-1}) stretching vibration of the carboxylate group is in line with a mono dentate type of coordination [44–46]. The band subsequent to the stretching vibration of the C=O group of the Hpic monomer is situated at $1700\text{--}1769\text{ cm}^{-1}$ and disappears in the complex. The IR spectra of picolinic acid contain broad absorption bands at 2607 cm^{-1} and 2152 cm^{-1} and indicate the existence

of O-H...N type of intermolecular hydrogen bonding, but it disappears in the complex whose observable fact confirms that the nitrogen atom is coordinated to the Copper ion. The absorption peaks at 771 cm^{-1} and 698 cm^{-1} for the complex are assigned to deformation vibration of the pyridine ring which confirms that the pyridyl N atom and carboxyl O atom are coordinated with the center Copper ion. The absorption peak found in the 455 cm^{-1} region is assigned to the Cu–N bond and in the 425 cm^{-1} region is assigned to the Cu–O bond [47].

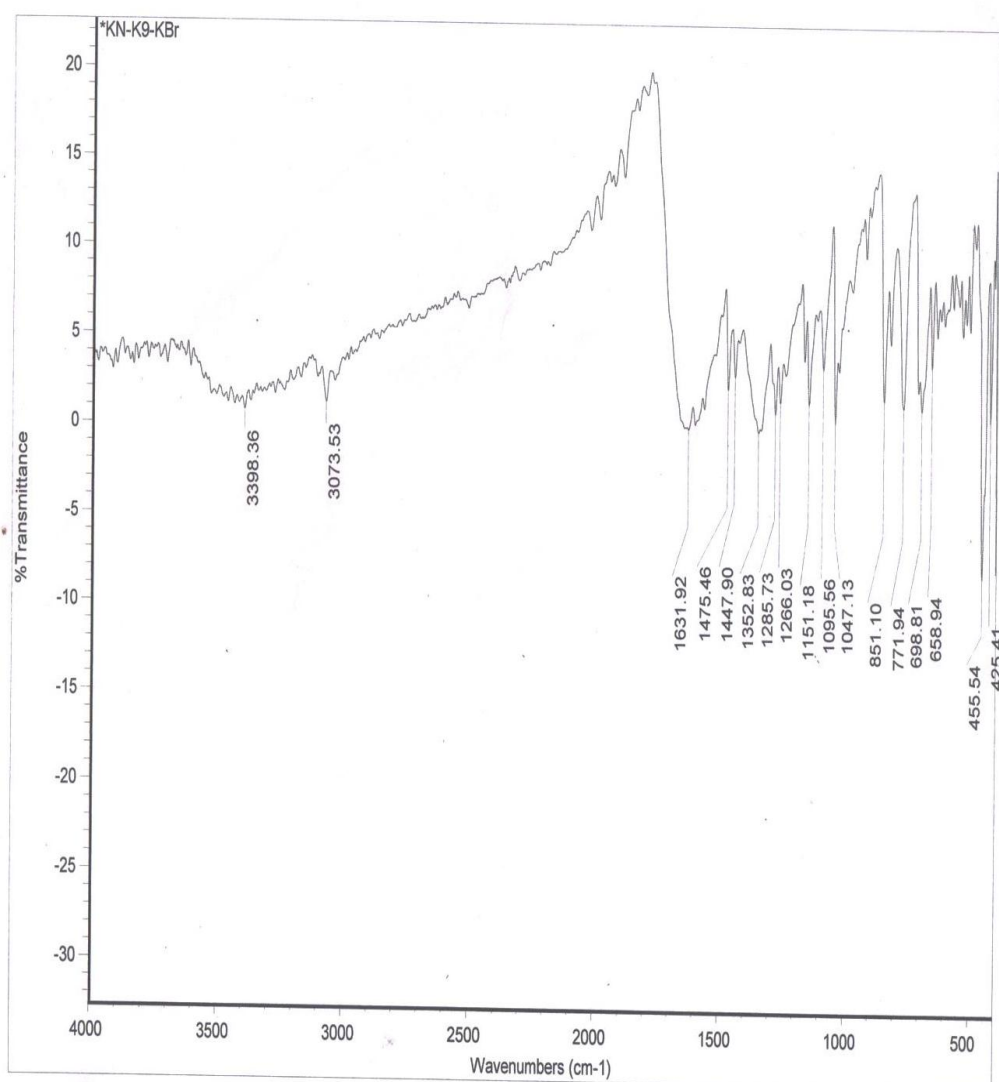


Fig 3.25 IR- spectrum of [Cu (2-pico)₂]. H₂O

3.6.3 Electronic spectrum of [Cu (2-pico)₂]H₂O

The maximum of the absorbance from the UV-visible spectra of Single Crystal Copperpicolinate complexes are shown in Figure 3.26. The maximum corresponded to the π - π transitions in the aromatic ring. The complex has a shoulder broad band at 259 and 310 nm may be assigned to the following charge transfer from metal to ligand. The electronic configuration of copper (II) complex was d^9 which confirms the absence of any d-d electronic transitions. There were differences in the UV spectra between ligand and metal complexes [43].

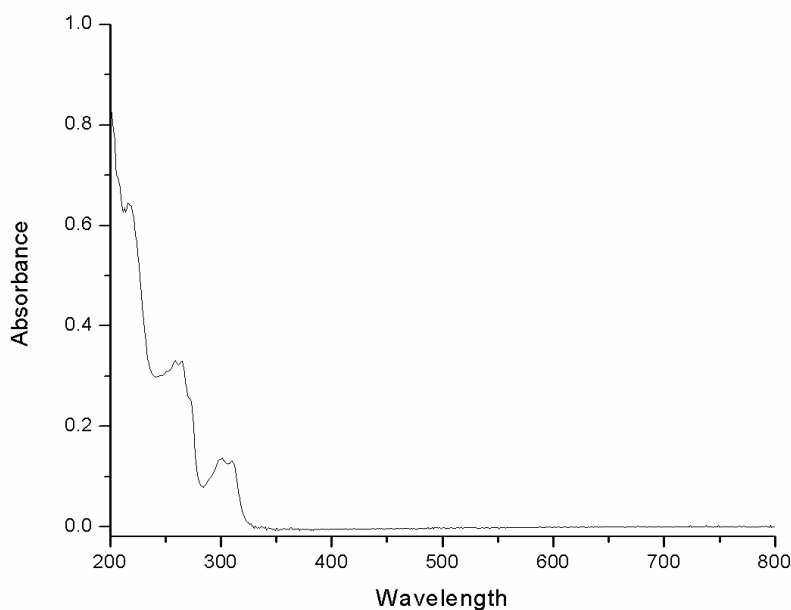


Fig 3.26 Electronic spectrum of [Cu (2-pico)₂ H₂O]

3.6.4 Fluorescent emission spectrum of [Cu (2-pico)₂ H₂O]

These complexes are also fluorescently examined in aqua media solution at room temperature, Fluorescence for free picolonic acid bands observed at 211 and 264 nm. The emission spectra of copper-picolonic acid complex are shown in Figure 3.27 respectively. The intensity of main visible emission lines of Copper picolonic acid observed at 524 nm increased in the presence of picolonic acid. The emission spectrum of copper complex is recorded at the excitation wavelength of 301 nm.

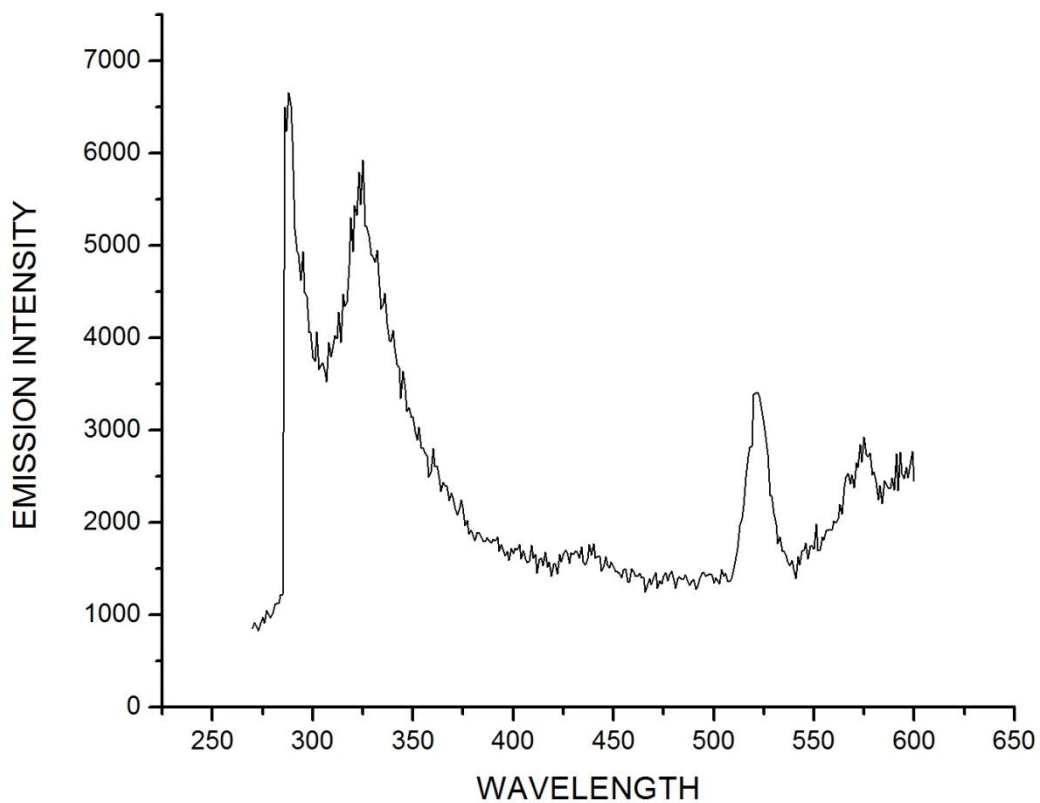


Fig 3.27 Electronic spectrum of [Cu (2-pico)₂.H₂O]

3.6.5 Powder X-Ray Diffractogram of [Cu (2-pico)₂. H₂O]

The X-ray powder diffraction (XRD) measurement of the complex [Cu(2-pico)₂.H₂O] is performed. The diffractogram obtained for complex 3 is given in Fig. 2.34 and with the help of the data obtained from the powder XRD, the crystallite size calculations are performed using Scherer equation.

[Cu (2-pico) ₃ .H ₂ O] n	2θ	FWHM	Crystallite size
	17.55	0.32°	27.54 nm

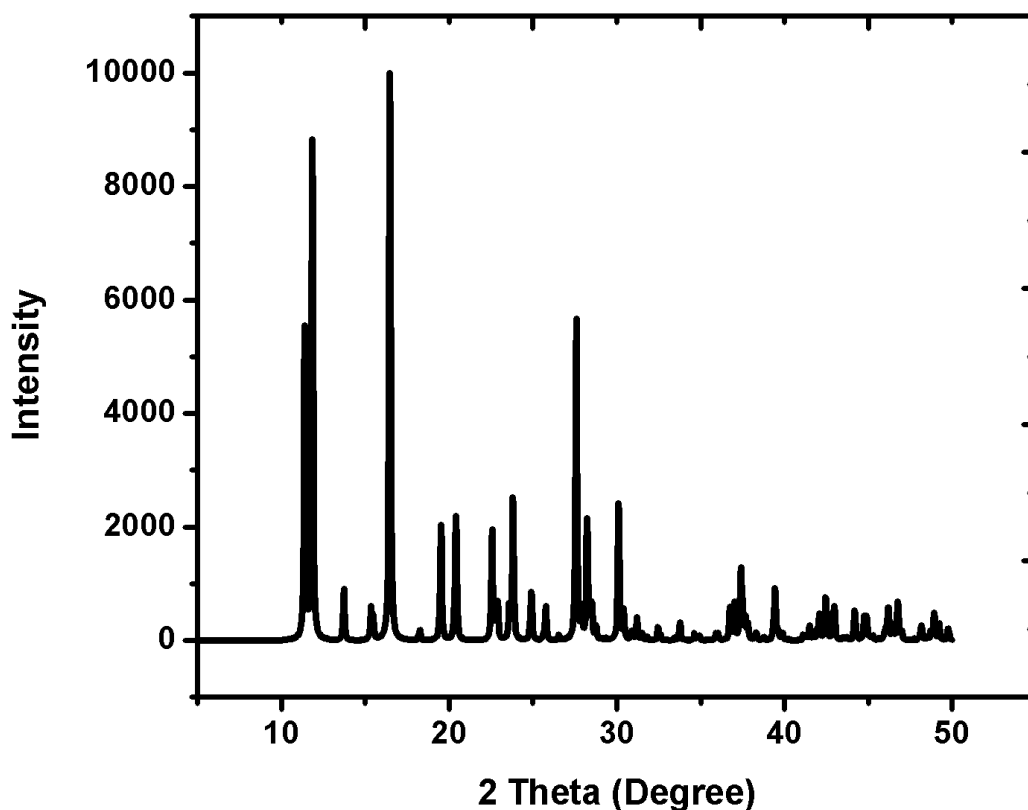


Fig 3.28 Powder X-Ray Diffractogram of [Cu (2-pico)₂ . H₂O]

3.6.6 ANTI PATHOGENIC IN VITRO STUDIES OF [Cu (2-pico)₂ . H₂O]

Antibacterial activity of sample [Cu (2-pico)₂ H₂O] is screened against 7 human pathogenic bacteria's such as Staphylococcus aureus MTCC 96, Pseudomonas aeruginosa MTCC 3216, Proteus mirabilis MTCC 1429, Vibrio cholera MTCC 3905, Escherichia coli MTCC 443, Shigella flexneri MTCC 1457, and Micrococcus luteus MTCC 106. The Anti Pathogenic screening data of crystal structure is summarized in the Table 3.10

Human Pathogens	Staphylococcus aureus	Pseudomonas aeruginosa	Proteus mirabilis	Vibri	Escherichia coli	Shigella flexneri	Micrococcus luteus
Inhibition Zone (mm)	14	14	12	14	14	14	16

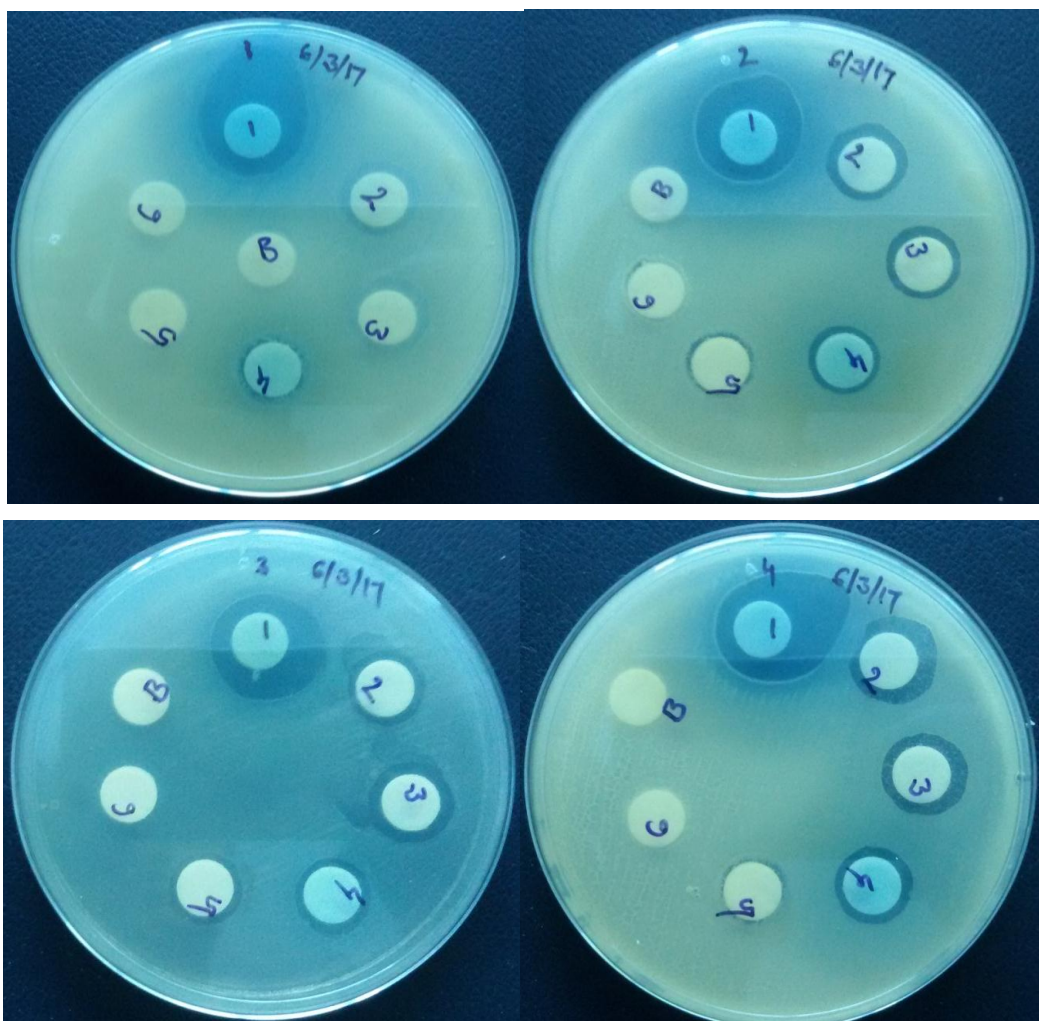


Fig 3.29 Inhibition zones for $[\text{Cu}(\text{2-pico})_2 \cdot \text{H}_2\text{O}]_2$ against *Staphylococcus aureus*,
56

***Pseudomonas aeruginosa*, *Proteus mirabilis* and *Vibrio cholera*.**

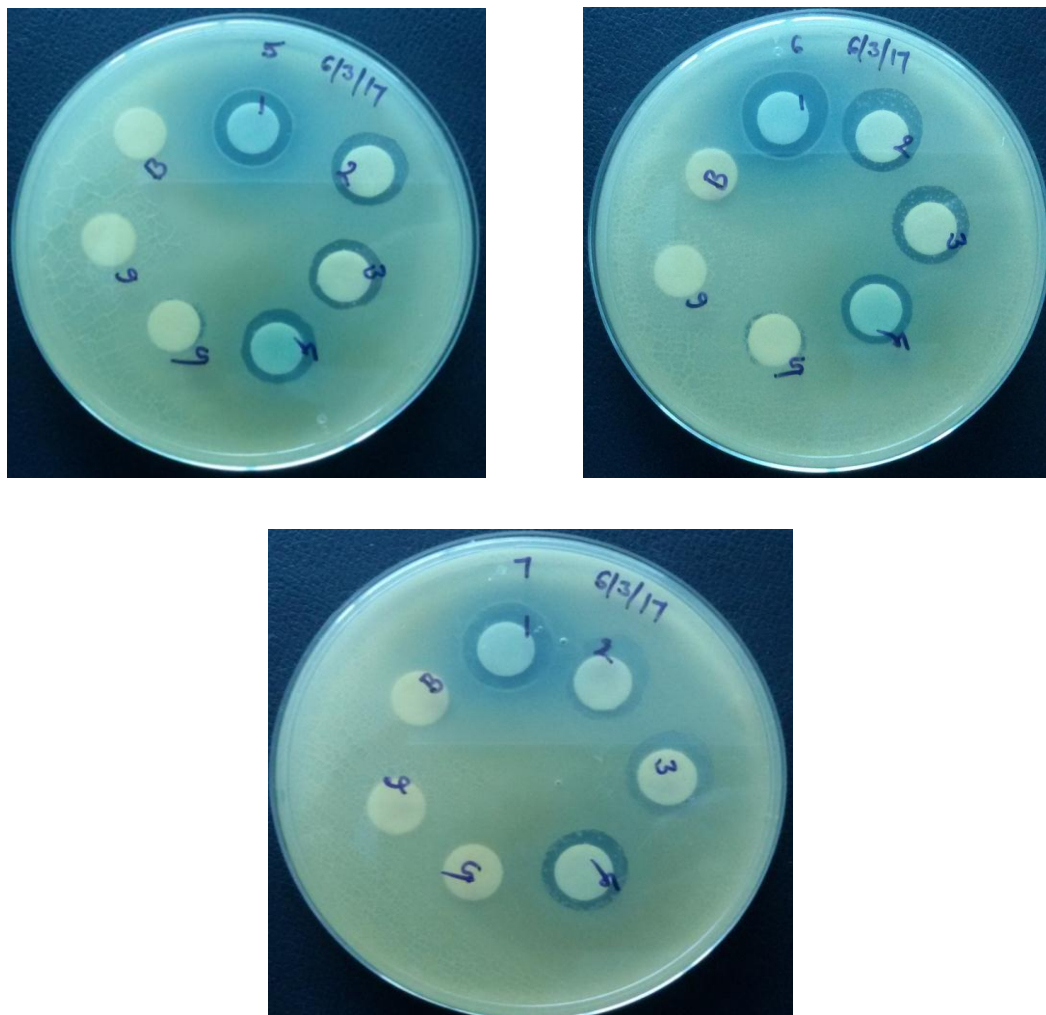


Fig 3.30 Inhibition zones for $[Cu(2-pico)_2H_2O]_2$ against *Escherichia coli*, *Shigella flexneri*, and *Micrococcus luteus*.

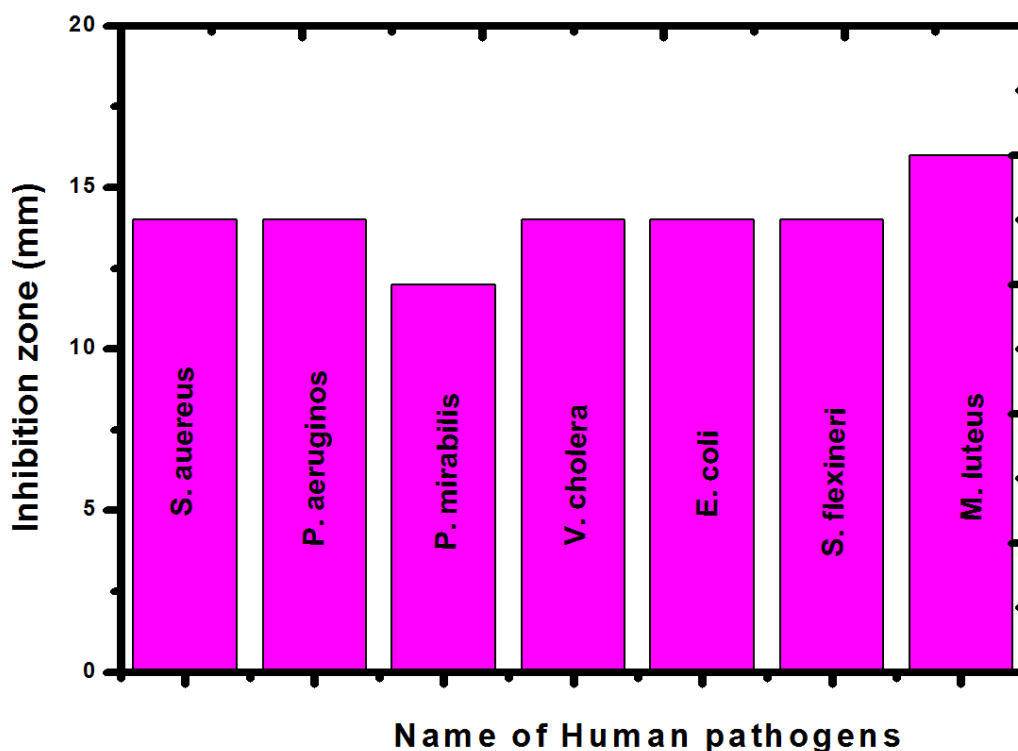


Fig 3.31 Bar chart of Antipathogenic activities of [Cu (2-pico)₂ H₂O]

From the above bar chart we explained that, the Antipathogenic activity is good for the tested microorganisms such as Staphylococcus aureus, Pseudomonas aeruginosa, Vibrio cholera, Escherichia coli, Shigella flexineri and Micrococcus luteus. The obtained inhibition zones are 14, 14, 14, 14, 14 and 16 mm.

3.7 CONCLUSIONS

In this chapter, we presented the results of synthesis and characterization studies for the two heterocyclic transition metal based single crystal compounds involving 2-picolonic acid and Acetate ligands. The transition copper metal is chelated with the heterocyclic ligand i.e. 2-picolonic acid and Acetate ligands the adopted methodology for synthesis of metal based single crystal compounds is self-assembly. The both complexes [Cu(2-pico)₃].H₂O and [Cu (2-pico)₂ H₂O] is characterized by using the single crystal X- ray analysis. The structure obtained by the single-X ray analysis is it confirms the structure of atomic bond distances and bond angles of both [Cu(2-pico)₂H₂O]_n and [Cu (2-pico)₂ H₂O]. The crystal packing diagrams shows, some organic

frame works, C-H...O interactions, π and π - π are obtained by using Mercury Software. The IR spectra reveals the existence of functional groups and anionic ligands such as O-H (water), C=C, C=N, C-H (pcy), The UV spectrum confirms the complexation of metal and ligand with the increase in the absorbance value compared to free ligand. The λ_{\max} values of d-d band are observed for the metal complexes in the range of 211 to 310 nm. The Fluorescence spectrum confirms the complexation.

The single crystal metal complexes are screened for antimicrobial activity by Kirby-Bauer method. The bacterial organisms used for this study are antibacterial activity of both $[\text{Cu}(\text{2-pico})_2 \cdot \text{H}_2\text{O}]_n$ and $[\text{Cu}(\text{2-pico})_2 \cdot \text{H}_2\text{O}]$ single crystal complexes are screened against 7 human pathogenic bacteria's such as Staphylococcus aureus, Pseudomonas aeruginosa, Proteus mirabilis, Vibrio cholera, Escherichia coli, Shigella flexneri, and Micrococcus luteus as the test microorganisms. The anti-Pathogenic screening data of complexes is summarized the observed inhibition zones in both complexes are in the range of 16-12 mm. The screened data in these reports are in good agreement with the previous data and the present observations.

4.1 Experimental

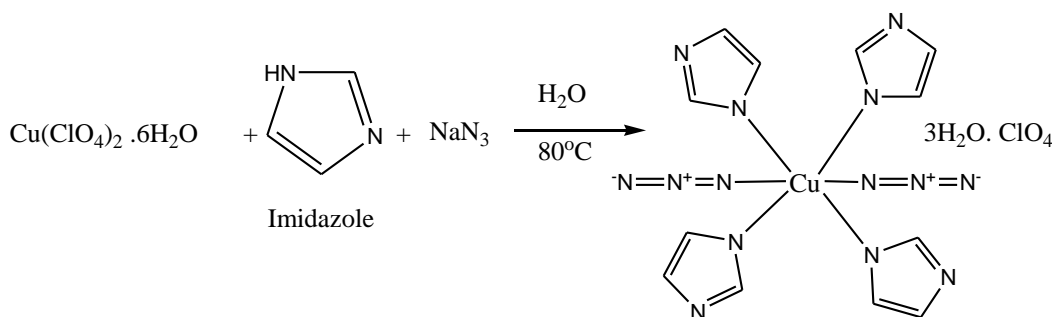
4.1.1 Reagents

Imidazole was purchased from sigma-aldrich and used without further purification. Ethanol, methanol used for synthesis of metal complexes were A.R. grade and used as received for synthetic work. $\text{Cu}(\text{ClO}_4)_2 \cdot 6\text{H}_2\text{O}$ were procured from Alfa aesar and $\text{CoSO}_4 \cdot 7\text{H}_2\text{O}$ were procured from Lobachemie..

Caution : Azides and perchlorates are explosive, handle with care.

4.1.2 Synthesis of $[\text{Cu}(\text{imd})_4(\text{N}_3)_2] \cdot 3\text{H}_2\text{O} \cdot \text{ClO}_4(1)$

An aqueous (5 ml) solution of copper perchlorate hexahydrate (0.185g, 0.5mmol) is added to an aqueous solution (5ml) of imidazole (0.068g, 1.0 mmol) under stirring conditions and the solution turned to blue colour and then aqueous solution (5 ml) of NaN_3 (0.065 g, 1.0 mmol) is added which turned to parrot green colour. After constant stirring at 80°C temperature for 30 minutes, the solution is filtered off. The green crystals are formed after 2 days and are washed with methanol and toluene. Crystal: Yield 0.098 g (53%). Anal. exptal. $\text{C}_{12}\text{H}_{18}\text{N}_{14}\text{CuClO}_7$ (M.Wt. 569.36) C, 25.31; H, 3.19; N, 34.44. Found: C, 25.21; H, 3.11; N, 34.21. Important IR absorptions (KBr disk, cm^{-1}): 3361, 3144, 3088, 2921, 2041, 1617, 1542, 1490, 1471, 1331, 950, 831, 747, 671, 655. Mass peaks (m/z): 380, 425, 441, 516, 570.



Scheme 1. Synthetic route and proposed structure of complex 1

The title mononuclear complex, $[\text{Cu}(\text{imd})_4(\text{N}_3)_2] \cdot 3\text{H}_2\text{O} \cdot \text{ClO}_4$ (imd is imidazole) has been synthesized. The Cu^{II} ion in the complex has a distorted octahedral coordination geometry comprised of four deprotonated N atoms of the four imidazole ligands, two azide N atoms in the coordination sphere and three aqua ligands and one perchlorate ion in the outersphere.

4.2 Measurements

IR spectra are obtained with a Shimadzu IR Prestige 21 FT-IR spectrophotometer. UV spectra are recorded on Thermoscientific UV spectrophotometer. Elemental analysis is obtained using a

FLASH EA 1112 SERIES CHNS analyser. Mass Spectra are recorded on AGILANT QQQ (ESI-MS) mass spectrometer. SEM data are recorded on ZEISS ULTRA-55.

4.2.1 IR Spectrum of $[\text{Cu}(\text{imd})_4(\text{N}_3)_2] \cdot 3\text{H}_2\text{O} \cdot \text{ClO}_4(1)$

The IR spectrum of the complex 1 (Fig 4.1) exhibits bands in the $3450\text{--}3300\text{ cm}^{-1}$ regions, which may be attributed to $\nu(\text{OH})$ of the coordinated water³² molecules. The coordination of imidazole ligand to metal is confirmed by presence of peak at 3088 cm^{-1} ($\nu\text{N-H}$) and the shifting of $\nu\text{C=N}$ of imidazole from 1577 to 1617 cm^{-1} indicates that the ligand is chelating through imidazolic nitrogens³³. The spectrum exhibits an intense absorption at 2042 cm^{-1} which is associated with the asymmetric stretching mode of the azide ligand. The $\nu\text{s}(\text{N}_3)$ stretching mode of the azide group is observed as a medium band at 1331 cm^{-1} . The deformation mode of the azido ligand is observed as a weak band at 671 cm^{-1} . The IR Spectral data of all the complexes are reported in Table 4.20.

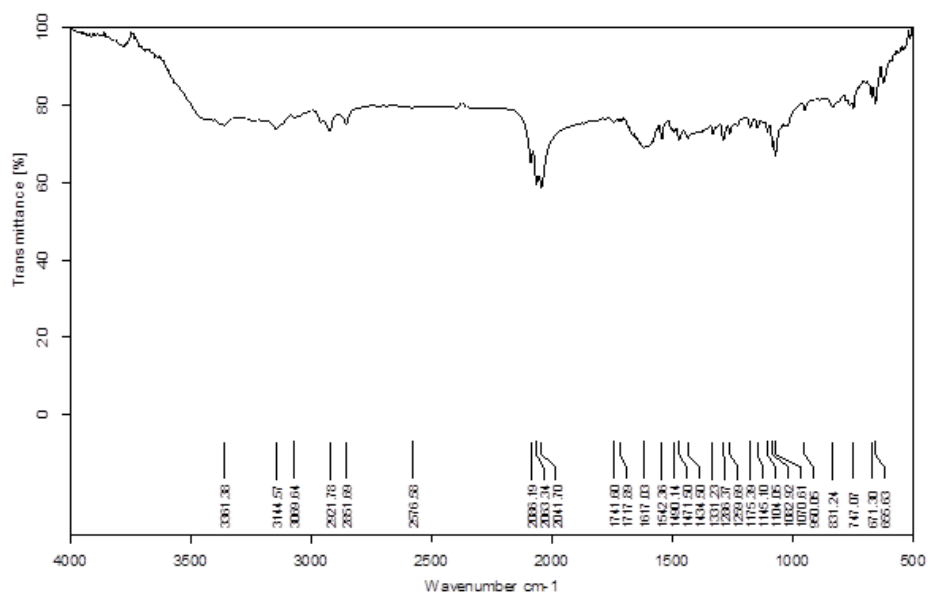


Fig 4.1 IR Spectrum of complex 1

4.2.2 Electronic Spectrum of $[\text{Cu}(\text{imd})_4(\text{N}_3)_2] \cdot 3\text{H}_2\text{O} \cdot \text{ClO}_4(1)$

The Electronic spectra of the imidazole complexes are taken in methanol. The free ligand has broad band at 215 and 243 nm. The electronic spectral details of ligand and all the complexes are listed in Table 4.21.

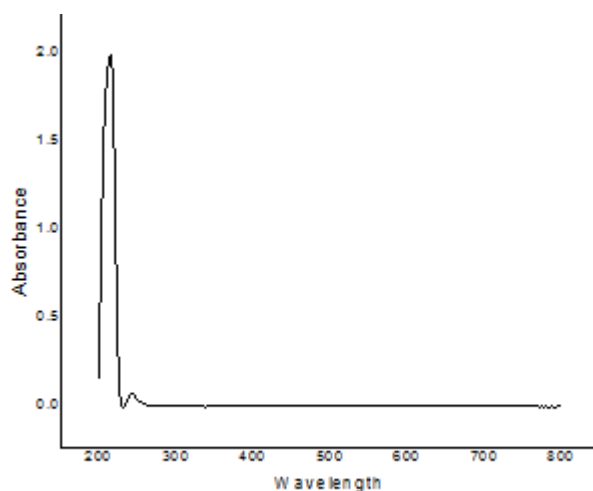


Fig 4.2 Electronic Spectrum of free ligand

The complex 1 has a shoulder broad band at 259 and 354 nm assigned to the d-d transition. This result confirms the complexation of metal ion.

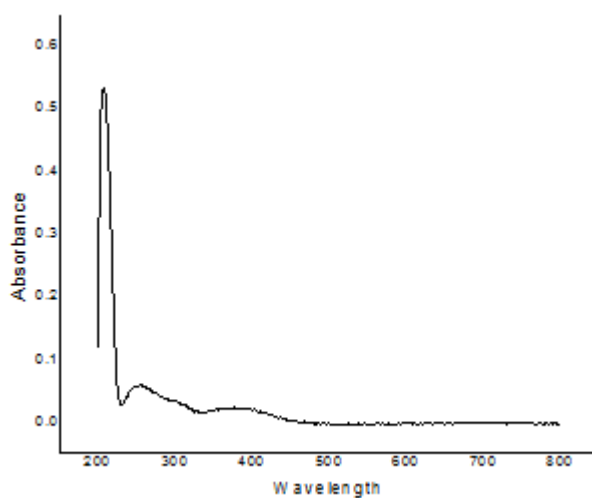


Fig 4.3 Electronic Spectrum of complex 1

4.2.3 LC-MS Spectrum of $[\text{Cu}(\text{imd})_4(\text{N}_3)_2] \cdot 3\text{H}_2\text{O} \cdot \text{ClO}_4(1)$

The peak at 380(m/z) is complex bound to four imidazoles and one azide molecules present in 4:1 ratio $[\text{Cu}(\text{imd})_4(\text{N}_3)]$ and the peak at 425(m/z) is complex bound to four imidazoles and two azide molecules, $[\text{Cu}(\text{imd})_4(\text{N}_3)_2]$. The peaks around 441(m/z) and 516 (m/z) refer to the $[\text{Cu}(\text{imd})_4(\text{N}_3)_2] \cdot \text{H}_2\text{O}$ and $[\text{Cu}(\text{imd})_4(\text{N}_3)_2](\text{ClO}_4)$ complexes respectively. The peaks around 570(m/z) refer to the $[\text{Cu}(\text{imd})_4(\text{N}_3)_2] \cdot 3\text{H}_2\text{O} \cdot \text{ClO}_4$ complex.

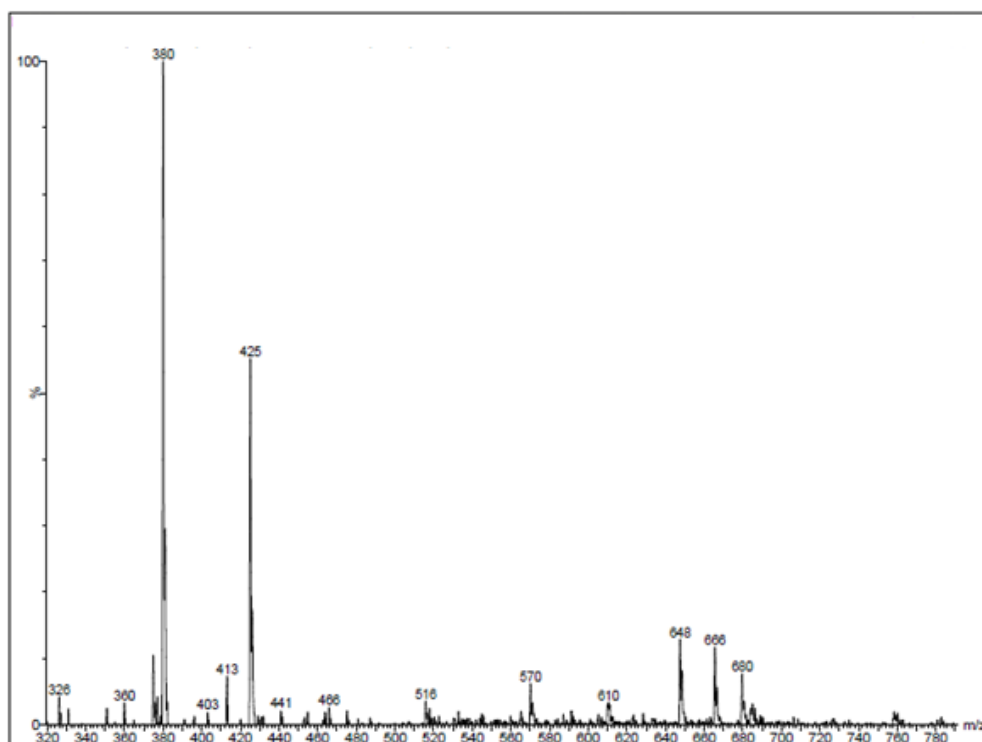


Fig 4.4 LC-MS Spectrum of Complex 1

4.2.4 Antimicrobial Screening of $[\text{Cu}(\text{imd})_4(\text{N}_3)_2] \cdot 3\text{H}_2\text{O} \cdot \text{ClO}_4(1)$

The complex 1 is screened *in vitro* for antibacterial activity against E.coli, S.aureus and antifungal activity against R.oligospores by disc diffusion method. Antimicrobial activities of all the complexes are reported in Table 4.22. The antimicrobial activities of complex 1 are listed in table 4.1.

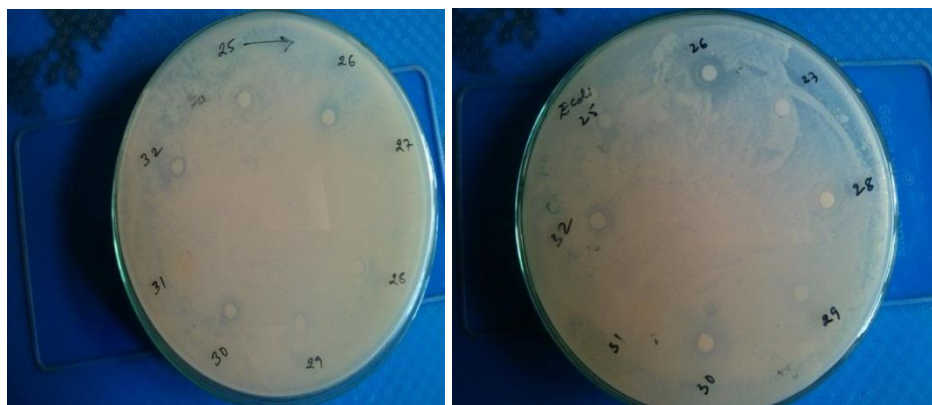


Fig 4.5 Inhibition zones for complex 1 (30) against S.aureus and E.coli



Fig 4.6 Inhibition zones for complex 1 (30) against R.oligospores

Table 4.1 Inhibition zones for complex 1 (30)

Bacteria	Inhibition zone (mm)
S.aureus	4
E.coli	4
Fungal	Inhibition zone (mm)
R.oligospores	Nil

The complex 1 showed good antibacterial activity against two organisms, but it did not show any activity against fungal organism.

4.2.5 Cytotoxic Studies of $[\text{Cu}(\text{imd})_4(\text{N}_3)_2] \cdot 3\text{H}_2\text{O} \cdot \text{ClO}_4(1)$

Among the synthesized complexes, complex 1 is screened *invitro* for their cytotoxicity (MCF-7, A-431 and HepG-2 cell lines). From the data, it is observed that the complex displayed their cytotoxic activities as IC_{50} ($\mu\text{g}/\text{mL}$) against breast cancer MCF-7, skin cancer A-431 and lung cancer HepG-2 cell lines. The IC_{50} values of the all the complexes are listed in Table 4.23.

Table 4.2 Dose Response of complex 1 on MCF-7(Breast Cancer) Cell line

Control : 0.509

Incubation period : 24 hours

Conc (µg/ml)	OD of extract	% Cell Survival	% Cell Inhibition
0.1	0.48	94.3	5.7
1	0.4335	85.16	14.84
10	0.325	63.85	36.15
100	0.081	15.91	84.09
500	0.065	12.77	87.23

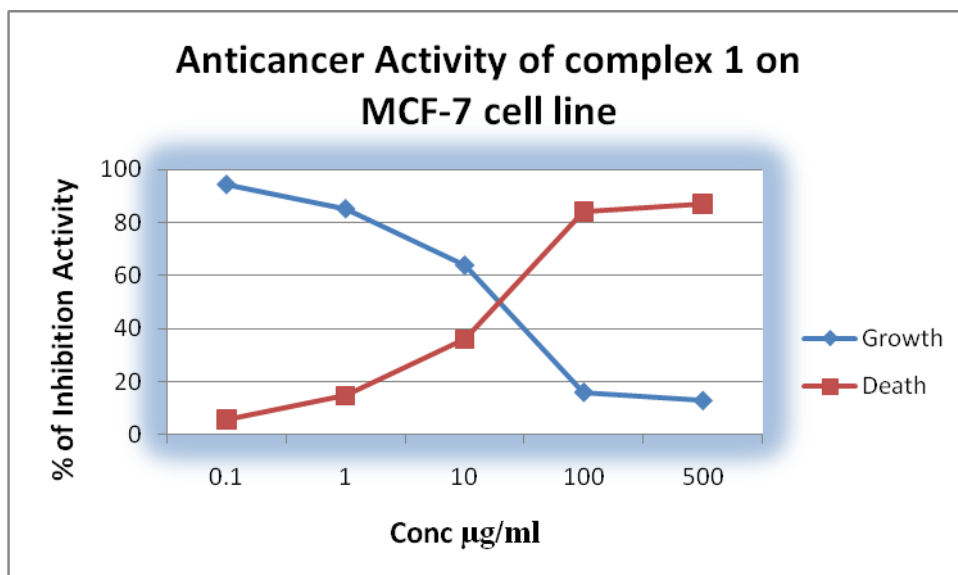


Fig 4.7 Effect of complex 1 on MCF-7 Cell Viability for 24 h Incubation Time.

IC50	36.19µg/mL
-------------	-------------------

Table 4.3 Dose Response of complex 1 on A-431 (Skin Cancer) Cell line

Control : 0.776

Incubation period : 24 hours

Conc (µg/ml)	OD of extract	% Cell Survival	% Cell Inhibition
0.1	0.769	99.09	0.91
1	0.738	95.1	4.9
10	0.6865	88.46	11.54
100	0.0725	9.34	90.66
500	0.0575	7.4	92.6

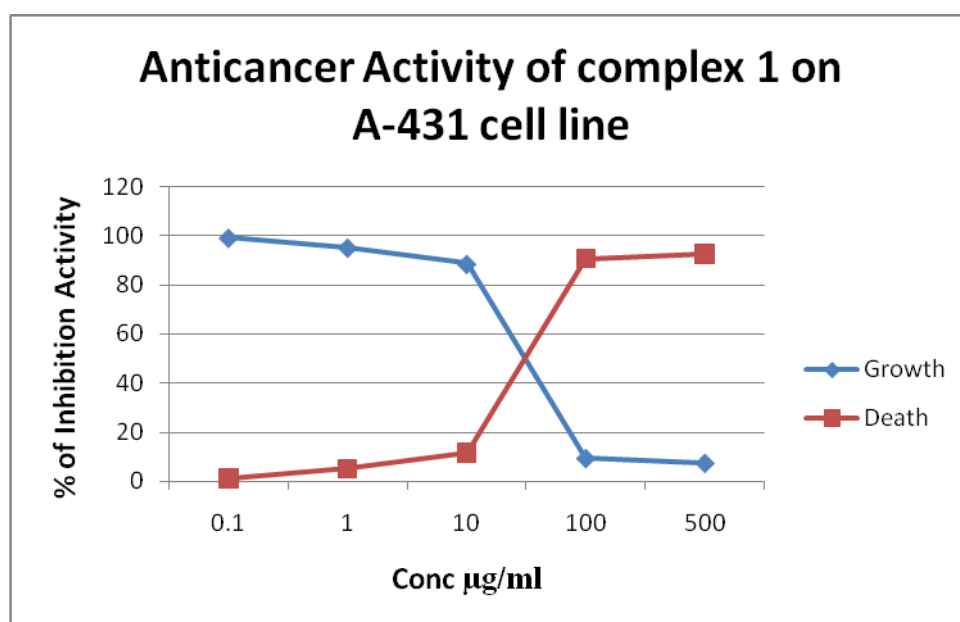


Fig 4.8 Effect of complex 1 on A-431 Cell Viability for 24 h Incubation Time.

IC50	53.72µg/mL
-------------	-------------------

Rational of the Study and the Research Gap

It is observed from the review of literature that there available a plethora of research being conducted all over the world to develop new pseudo halide metal complexes and Schiff bases and establish the procedures for the application at the

lab level and in scaling up process. Very few of the available researches have been presented in this part.

Further, keeping in view of the advantages of nano particulate metal complex systems, many new reactions have been studied in the limited time framework of research to be completed and submitted as part of the course work. Many areas could be studied and many factors could also be considered in selecting the objectives and scope of the work, but finally keeping in view of the framework of the course, the study confined to the objectives selected.

The main aim of this research work is on the synthesis and characterization of nano crystalline complexes and study their biological application in the synthesis of some new class of organo metallic compounds by self assembly synthesis using chemical strategies. The bioactive compounds have been prepared by self-assembly method and hydrothermal method. Phase pure nano crystalline nanoparticulate metal complexes with different compositions. The bio active compounds have been characterised and used in the research as pharmacological active compounds. This technique produced good yield and ensured complete homogeneity. Hence this process could be scaled.

The objectives of the study are:

5. To synthesize nano particulate compounds and its metal chelates by self assembly and hydrothermal methods.
6. To characterize the synthesized nano ferrites using FT-IR, XRD, SEM, EDAX, TEM and BET surface area techniques to interpret their structure, morphology and size.
7. To characterise the structure of the newly synthesized metal complexes and its nanostructures using FT-IR, ^1H NMR and MASS spectral analysis
8. To study the biological activity of the newly synthesized Metal complex compound

Self -assembly synthesis of Nanoparticulate metal complexes

All compounds were prepared by using self assembly method. The efficiency of the bio active compounds are compared with the reported literature and it is found that these Nanoparticulate metal complexes have found to be excellent biological efficacy.

A number of compounds have been synthesized and their structures have been assigned with the help of FT-IR, ¹H NMR and MASS spectral analysis. The supporting spectra are also provided.

Antibacterial Activity and cytotoxic activity of metal chelates and Nanoparticulate metal complexes:

In this chapter antibacterial activity studies of all the Nanoparticulate metal complexes synthesized by various synthetic strategies using self assembly method.

And finally 50 samples of one-pot synthesized compounds were screened for their antibacterial activity on gram positive (*Bacillus subtilis*, *Staphylococcus aureus*) and gram negative bacteria (*Salmonella typhi*, *Enterobacter aerogenes*). Out of these 50 compounds, all compounds showed zone of inhibition for *Bacillus subtilis*, and *Staphylococcus aureus*. For gram negative bacteria, all compounds showed zone of inhibition from moderate to high in comparison with the standard drug. 26 compounds are screened for cytotoxic activity and show high potent towards breast, liver and skin cancer studies. so much of work will be published in the coming period and it will be published in the account of UGC-MRP.

Conclusions

The summary of the work presented and the final conclusions of the work carried out. high potent antibacterial and anti-cancer compounds are prepared and published.

14.	Contributions to the Society	:	The results have been incorporated in many other studies
15.	Whether any Ph.D enrolled/produced out of the project:	:	YES Project Fellow Mr. M o h a n a R a o K o t a Enrolled as PhD Research Scholar Completed his course work and Submitted his Thesis He has been awarded PhD in Chemistry from Andhra University on the TOPIC <i>"Novel Crystalline Metal Organic Frame works: Anti-Pathogenic and Anti-Cancer Studies"</i> <i>PhD Degree Proceedings Enclosed</i>
16.	No. of publications out of the project:	:	8 Research papers were published.

S. No	Title of the Publication, Authors, Journal	Year
1	<p>CYTOTOXIC STUDY OF NICKEL OROTATE IMIDAZOLE COMPLEX AND ITS SPECTROSCOPIC DETERMINATION</p> <p>K. PRAVEEN¹, CH. V. PADMARAO¹, K. MOHANA RAO¹, B. KISHORE BABU¹ & B. SWARNALATHA²</p> <p>International Journal of Medicine and Pharmaceutical Sciences (IJMPS)</p> <p>ISSN 2250-0049 Vol. 3, Issue 4, Oct 2013, 49-56</p>	2013
2	<p>NEW DIMETHYLGLYOXIME PSEUDOHALIDE COMPLEXES</p> <p>K. PRAVEEN¹, CH.V. PADMARAO², B. KISHORE BABU³, B. SWARNALATHA⁴ & V.VEERAIHAH⁵</p> <p>International Journal of Applied and Natural Sciences (IJANS)</p> <p>ISSN 2319-4014 Vol. 2, Issue 4, Sep 2013, 61-66</p>	2013
3	<p>Synthesis and characterization of the pseudohalide metal complexes</p> <p>Praveen. K, Padma Rao. Ch. V., Kishorebabu. B.*, Naga Sirisha. J., Swarna Latha. B., Suseelabai. G., Venketeswara Rao. B., Raghu Babu. K. and Padma. M.</p> <p>Der Pharma Chemica, 2013, 5(2):149-153</p>	2013
4	<p>Zinc dimethylglyoxime complexes</p> <p>Padma Rao. Ch. V.1, Praveen K.1, Kishorebabu B.*1, Padma M.1, Anna Sudheer K.1, Sandhya Rani K.1, Koteswarao K.1, Suseelabai G.1, Venkateswara Rao B.1, Mohana Rao K. and Swarna Latha B.2</p> <p>Der Pharma Chemica, 2013, 5(5):280-284</p>	2013
5	<p>Evaluation of antiproliferative potential of manganese (II)-dafone complex</p> <p>Reena¹, Megha P Nambiar², Bonige Kishore Babu³ & Biju AR²</p> <p>Indian Journal of Biochemistry & Biophysics Vol. 58, February 2021, pp. 62-70</p>	2021 accepted
6	<p>Efficacy of ZnO: SnO₂ Nano composite clusters Synthesis and characterization for Gas sensor and anti microbial applications IJBB-1638</p>	2021 Accepted
7	<p>Computational studies on the structural variations of selected MAO-A and MAO-B inhibitors- An in-silico docking approach IJBB-1105</p>	2021 accepted

8	Anti pathogenic <i>in vitro</i> studies of heterocyclic metal complexes-IJBB-1578	2021 accep ted
---	---	----------------------

References

1. Li, Y.W., Tao, Y and Hu, T.L. *Solid State Sciences*. **2012**, vol.14,8,1117–1125
2. Colacio, E., Maria,A., Palacios, A.R. AntonioRodrguezDieguez, *Inorganic Chemistry*. **2010**,vol.49, 4, 1826–1833.
3. unay, G., Yes,O.Z., ilel,M., Soylu,S., Keskin,G and Dal, H. *Synthetic Metals*. **2011**,vol.161, 21-22, 2471–2480.
4. Cui,J., Li, Y., Guo, Z and Zheng, H. *Chemical Communications*. **2013**, vol.49, 6,555–557.
5. Fang, S. M., SaE. C., nudo, M., Hu. *Crystal Growth and Design*. **2011**, vol. 11, 3, 811–819.
6. Yang,J., Zhao, B., Hu, X., Zhang,T and Bu,X. *Inorganic Chemistry*. **2010**,vol.49, 8, 3746–3751.
3. Hu, Y., Zeng, Z., Chen,X. *Crystal Growth and Design*. **2009**, vol.9, 1,421–426.
4. Tanner, P. A and C. Duan, P. A. *Coordination Chemistry Reviews*. **2010**, vol.254, 23-24, 3026–3029.
5. Huang,Y.G., Jiang,F.L and Hong, M. C. *Coordination Chemistry Reviews*, **2009**,vol.253, 23-24, 2814–2834.
6. Cui, G., He, C.H., Jiao, C.H., Geng, J.C and Blatov,V.A. *CrystEngComm*. **2012**,vol.14, 12, 4210–4216.
7. Novitski, A., Borta,S., Shova,O., Kazheva, M., Gdaniec. X and Simonov, Y.A. *Russian Journal of Inorganic Chemistry*. **2008**,vol.53, 2, 202–208.
8. Kukovec, B.M., Popovi, Z., Pavlovi, G. and M. Raji,G. *Journal of Molecular Structure*. **2008**,vol.882, 1–3, 47–55.
8. Luo, J.H., Hong, M.C., Shietal, Q. *TransitionMetal Chemistry*. **2002**, vol.27, 3, 311–315.
9. Vargov, Z. Zele, V., isaøov, I.C., oryov, T. *Thermo chimicaActa*. **2004**,vol.423,1-2,149–157.

10. Zhong, G.Q., Zhong, W.W., Jia, R.R., Jia, Y.Q. *Journal of Chemistry*. **2013**, vol, ArticleID217947.
11. Zhong, G. Q., Jia, R. R., Jia, Y. Q. "Advanced Materials Research. **2012**, vol.549, 292–296.
12. Min, C.Y., Yang, X.F., Zhang, R.X., Yao, F., Ouyang, W.M.," *Journal of Coordination Chemistry*. **2011**, vol.64, 9, 1617–1625.
13. Eret, M. M., Bienz, S. *European Journal of Organic Chemistry*. **2008**, 33, 5518–5525.
14. Kukovec, B. M., Kodrin, I., Mihali, Z., Furi, K., Popovič, Z., *Inorganica Chimica Acta*. **2010**, vol. 363, 8, 1887–1896.
15. Failes, T. W., Cullinane, C., Diakos, I., Yamamoto, N, J. G. Lyons, and T. W. Hambley, *Chemistry*. **2007**, vol.13,10, 2974–2982.
16. Lopez-Sandoval, V. M., Londoño-Lemos, E., Garza-Velasco et al., " *Journal of Inorganic Biochemistry*, **2008**, vol.102, no. 5-6, pp.1267–1276.
17. Dimiza, F., Papadopoulos, A.N., Tangoulis, V, et al. *Dalton Transactions*. **2010**, vol.39, 19, 4517–4528.
18. Yesilcelik, O. Z., Mutlu, A, C., Darcan, O., Uyukgung, B. *Journal of Molecular Structure*. **2010**, vol 964, 1–3, 39–46.
19. Segl'ar, P., Miklovič, J., Miklo, Ds et al., " *Transition Metal Chemistry*. **2008**, vol.33, 8, 967–974.
20. Georgiou, D., *Hydrometallurgy*. **2009**, vol.100, 1-2, 35–40.
21. Mamula, O., von Zelewsky, A., Bark, T., Bernardinelli, G., *Angew. Chem. Int. Ed.* **1999**, 38, 2945.
22. Kaes, C., Hosseini, M.W., Rickard, C.E., F.B.W. Skeleton, White, A., H., *Angew. Chem. Int. Ed.* **1998**, 37, 920.
23. McMorran, D.A., Steel, J., *Angew. Chem. Int. Ed.* **1998**, 37, 3295.
24. Siddiqui, K.A., Mehrotra, G.K., Mrozinski, J. *J. Coord. Chem.* **2011**, 64, 2367.

25. Siddiqui, K.A., Mehrotra, G.K., Mrozinski, J., Butcher, R.J. *Eur. J. Inorg. Chem.* **2000**, 4166.
26. Atwood, J.T., L.J. Barbour, T.J. Ness, C.L. Ratson, P.L. Ratson. *J. Am. Chem. c.* **2001**, 123, 7192.
27. Barbour, L.J., Orr, W.G., Atwood, J.L. *Nature.* **1998**, 393, 671.
28. Infantes, L., J. Chisholm, S., Motherwell. *CrystEngComm.* **2003**, 5, 480,
29. Pal, S., Sankaran, N. B., Sumanta., A. *Angew. Chem. Int. Ed.* **2003**, 42, 1741.

COPY OF THE Ph.D. DEGREE PRODUCED FROM THE RESEARCH



Evaluation of antiproliferative potential of manganese (II)-dafone complex

Reena¹, Megha P Nambiar², Bonige Kishore Babu³ & Biju AR^{2*}

¹Department of Chemistry, Pazhassi Raja N.S.S. College, Mattanur-670 702, Kerala, India

²Department of Chemistry, Sir Syed College, Taliparamba-670142, Kerala, India

³Department of Engineering Chemistry, Andhra University College of Engineering (A), Visakhapatnam-530 003, Andhra Pradesh, India

Received 06 November 2020; revised 27 January 2021

Cytotoxicity is the quality of being toxic to cells. *In vitro* toxicity is the scientific analysis of the effect of toxic chemical substances on cultured bacteria or mammalian cells. In our work Manganese-4,5-Diazafluoren-9-one complex was prepared and its cytotoxicity was studied by standard MTT Assay in Cervical carcinoma cells HeLa. The result was compared with the normal fibroblast cell to check its influence on normal cells. On comparing the results, the complex is found to be more toxic to cervical carcinoma cells than the normal fibroblast cells. The photocatalytic activity of the complex was studied on the basis of the decomposition reaction of methylene blue dye in presence of the complex. The compound $[\text{Mn}(\text{C}_{11}\text{H}_6\text{N}_2\text{O})_2(\text{NCS})_2]$ was synthesised and characterised by various spectroscopic methods and the structure was confirmed by single-crystal XRD analysis. The molecular structure of the complex was optimized using density functional theory (DFT) at the B3LYP/6-311 G (d,p) level. The smallest HOMO-LUMO energy gap (0.66 eV) indicates the soft acid nature of the complex.

Keywords: Crystal structure, Cytotoxicity, DFT studies, 4,5-Diazafluoren-9-one, Photocatalyst

Cancer, also called malignancy, is an abnormal growth of cells. There are five types of cancer known as carcinoma, lymphoma, melanoma, sarcoma, and leukemia. Carcinoma is the most commonly diagnosed cancer, originate in the skin, lungs, breasts, pancreas, and other organs and glands. In cervical carcinoma lowermost part of the uterus (cervix) was affected. It is the fourth most common cancer in women. According to WHO, in 2018, approximately 5,70,000 women were diagnosed with cervical cancer worldwide and about 3,11,000 women died from the disease.

Dafone is a bidentate ligand similar to 1,10-phenanthroline and bipyridine. It is a derivative of 1,10-phenanthroline, having an exocyclic keto group^{1,2}, which make it suitable for further derivatisation, to yield multinuclear metal complexes having interesting catalytic and biological properties³. Metal coordination complexes have been widely studied for their anticancer activities⁴⁻⁹. Earlier platinum-based complexes like cisplatin and carboplatin were used for the treatment of various

cancers. In spite of their effectiveness, they lack selectivity for tumour tissues, which leads to severe side effects like neurotoxicity and ototoxicity. Moreover, some tumor cell lines are now growing resistant to cisplatin. So researchers are trying to synthesize new compounds that are selectively toxic to tumor cells^{10,11} and cause no harm to normal cells. Titanium complex titanocene dichloride was clinically approved for its higher cytotoxicity in renal cell carcinoma¹² and human ovarian cancer¹³. Recent studies support the cytotoxicity of phenanthroline derivative against various cell lines including cisplatin-resistant cell lines^{14,15}. A cisplatin analogue cis-Pt(dafone)Cl₂ shows considerable cytotoxicity against HeLa and Hacat cell lines¹⁶. Silver complexes have been reported to have anticancer activity. Silver carboxylate dimers possess anticancer activity against human carcinoma cells¹⁷ and silver phosphine complexes are active against cisplatin-resistant cell lines¹⁸. Several Cu (II) chelates have been reported to exhibit enhanced antiproliferative activity^{19,20}. On analysing these results we decided to find out the cytotoxic character of the title complex.

A photocatalyst is a material that absorbs light to bring it to a higher energy level and provides such energy to a reacting substance to make a chemical reaction occur. Environmental pollution gets more and

*Correspondence:

E-mail: biju@sirsyedcollege.ac.in

Abbreviations: dafone, 4,5-diazafluoren-9-one; DFT, density functional theory; FMO, Frontier Molecular Orbitals; LC₅₀, Lethal concentration⁵⁰

more public concern in our society^{21,22}. Wastewater containing dyes coming from textile and paper industry is generally high in both color and organic content²³. Therefore, decolourization process were important in waste water treatment. Decontamination of polluted water by photocatalysis was low cost and effective²⁴. A lot of work has been done to develop heterogeneous photocatalyst with high photocatalytic activities for environmental applications such as water disinfection, hazardous waste remediation, and water purification²⁵⁻²⁷.

Even though the DNA interaction properties²⁸⁻³⁰ of dafone attracted the attention of many researchers, the co-ordination chemistry of dafone is still restricted to a few metals³¹⁻³⁴. There is only one report³⁵ for Mn(II) dafone coordination complex $[\text{Mn}(\text{dafone})_2\text{Cl}_2]$, in which dafone coordinates to Mn(II) in *cis*-mode. There is also report of crystallography of Co(II) $[\text{Co}(\text{dafone})_2(\text{NCS})_2]$ ³⁶, Zn(II) $[\text{Zn}(\text{dafone})_2\text{I}_2]$ ³⁷, Cu(II) $[\text{Cu}(\text{dafone})_2(\text{SCN})_2]$ ³⁸ and $[\text{Cu}(\text{dafone})_2(\text{NCO})_2]$ MeCN³⁵, Ni(II) $[\text{Ni}(\text{dafone})_2(\text{SCN})_2]$ ³⁸ and $[\text{Ni}(\text{dafone})_2(\text{NCS})_2]$ ³⁹ and Hg(II) $[\text{Hg}(\text{dafone})(\text{SCN})_2]$ ³⁸ complexes. In both cobalt and zinc complexes, dafone coordinates in *cis*-mode. The crystallography of the title compound was analysed by various spectroscopic methods and confirmed by single-crystal XRD studies.

Our research work was conducted to find out the cytotoxicity of Manganese – 4,5-Diazafluoren-9-one Complex by standard MTT Assay in Cervical carcinoma cells HeLa (an immortal cell line derived from cervical cancer cells). Selectivity for tumour tissue was checked by its action on Fibroblast cells (L929) (a type of biological cell that synthesises the extracellular matrix and collagen and the most common connective tissue in animals). A compound that is toxic to HeLa cell lines and non-toxic to fibroblast cell lines will be safe for cancer treatment. The photocatalytic activity of the prepared complex was carried out based on degradation of methylene blue dye in presence of the complex using a UV lamp as the source of radiation. The crystallography of the Manganese – 4,5-Diazafluoren-9-one complex was analysed by various spectroscopic methods and confirmed by single-crystal XRD studies.

Materials and Methods

All chemicals were purchased from Ranbaxy chemicals and Sigma Aldrich and used without further purification. Dafone was prepared as per the reported procedure¹. It was precipitated as yellow-orange needles within 1-2 days. IR spectra were measured by using the Thermo Nicolet AVATAR

model FTIR spectrometer using the KBr pellets. An elemental analysis experiment was conducted from SAIF STIC Cochin, Kerala, India.

Synthesis of $[\text{Mn}(\text{dafone})_2(\text{NCS})_2]$

Manganese perchlorate (0.3619 g, 1 mmol) and Ammonium Thiocyanate (0.152 g, 2.00 mmol) were dissolved in a minimum amount of water. To this solution, dafone (0.364 g, 2.00 mmol) dissolved in a minimum amount of acetonitrile was added slowly and kept undisturbed. Golden yellow shining needles were formed within ten days. Yield 0.4113 g (76.81 mmol, 76.81%). Anal (%) Calcd. for $\text{C}_{24}\text{H}_{12}\text{MnN}_6\text{O}_2\text{S}_2$: C, 53.78; H, 2.24; N, 15.69; S, 11.97. Found: C, 54.05; H, 1.32; N, 16.36; S, 11.24; IR (KBr, cm^{-1}) 3431, 3088, 2067, 2053, 1735, 1570, 1412, 1248, 1101, 755 and 524. The crystals are stable in air and melt above 280°C.

Cytotoxic Study

Cytotoxicity of the complex was conducted from Biogenix Research Centre, Thiruvananthapuram, Kerala, India using cervical carcinoma cells (HeLa) and compare the result obtained with normal fibroblast cells (L929). Viability of the cell was evaluated by direct observation of cells by inverted phase-contrast microscope followed by MTT assay method. Any detectable changes in the morphology of the cells, such as rounding or shrinking of cells, granulation, and vacuolization in the cytoplasm of the cells were considered as indicators of cytotoxicity.

Photocatalytic activity

Photocatalytic activity of the prepared complex was carried out using methylene blue dye as the pollutant and UV lamp as the source of radiation. The metal complex (0.01 g) and an aqueous solution of methylene blue (70 mL) were mixed in a beaker and were equilibrated by constant stirring at room temperature in dark for 30 min to allow the adsorption of methylene blue dye, if any, by the complex. The solution is stirred under UV light. The sample was allowed to absorb UV light and 5 mL aliquots were taken and filtered at a definite time interval of 30 min. The filtrate was analysed using a UV-Visible spectrophotometer. When the reaction mixture was stirred, the complex absorbs UV rays and get excited due to the appropriate bandgap. The photogenerated electron-hole pairs produce hydroxyl radicals in the system which decolorises the blue-colored methylene blue solution^{38,39}. The intensity of absorption peak of methylene blue at 663 nm gets diminished gradually

with the extension of the exposure time indicating the degradation of methylene blue dye⁴⁰⁻⁴¹.

X-Ray Crystallography

X-ray diffraction data were collected on a Bruker Kappa APEX2 CCD diffractometer, equipped with graphite monochromated Mo K α radiation ($\lambda = 0.71073\text{\AA}$) at 298 K. Datas were reduced using Computer programs: APEX2⁴², SIR92⁴³, SHELXL2014/7⁴⁴, Mercury⁴⁵, publCIF⁴⁶. The analysis was carried out from SAIF STIC, Kochin.

Computational Analysis

The highest occupied molecular orbital (HOMO) and lowest unoccupied molecular orbital (LUMO) are called Frontier Molecular Orbitals (FMO). The molecular structure of the complex was optimized using density functional theory (DFT). DFT calculations were performed for the complex $[\text{Mn}(\text{dafone})_2(\text{NCS})_2]$ with computational program Gaussian09⁴⁷ using the basis set B3LYP/6-311 G(d,p)⁴⁸.

Results and Discussion

Characterization of the ligand and the complex

Ligand and complex were characterized by various spectroscopic studies. IR Spectrum of dafone shows three characteristic bands, whose wavelengths corresponding to the stretching vibrations of its three types of bonds: 3304 cm^{-1} ($\nu_{\text{C-H}}$), 1714 cm^{-1} ($\nu_{\text{C=O}}$), and 1461 cm^{-1} ($\nu_{\text{C=N}}$). In the IR spectrum of the complex, a strong band in 1410 cm^{-1} may be due to azomethine group (C=N) and a broadband in 1740 cm^{-1} may be due to stretching vibrations of C=O group. The absorption band at 590 nm may be assigned to ${}^6\text{A}_{1g} \rightarrow {}^4\text{T}_{1g}$ (G) transition indicate the octahedral geometry of the complex $[\text{Mn}(\text{dafone})_2(\text{NCS})_2]$.

Molar conductivity of $\sim 10^{-3}$ M solution of the complex in DMF was found to be 12 $\text{Sm}^2\text{mol}^{-1}$ at room temperature, indicate the non-electrolytic nature of $[\text{Mn}(\text{dafone})_2(\text{NCS})_2]$ ⁴⁹.

Application of the complex $[\text{Mn}(\text{dafone})_2(\text{NCS})_2]$

Cytotoxicity

Complex $[\text{Mn}(\text{dafone})_2(\text{NCS})_2]$ was tested for anticancer activity against cervical carcinoma cells. The result was compared with the normal fibroblast cell to check its influence on normal cells. Percentage of viability can be calculated by the equation:

$$\text{Percentage viability} = \frac{\text{Mean OD of Samples}}{\text{OD of Control group}} \times 100$$

Percentage viability of $[\text{Mn}(\text{dafone})_2(\text{NCS})_2]$ against HeLa cells and Fibroblast cells (Tables 1 & 2) and the corresponding photographs (Figs. 1 & 2) are given. From the graphical comparison (Fig. 3) of the percentage viability of HeLa and fibroblast cells against $[\text{Mn}(\text{dafone})_2(\text{NCS})_2]$, it is clear that the complex is more toxic to HeLa cells than the fibroblast cells in a metal concentration varying from 0-100 $\mu\text{g/mL}$. The concentration of the complex that can kill 50% of the unwanted cell (LC_{50} Value) was calculated (Table 3) using ED50 PLUS V1.0 Software.

Photocatalytic activity

The photocatalytic activity of the complex was studied based on its degradation reaction with methylene blue dye. On analyzing the absorbance vs wavelength graph (Fig. 4) of methylene blue dye, the intensity of the characteristic absorption peak of methylene blue at 663 nm gets diminished gradually with the extension of the exposure time. It is an indication of

Table 1 — Percentage viability of $[\text{Mn}(\text{dafone})_2(\text{NCS})_2]$ against HeLa cells

Sample Conc. ($\mu\text{g/mL}$)	OD value I	OD value II	OD value III	Average OD	% Viability
0	0.4952	0.4896	0.4935	0.4928	100
6.25	0.4015	0.4115	0.4137	0.4089	82.97
12.5	0.3878	0.3892	0.3964	0.3911	79.37
25	0.3620	0.3742	0.3685	0.3682	74.72
50	0.3280	0.3364	0.3295	0.3313	67.23
100	0.2851	0.2973	0.2984	0.2936	59.58

Table 2 — Percentage viability of $[\text{Mn}(\text{dafone})_2(\text{NCS})_2]$ against Fibroblast cells

Sample Conc. ($\mu\text{g/mL}$)	OD value I	OD value II	OD value III	Average OD	% Viability
Control	0.7225	0.7376	0.7282	0.7294	100.00
6.25	0.6988	0.6982	0.6801	0.6924	94.92
12.5	0.6408	0.6319	0.6328	0.6352	87.08
25	0.5532	0.5616	0.5572	0.5573	76.41
50	0.5121	0.5270	0.5206	0.5199	71.28
100	0.4431	0.4574	0.4584	0.4530	62.10

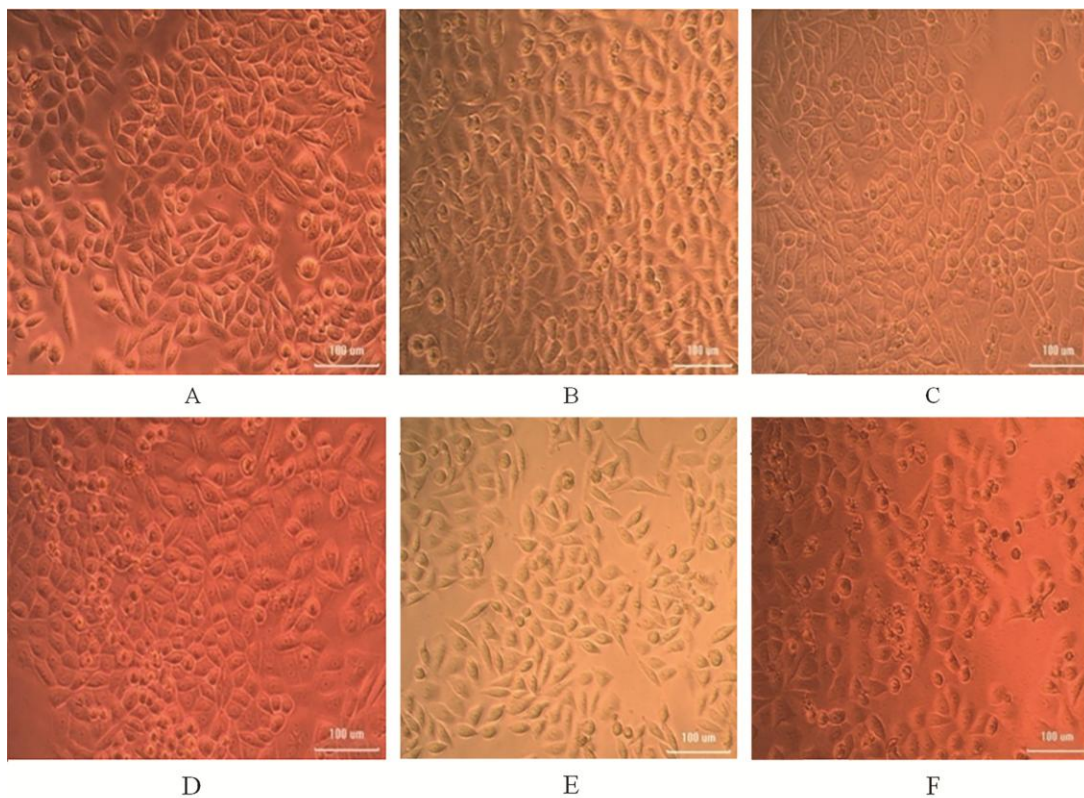


Fig. 1 — Microscopic image of Cervical carcinoma cells (HeLa) when treated with the $[Mn(dafone)_2(NCS)_2]$ in the order of increasing concentration (A) Control; (B) 6.25 µg/mL; (C) 12.5 µg/mL; (D) 25 µg/mL; (E) 50 µg/mL; and (F) 100 µg/mL

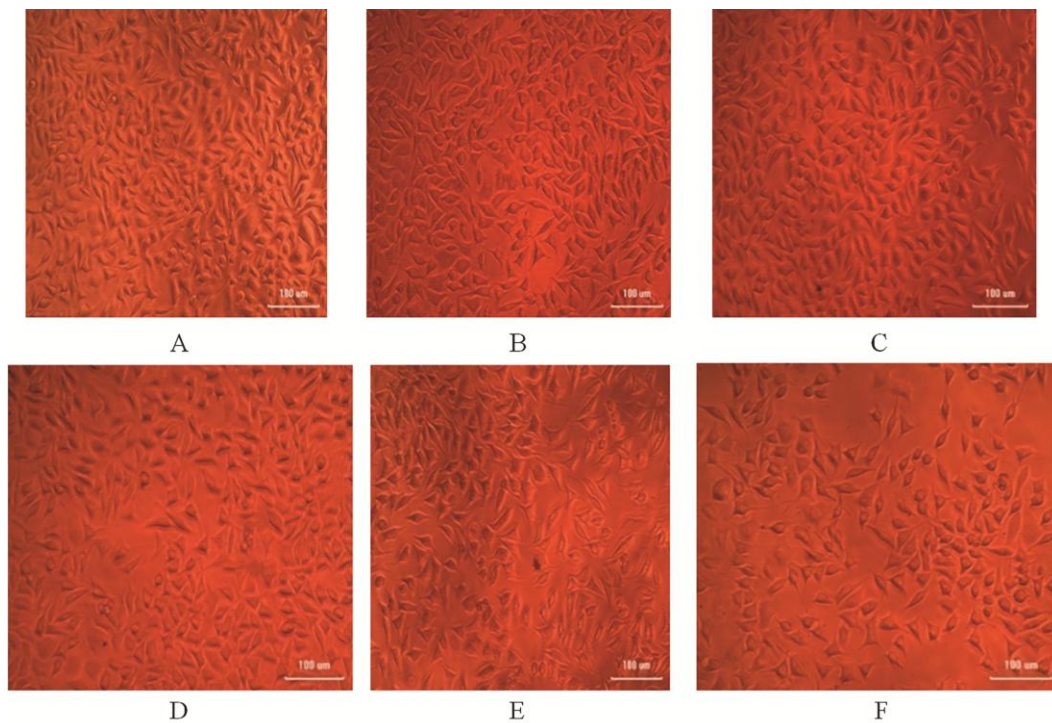


Fig. 2 — Microscopic image of Fibroblast (L929) when treated with the $[Mn(dafone)_2(NCS)_2]$ in the order of increasing concentration (A) Control; (B) 6.25 µg/mL; (C) 12.5 µg/mL; (D) 25 µg/mL; (E) 50 µg/mL; and (F) 100 µg/mL

degradation of methylene blue dye which supports the photocatalytic activity of the complex.

Crystal structure description of $[Mn(dafone)_2(NCS)_2]$

Single crystal X-ray diffraction analysis reveal that the complex $[Mn(dafone)_2(NCS)_2]$ crystallizes in the orthorhombic, $Pbcn$ with cell parameters $a = 3.3803(10)$ Å, $b = 10.4789(7)$ Å and $c = 16.6256(9)$ Å, $\alpha = 90^\circ$, $\beta = 90^\circ$, $\gamma = 90^\circ$ and $Z = 4$ (Fig. 5). Central atom Mn(II) octahedrally coordinated to two thiocyanate anions through nitrogen atoms and two dafone molecules (Fig. 6).

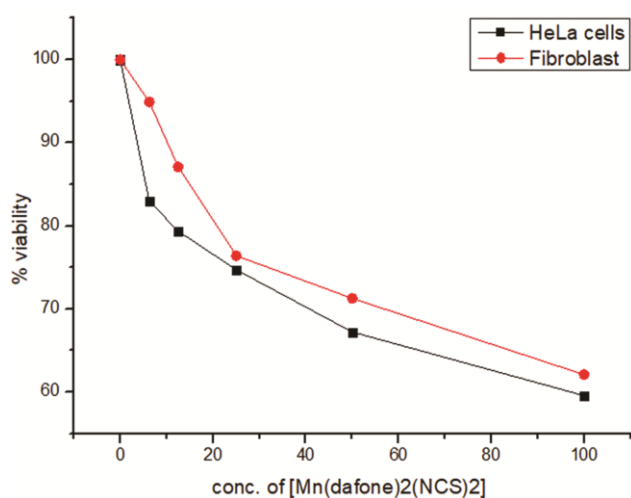


Fig. 3 — A comparison of the percentage viability of HeLa and fibroblast cells against the different concentration of $[Mn(dafone)_2(NCS)_2]$

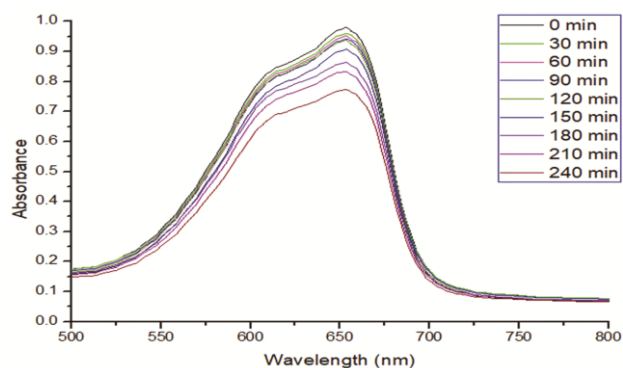


Fig. 4 — Photodegradation plot of methylene blue dye under UV light in presence of $[Mn(dafone)_2(NCS)_2]$ at various time intervals

Table 3 — LC_{50} Value for the complex $[Mn(dafone)_2(NCS)_2]$

Cell lines	Average LC_{50} Value in µg/mL
Cervical carcinoma cells	133.183
Fibroblast cells	129.523

The Mn(II) ions have an octahedral configuration and are located in a special position. Two dafone ligands chelate in cis-mode with an average Mn—N distance of 2.367 Å. The multidentate NCS⁻ ligand coordinates through the nitrogen atom. The Mn—N(NCS) distance is 2.095 Å, which is much shorter than the Mn—dafone distance. The *cis* mode of coordination has been previously observed for both Co(II) and Zn(II) complexes with dafone.

Supramolecular features

The crystal packing of the title compound (Fig. 7) shows several weak intermolecular short contacts and hydrogen bonding interactions, such as C11—H11...N3 (2.721 Å), C11—H11...C12 (2.707 Å), C3—H3...S1 (2.949 Å), C1—H1...C12 (2.870 Å), S1...O1 (3.195 Å) and the contacts expands to become three-dimensional architecture.

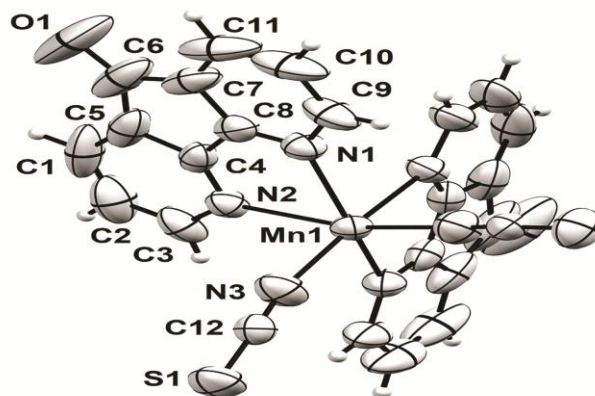


Fig. 5 — The molecular structure of $[Mn(dafone)_2(NCS)_2]$, with the atom labelling. Displacement ellipsoids are drawn at the 50% probability level

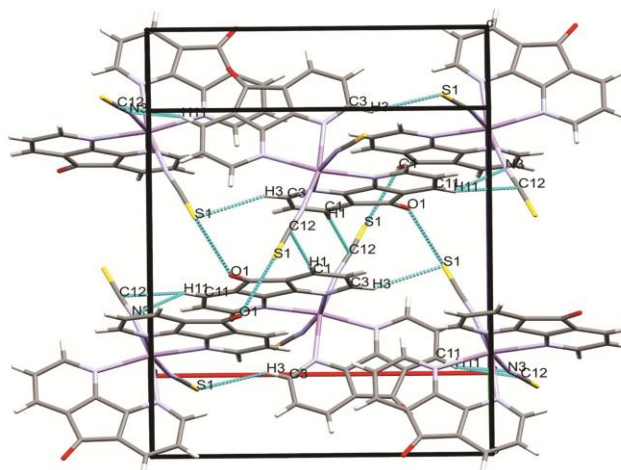


Fig. 6 — A view of the crystal packing of the complex. Dashed lines denote the intermolecular short contact

Refinement

Crystal data, data collection, and structure refinement details (Table 4) are summarized. The C-bound H atoms were positioned geometrically and refined using a riding model, with C—H = 0.93 Å and with $U_{iso}(H) = 1.2U_{eq}(C)$. Selected bond length and bond angles (Table 5) are given.

Frontier Molecular orbital studies

Frontier Molecular Orbitals decides the optoelectronic properties of the molecule. A molecule can be classified into soft and hard acids depending upon the HOMO-LUMO gap. The geometry of the complex is optimised (Fig. 7), and the calculated energy of HOMO and LUMO orbital's of the complex been found to be negative, indicates its stability. The optimized geometry is slightly different from the crystal structure, in which the average Mn1—N2 bond length is increased to 2.64 Å from 2.39 Å and Mn1—N1 and Mn1—N3 distance remains similar 2.32 from 2.34 Å and 2.04 from 2.09 Å, respectively. The HOMO-LUMO gap is calculated to be 0.66 eV, which indicates that the complex molecule is a soft acid. The hardness parameter, which is calculated by the formula of the complex, is

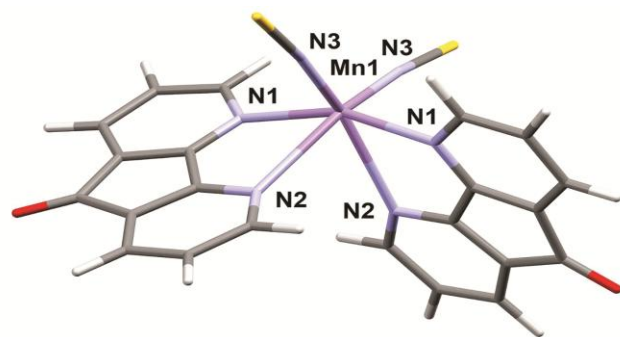


Fig. 7 — Optimized structure of $[Mn(dafone)_2(NCS)_2]$ from computational analysis

Table 4 — Crystal data and structure refinement for $[Mn(dafone)_2(NCS)_2]$

Empirical formula	$C_{24}H_{12}Mn N_6O_2S_2$
Formula weight	535.46
Temperature (K)	296(2)
Wavelength(Å)	0.71073
Crystal system	Orthorhombic
Space group	<i>Pbcn</i>
Unit cell dimensions	
a(Å)	13.3803(10)
b(Å)	10.4789(7)
c(Å)	16.6256(9)
α (°)	90
β (°)	90
γ (°)	90
Volume (Å ³ Å ³)	2331.1(3)
Z	4
D_{calc} (g cm ⁻³)	1.526
μ (mm ⁻¹)	0.781
F (000)	1084
Crystal size (mm)	0.30 x 0.20 x 0.20
Theta range for data collection	2.469 to 28.422 deg.
Limiting indices	$17 \leq h \leq 17$,
Reflections collected / unique	17638 / 2877 [R(int) = 0.0381]
Completeness to theta = 25.242	100.0 %
Absorption correction	Semi empirical from equivalents
Max. and min. transmission	0.859 and 0.800
Refinement method	Full-matrix least-squares on F ²
Data / restraints / parameters	2877 / 0 / 159
Goodness-of-fit	0.919
R_I [$I > 2\sigma(I)$]	0.0470
wR2	0.0796
Largest diff. peak and hole	0.413 and -0.293 e.Å ⁻³

Table 5 — Selected bond length in [Å] and bond angles in [°] for $[Mn(dafone)_2(NCS)_2]$

Mn1—N3i 2.095 (3)	Mn1—N2i 2.395 (2)
Mn1—N1i 2.338 (2)	
N3—Mn1—N3i 98.51 (15)	N1i—Mn1—N2i 76.02 (8)
N3—Mn1—N1i 107.81 (11)	N1—Mn1—N2i 83.97 (8)
N3i—Mn1—N1i 89.96 (11)	N3—Mn1—N2 165.32 (10)
N3—Mn1—N1 89.96 (11)	N3i—Mn1—N2 90.03 (9)
N3i—Mn1—N1 107.81 (11)	N1i—Mn1—N2 83.97 (8)
N1i—Mn1—N1 152.96 (12)	N1—Mn1—N2 76.02 (8)
N3—Mn1—N2i 90.03 (9)	N2i—Mn1—N2 84.28 (11)
N3i—Mn1—N2i 165.32 (10)	
Symmetry code: (i) $-x+1, y, -z+1/2$	

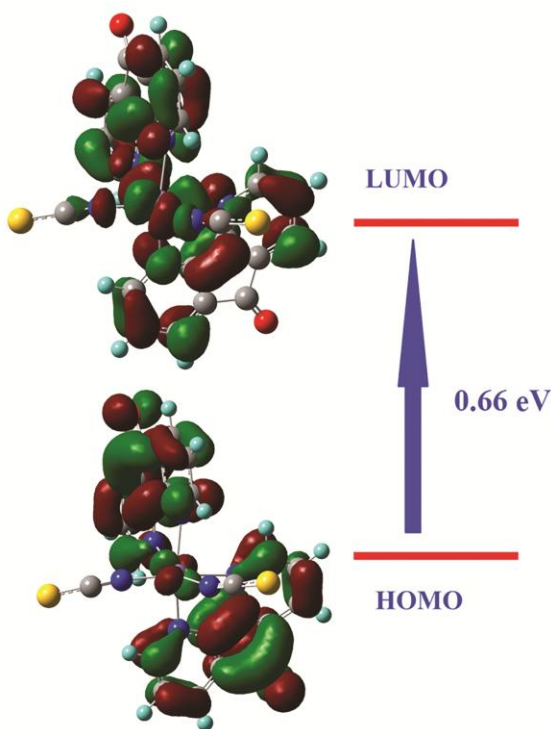


Fig. 8 — Electron distribution of the HOMO-LUMO orbitals of the $[\text{Mn}(\text{dafone})_2(\text{NCS})_2]$

found to be 0.0053 which indicates that the complex is soft. The electron distribution of the HOMO-LUMO orbital's of $[\text{Mn}(\text{dafone})_2(\text{NCS})_2]$ is given (Fig. 8).

Conclusion

Complex $[\text{Mn}(\text{dafone})_2(\text{NCS})_2]$ was prepared by solvent-based synthesis method using acetonitrile and methanol as solvent. Characterisation of ligand and complexes were done by elemental and various spectral analysis. The structure of the complex was confirmed by Single-crystal X-ray diffraction studies. The complex shows octahedral geometry. Cytotoxicity of the complex was studied based on percentage viability of the cell evaluated by direct observation of cells by inverted phase-contrast microscope followed by MTT assay method. The complex was found to be more active against cervical carcinoma cells than fibroblast cells in any of the metal concentrations varying from 0-100 $\mu\text{g}/\text{mL}$. Its photocatalytic activity was clear from the photodegradation plot of methylene blue dye.

Acknowledgement

CCDC deposit number for the single crystal x-ray structure is CCDC- 2039258. We thank Biogenix

Research Centre, Thiruvananthapuram, Kerala, India for cytotoxic studies, SAIF STIC CUSAT, Kerala, India for the XRD analysis, Solid-state electronic spectra & CHN analysis, & National Institute for Interdisciplinary Science and Technology, Thiruvananthapuram, Kerala, India for ^1H NMR spectra.

Reena thank University Grants Commission for the FDP fellowship and ARB thank the FIST-UGC fund for the IR spectrophotometer at Sir Syed College, Taliparamba, Kerala.

B. Kishore babu and K.Mohana Rao acknowledge grants from the Ref No: 42-354/2013 UGC (INDIA), New Delhi. We are grateful for the technical assistance provided by the Department of Engineering Chemistry at the Andhra University, Visakhapatnam (INDIA) and the University of Hyderabad for providing the spectral data.

Conflict of interest

All authors declare no conflict of interest.

References

- Henderson Jr LJ, Fronczek FR & Cherry WR, Selective perturbation of ligand field excited states in polypyridine ruthenium(II) complexes. *J Am Chem Soc*, 106 (1984) 5876.
- Prasad K, Subhash P & Ekkehard S, Neutral metal complex in an ionic pocket: synthesis, physicochemical properties and X-ray structure of a copper(II) complex containing neutral as well as cationic dafone ligands and dafonium perchlorate. *Inorganica Chimica Acta*, 321 (2001) 193.
- Lu Z, Duan C, Tian Y & You X, Synthesis, Characterization, and Crystal Structure of a Novel Copper(II) Complex with an Asymmetric Coordinated 2,2'-Bipyridine Derivative: A Model for the Associative Complex in the Ligand-Substitution Reactions of $[\text{Cu}(\text{tren})\text{L}]^{2+}$. *Inorg Chem*, 35 (1996) 2253.
- Treshchalina EM, Konovalova AL, Presnov MA, Chapurina LF & Belichuk NI, Antitumor properties of mixed coordination compounds of copper (II) and alpha-amino acids. *Dokl Akad Nauk (SSSR)*, 248 (1979) 1273.
- Brown DB, Khokhar AR, Hacker MP, Lokys L, Burchenal JH, Newman RA, McCormack JJ & Frost D, Synthesis and antitumor activity of new platinum complexes. *J Med Chem*, 25 (1982) 952.
- Saeed-ur-Rehman, Muhammad I, Sadia R, Alia F & Shahnawaz, Synthesis, characterization and antimicrobial studies of transition metal complexes of imidazole derivative. *Bull Chem Soc Ethiop*, 24 (2010) 201.
- Mirabelli CK, Hill DT, Faucette LF, McCabe FL, Girard GR, Bryan DB, Sutton BM, Bartus JO, Crooke ST & Johnson RK, Antitumor activity of bis(diphenylphosphino)alkanes, their gold(I) coordination complexes, and related compounds. *J Med Chem*, 30 (1987) 2181.
- Kelland LR, New platinum antitumor complexes. *Crit Rev Oncol Hematol*, 15 (1993) 191.
- Kelland LR, Barnard CF, Mellish KJ, Jones M, Goddard PM, Valenti M, Bryant A, Murrer BA & Harrap KR, A novel

- trans-platinum coordination complex possessing *in vitro* and *in vivo* antitumor activity. *Cancer Res*, 54 (1994) 5618.
- 10 Ganesh KN, Satya D P, Sathi M, Sudip K G, Panchanan P & Anindya S G, Thiol stabilized copper nanoparticles exert antimicrobial properties by preventing cell division in *Escherichia coli*. *Indian J Biochem Biophys*, 57 (2020) 151.
 - 11 Swadesh S, Amrita P, Anirban C & Santanu P, A novel compound β -sitosterol-3-O- β -D-glucoside isolated from *Azadirachta indica* effectively induces apoptosis in leukemic cells by targeting G0/G1 populations. *Indian J Biochem Biophys*, 57 (2020) 27.
 - 12 Kurbacher CM, Nagel W, Mallmann P, Kurbacher JA, Sass G, Hubner H, Andreotti PE & Krebs D, *In vitro* activity of titanocenedichloride in human renal cell carcinoma compared to conventional antineoplastic agents. *Anticancer Res*, 14 (1994) 1529.
 - 13 Friedrich M, Villena-Heinsen C, Farnhammer C & Schmidt W, Effects of vinorelbine and titanocene dichloride on human tumour xenografts in nude mice. *Eur J Gynaecol Oncol*, 19 (1998) 333.
 - 14 Roy S, Hagen KD, Maheswari PU, Lutz M, Spek AL, Reedijk J & Van Wezel GP, Phenanthroline derivatives with improved selectivity as DNA-targeting anticancer or antimicrobial drugs. *Chem Med Chem*, 3 (2008) 1427.
 - 15 Marzano C, Pillei M, Tisato F & Santini C, Copper complexes as anticancer agents. *Anticancer Agents Med Chem*, 9 (2009) 185.
 - 16 Biju AR, Rajasekharan MV, Satish S Bhat, Ayesha A Khan & Avinash S Kumbhar Synthesis, crystal structure and cytotoxicity studies of cis-dichloro(4,5-diazafluoren-9-one)platinum(II). *Inorganica Chimica Acta*, 423 (2014) 93.
 - 17 Zhu HL, Zhang XM & Liu XY, Clear Ag-Ag bonds in three silver(I) carboxylate complexes with high cytotoxicity properties. *Inorg Chem Commun*, 6 (2003) 1113
 - 18 Liu JJ, Galettis P, Farr A, Maharaj L, Samarasinha H, McGechan AC, Baguley BC, Bowen RJ, Berners-Price SJ & McKeage MJ, *In vitro* antitumour and hepatotoxicity profiles of Au(I) and Ag(I) bidentate pyridyl phosphine complexes and relationships to cellular uptake. *J Inorg Biochem*, 102 (2007) 303.
 - 19 Solomon EI, Sundaram UM & Machonkin TE, Multicopper oxidases and oxygenases. *Chem Rev*, 96 (1996) 2563.
 - 20 Tripathi L, Kumar P, Singhai AK, Role of chelates in treatment of cancer. *Indian J Cancer*, 44 (2007) 62.
 - 21 Shannon MA, Bohn PW, Elimelech M, Georgiadis JG, Marinas BJ & Mayes AM, Science and technology for water purification in the coming decades. *Nature*, 452 (2008) 301.
 - 22 Hoffmann MR, Martin ST, Choi W & Bahneman DW, Environmental applications of semiconductor photocatalysis. *Chem Rev*, 95 (1995) 69.
 - 23 Zhiyong Y, Laub D, Bensimon M & Kiwi J, Flexible polymer TiO₂ modified film photocatalysts active in the photodegradation of azo-dyes in solution. *Inorg Chim Acta*, 361 (2008) 589.
 - 24 Macwan DP, Dave PN & Chaturvedi S, A review on nano-TiO₂ sol-gel type syntheses and its applications. *J Mater Sci*, 46 (2011) 3669.
 - 25 Ungelenk J & Feldmann C, Adjustable kinetics in heterogeneous photocatalysis demonstrating the relevance of electrostatic interactions. *Appl Catal B: Environ*, 127 (2012) 11.
 - 26 Mena E, Reya A, Acedo B, Beltrán FJ & Malato S, TiO₂ photocatalytic oxidation of a mixture of emerging contaminants: A kinetic study independent of radiation absorption based on the direct-indirect model. *Chem Eng J*, 204–206 (2012) 131.
 - 27 Ge L & Liu J, Photocatalytic active Bi₂WO₆ sensitized by CdS quantum dots (QDs). *Appl Catal B: Environ*, 105 (2011) 289.
 - 28 Pyle AM, Rehmann JP, Meshoyrer R, Kumar CV, Turro NJ & Barton JK, Mixed-ligand complexes of ruthenium(II): factors governing binding to DNA. *J Am Chem Soc*, 111 (1989) 3051.
 - 29 Kumari NKP & Jagannadham MV, Organic solvent induced refolding of acid denatured heynein: molten: Evidence of domains in the molecular structure of the protein and their sequential unfolding. *J Protein Proteomics*, 2 (2011) 11.
 - 30 Prasanna Kumari NK & Jagannadham, MV, Deciphering the molecular structure of cryptolepain in organic solvents. *Biochimie*, 94 (2012) 354.
 - 31 Menon S, Balagopalakrishna C, Rajasekharan MV & Ramakrishna BL, Synthesis, Crystal Structure, Magnetic Susceptibility, and Single-Crystal EPR Studies of [DafoneH₂][(CuCl₃H₂O)Cl]. *Inorg Chem*, 33 (1994) 950.
 - 32 Menon S & Rajasekharan MV, A Channel-Forming Polyiodide Network in [Cu(dafone)₃]I₁₂. A Tris Chelate of Dafone and a New Planar Structure for the I₁₂²⁻ Ion (Dafone = 4,5-Diazafluoren-9-one). *Inorg Chem*, 36 (1997) 4983.
 - 33 Menon S & Rajasekharan MV, Bis chelate Cu(II) complexes of dafone—synthesis, structural, EPR and optical spectral studies. *Polyhedron*, 17 (1998) 2463.
 - 34 Miao S, Kang H, Du C & Ji B, Nickel complexes of 4, 5-Diazafluoren-9-one. *X-Ray Struct Anal Online*, 22 (2006) 45.
 - 35 Wu ZY & Xu DJ, cis-Dichlorobis(4,5-diazafluoren-9-one-K²N,N')manganese(II) ethanol Solvate. *Acta Cryst E*, 60 (2004) m839.
 - 36 Shi XU, You XZ, Li C & Xiong RG, Synthesis, spectral and magnetic studies on mixed-ligand complexes M(DIAFO)₂(NCS)₂ and M(DIAFH)₂X₂ (M = Fe^{II}, Co^{II}, Ni^{II}). The crystal structure of Co(DIAFO)₂(NCS)₂. *Trans Met Chem*, 20 (1995) 191.
 - 37 Maguire L, Seward CM, Baljak S, Reumann T, Ortin Y, Banide E & Nikitin K, Muller-Bunz H, McGlinchey MJ, A Synthetic and X-ray Crystallographic Study of Zinc and Platinum Complexes of 4,5-Diazafluoren-9-one (Dafone) and Dicobalt Hexacarbonyl Derivatives of 9-Phenylethynyl-4,5-Diazafluoren-9-ol: Chelation vs Monocoordination. *Eur J Inorg Chem*, (2009) 3250.
 - 38 Barbara M, Mariusz W, Joanna P, Anna S, Nawrot I & MichalikKrishna K, Cu(II), Ni(II) and Hg(II) thiocyanate complexes incorporating 4,5-diazafluoren-9-one: Synthesis spectroscopic characterization X-ray studies & magnetic properties. *Struct Chem*, 22 (2011) 1053.
 - 39 Kishore BB, Elahi SM, Krishna CT & Rajasekharan, Synthesis and Structural Studies of copper(II) and nickel(II) complexes containing 4,5-diazafluoren-9-one and pseudohalides: Metal ion directed isomer preference. *Indian J Chem*, 50A (2011) 1318.
 - 40 Tabbi G, Fry SC & Bonomo RP, ESR study of the non-enzymic scission of xyloglucan by an ascorbate-H₂O₂-copper system: the involvement of the hydroxyl radical and the degradation of ascorbate. *J Inorg Biochem*, 84 (2001) 179.

- 41 Verma P, Baldrian P & Nerud F, Decolorization of structurally different synthetic dyes using cobalt (II)/ascorbic acid/hydrogen peroxide system. *Chemosphere*, 50 (2003) 975.
- 42 Bruker SAINT, XPREP, APEX2 and SADABS. (Bruker AXS Inc, Madison, Wisconsin, USA) (2004).
- 43 Altomare A, Cascarano G, Giacovazzo C, Guagliardi A, Burla MC, Polidori G & Camalli M, SIR92 - a program for automatic solution of crystal structures by direct methods. *J Appl Cryst*, 27 (1994) 435.
- 44 Sheldrick GM, Crystal structure refinement with *SHELXL*. *Acta Cryst C*, 71 (2015) 3.
- 45 Macrae CF, Edgington PR, McCabe P, Pidcock E, Shields GP, Taylor R, Towler M & Van de Streek J, Mercury: Visualization and Analysis of Crystal Structures. *J Appl Cryst*, 39 (2006) 453.
- 46 Westrip SP, publCIF: software for editing, validating and formatting crystallographic information files. *J Appl Cryst*, 43 (2010) 920.
- 47 Frisch MJ, Trucks GW, Schlegel HB, Scuseria GE, Robb MA, Cheeseman JR, Scalmani G, Barone V, Mennucci B, Petersson GA, Nakatsuji H, Caricato M, Li X, Hratchian HP, Izmaylov AF, Bloino J, Zheng G, Sonnenberg JL, Hada M, Ehara M, Toyota K, Fukuda R, Hasegawa J, Ishida M, Nakajima T, Honda Y, Kitao O, Nakai H, Vreven T, Montgomery JA, Jr Peralta JE, Ogliaro F, Bearpark M, Heyd JJ, Brothers E, Kudin KN, Staroverov VN, Kobayashi R, Normand J, Raghavachari K, Rendell A, Burant JC, Iyengar SS, Tomasi J, Cossi M, Rega N, Millam JM, Klene M, Knox JE, Cross JB, Bakken V, Adamo C, Jaramillo J, Gomperts R, Stratmann RE, Yazyev O, Austin AJ, Cammi R, Pomelli C, Ochterski JW, Martin RL, Morokuma K, Zakrzewski VG, Voth GA, Salvador P, Dannenberg JJ, Dapprich S, Daniels AD, Farkas Ö, Foresman JB, Ortiz JV, Cioslowski J, Fox DJ, Gaussian 09, Revision E.01.(Gaussian, Inc., Wallingford CT) (2009).
- 48 Becke AD, A new mixing of Hartree-Fock and local density-functional theories. *J Chem Phys*, 98 (1993) 1372.
- 49 Geary WJ, The Use of Conductivity Measurements in Organic Solvents for the Characterisation of Coordination Compounds. *Coord Chem Rev*, 7 (1971) 81.

CYTOTOXIC STUDY OF NICKEL OROTATE IMIDAZOLE COMPLEX AND ITS SPECTROSCOPIC DETERMINATION

K. PRAVEEN¹, CH. V. PADMARAO¹, K. MOHANA RAO¹, B. KISHORE BABU¹ & B. SWARNALATHA²

¹Department of Engineering Chemistry, AUCE (A), Andhra University, Visakhapatnam, Andhra Pradesh, India

²Department of Physics, SKRC Women's College, Rajahmundry, Andhra Pradesh, India

ABSTRACT

Many activities of metal ions in biology have stimulated the development of metal-based therapeutics. In metal complexes metal centers, being positively charged, are favored to bind to negatively charged biomolecules; the constituents of proteins and nucleic acids offer excellent ligands for binding to metal ions. The pharmaceutical use of metal complexes therefore has excellent potential. A broad array of medicinal applications of metal complexes have been investigated, and several recent reviews summarize advances in these fields¹⁻⁵. Some selected compounds that are currently used in clinical diagnosis and treatment. Designing ligands that will interact with free or protein-bound metal ions is also a recent focus of medicinal inorganic research⁶⁻⁸. Antimicrobial screening of $[\text{Ni}(\text{H}_2\text{Or})(\text{H}_2\text{O})_2(\text{imd})_2]$ complex was already done and published by B. Kishore Babu et al⁹ in recent international article.

KEYWORDS: Orotic Acid, Complex, Imidazole, Cytotoxic Activity

INTRODUCTION

EXPERIMENTAL

Reagents

All chemicals were purchased from SRL chemicals and used without further purification.

Synthesis

Synthesis of $[\text{Ni}(\text{H}_2\text{Or})(\text{H}_2\text{O})_2(\text{imd})_2]$ (1)

An methanolic (5 ml) solution of Nickel nitrate (0.291g, 1.0 mmol) was added to an sodium hydroxide solution(10ml) of Orotic acid under stirring conditions and the solution turned to sky blue with little turbidity and then aqueous solution(5 ml) of imidazole (0.068 g, 1.0 mmol) was added which resulted into a clear greenish blue solution. After constant stirring at room temperature for 30 minutes, The clear solution was filtered off and the solution is left for slow evaporation in the beaker and blue crystals were obtained in 2 weeks . The crystals were washed with methanol. They were soluble in methanol. Yield 0.190 g (0.652 mmol, 65.29 %). Anal. exptal. $\text{C}_{12}\text{H}_{14}\text{N}_5\text{NiO}_6$ (M.Wt. 382.99) C, 32.84; H, 4.110; N, 23.78. theoretical: C, 32.33; H, 3.81; N, 23.24. Important IR absorptions (KBr disk, cm^{-1}): 3445, 3227, 3137, 2614, 1620, 1559, 1491, 1260, 1097, 760, 746, 588 and 479, 454.

Measurements

IR spectrum was obtained with a Shimadzu FT-IR 8000 spectrometer. Elemental analysis was obtained using a FLASH

EA 1112 SERIES CHNS analyzer. Electronic spectrum was recorded on Shimadzu UV/Vis/NIR spectrophotometer.

SEM were recorded on JSM-6610. P-XRD Spectrum was recorded on D8 Advance diffractometer, Bruker.

Structure of Ni (H₂Or)(imd)₂(H₂O)₂

mer-Diaquabis(1*H*-imidazole-κ³N³)(orotato-κ²N³,O⁴)nickel(II)

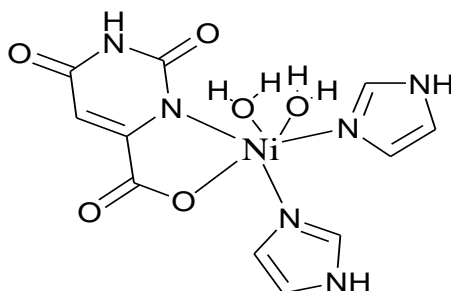


Figure 1: Structure of Ni (H₂Or)(imd)₂(H₂O)₂

The title mononuclear complex, [Ni(C₅H₂N₂O₄)(C₃H₄N₂)₂(H₂O)₂] has been synthesized. The Ni^{II} ion in the complex has a distorted octahedral coordination geometry comprised of one deprotonated pyrimidine N atom and the adjacent carboxylate O atom of the orotate ligand, two tertiary imidazole N atoms and two aqua ligands.

IR Spectrum of Ni (H₂Or) (Imd)₂ (H₂O)₂

The strong and broad absorption bands of m(OH) vibrations of H₂O in complexes is observed at 3445 cm⁻¹. IR spectra of the complexes exhibit a medium intensity and broad band in the 3227–3137 cm⁻¹ region which can be attributed to the N–H stretching vibration. The relatively weak two close bands at 2752–2964 cm⁻¹ are due to the m(CH) vibrations. The strong and broad bands appeared at 1620 and 1491 cm⁻¹ regions in this complex is ascribed to the asymmetric and symmetric stretching vibrations of the coordinated carboxylate groups of the orotate ligand, respectively. In IR spectra of the complexes, m(OHacid) band at 2500 cm⁻¹ in the orotic acid completely disappeared and a new carboxylate band m(COO) appeared between 1491cm⁻¹, indicating that the carboxylate group participates in the coordination with the metal ions by deprotonation.

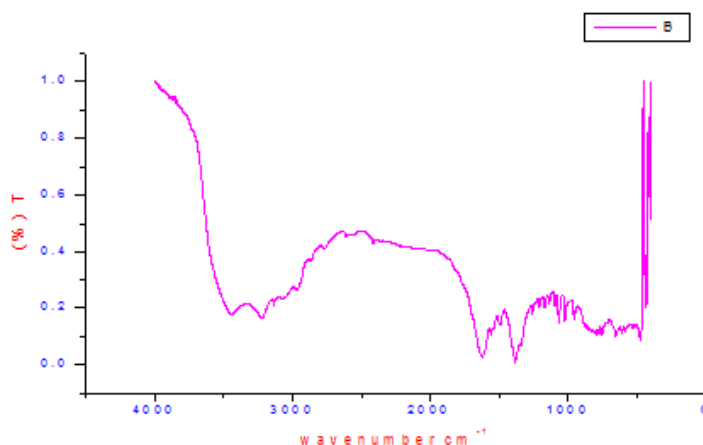


Figure 2: IR Spectrum of Ni (H₂Or) (Imd)₂ (H₂O)₂ (400-4000 cm⁻¹)

Electronic Spectrum of Ni (H₂Or) (Imd)₂ (H₂O)₂

The complex has a shoulder broad band at 325 nm may be assigned to the following d–d transition. This result confirms the complexation of metal ions via carboxylic group. The spectra of the complex was done in DMSO. There are two detected absorption bands at around (210, 235 nm) and 280 nm assigned to π–π* and n–π* transitions, respectively, in the electronic spectrum of the ligand. These transitions also found in the spectra of the complexes, but they are shifted towards lower wavelength, confirming the coordination of the ligand to the metallic ions. The first band around 210 and

235 nm is probably due to a $\pi-\pi^*$ of the exocyclic band in heterocyclic ring and also assigned to the two carbonyl groups. However, the second band around 280 nm is due to presence of COOH group¹⁰. In case of orotate complexes, the carboxylic group is blue shifted with increase the intensity (absorbance). This result confirms the complexation of metal ions via carboxylic group (monodentate chelating). The complex has a shoulder broad band at 325 nm may be assigned to the following d-d transition.

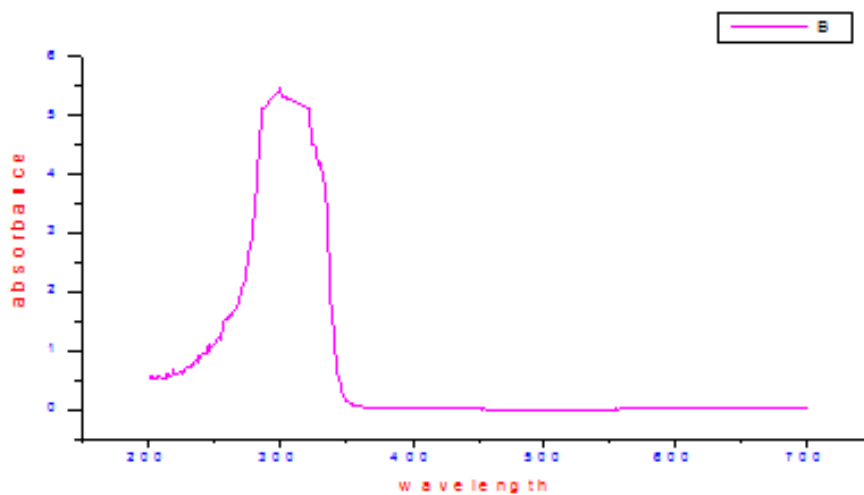


Figure 3: Electronic Spectrum of Ni (H₂Or) (Imd)₂ (H₂O)₂

Raman Spectrum of Ni(H₂Or)(imd)₂(H₂O)₂:

The strong Raman band at 1628.92 cm⁻¹ is assigned to the stretching vibration of the carboxylate group, and asymmetric COO stretching vibration should be assigned to the strong band at 1335.90 cm⁻¹ in the IR spectrum (the corresponding Raman band at 1335.90 cm⁻¹ is weak). The large frequency difference (293 cm⁻¹) between the two stretching frequencies gives the additional evidence for the unidentate type of coordination of the carboxylate group to the nickel(II) ion. This assignment is also confirmed by the recently reported Raman spectrum of cis- [Cu(H₂Or)₂](NH₃)₂, where the corresponding two carboxylate stretching vibrations have been observed at 1631 and 1315 cm⁻¹, respectively¹¹.

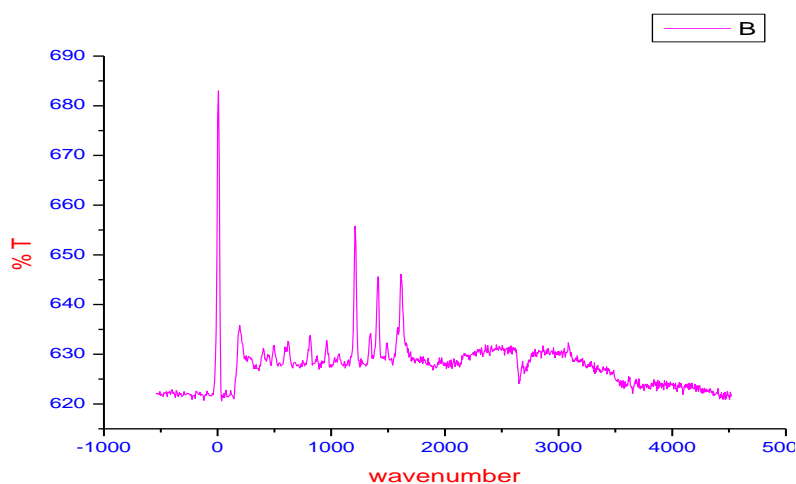


Figure 4: Raman Spectrum of Ni (H₂Or) (imd)₂ (H₂O)₂

Powder XRD Spectrum of Ni (H₂Or) (imd)₂ (H₂O)₂

Although single crystal X-ray crystallographic investigation is the most precise source of information regarding the structure of a complex, the difficulty of obtaining crystalline complexes renders this method unsuitable for such a

study. However, a variety of other spectroscopic techniques could be used with good effect for characterizing the metal complexes as X-ray power diffraction. The crystallite size calculations were performed using Scherrer equation^{12,13}. According to the crystallite size of the complex, the presented metal complex is in the form of nano.

Table 1: Crystallite Size of Ni (H₂Or) (imd)₂ (H₂O)₂

Complex	2θ	FWHM	Crystallite Size
Ni(H ₂ Or)(imd) ₂ (H ₂ O) ₂	22.468	0.269 ⁰	298.02 Å ⁰ (29.8 nm)

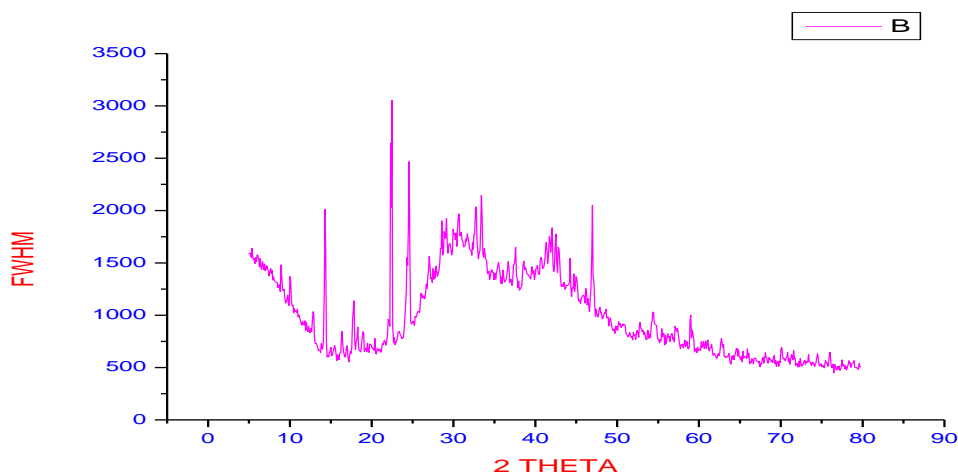


Figure 5: Powder XRD Spectrum of Ni (H₂Or) (imd)₂ (H₂O)₂

Scanning Electron Microscopy

SEM photographs of the free ligand and synthesized metal complex were presented in Figure 6 and 7. From the SEM photographs, we noted that there is a uniform matrix of the synthesized complex, i.e., the complex is homogeneous phase material. The free ligand shows flakes and the particle size recorded in the range of 5–10 μm. The complex is ice bar shaped morphology with 5-11 μm particle size. SEM images Orotic acid ligand differ significantly from that of the metal complexes due to the coordination of the metal ions to the donor sites of the ligands.

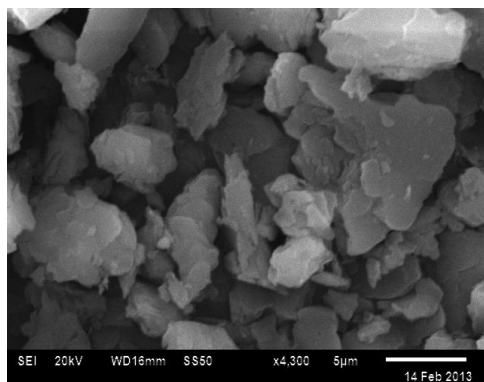


Figure 6: SEM Micrograph of H₃Or at the Range of 5 μm

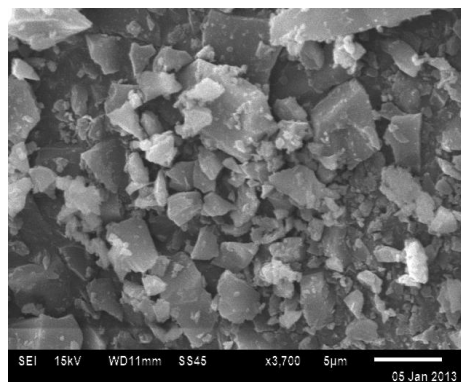


Figure 7: SEM Micrograph of Ni(H₂Or) (imd)₂ (H₂O)₂ at the Range of 5 μm

Cytotoxic Studies

Cell Culture

Human cancer cell lines used in this study were procured from National Centre for Cell Science, Pune. All cells were grown in Minimal essential medium (MEM, GIBCO) supplemented with 4.5 g/L glucose, 2 mM L-glutamine and 5% fetal bovine serum (FBS) (growth medium) at 37°C in 5% CO₂ incubator.

MTT Assay¹⁴

The MTT assay developed by Mosmann¹ was modified and used to determine the inhibitory effects of test compounds on cell growth *in vitro*. In brief, the trypsinized cells from T-25 flask were seeded in each well of 96-well flat-bottomed tissue culture plate at a density of 5×10^3 cells/well in growth medium and cultured at 37°C in 5% CO₂ to adhere. After 48hr incubation, the supernatant was discarded and the cells were pretreated with growth medium and were subsequently mixed with different concentrations of test compounds (12.5,25,50,100,200 µg/ml) in triplicates to achieve a final volume of 100 µl and then cultured for 48 hr. The compound was prepared as 1.0 mg/ml concentration stock solutions in DMSO. Culture medium and solvent are used as controls. Each well then received 5 µl of fresh MTT (0.5mg/ml in PBS) followed by incubation for 2hr at 37°C. The supernatant growth medium was removed from the wells and replaced with 100 µl of DMSO to solubilize the colored formazan product. After 30 min incubation, the absorbance (OD) of the culture plate was read at a wavelength of 492 nm on an ELISA reader, Anthos 2020 spectrophotometer.

Breast Cancer Activity of Ni (H₂Or) (imd)₂ (H₂O)₂

Nickel Orotate Imidazole complex was screened for their cytotoxicity (MCF-7). From the data, it was observed that the complex displayed their cytotoxic activities as IC₅₀ (µg/mL) against Breast cancer MCF-7, the IC₅₀ values of all the nickel complexes are listed in table 2. The activity is similar to standard tamoxifen. The Untreated and treated inhibition zones are shown in the figure 9 to 10. The cellular response on hormone (Tamoxifen) is almost same in this study. Some more studies are required to finalise this complex as a potential drug.

Blank : 0.040

Control : 0.627

Table 2: Dose Response of Ni(H₂Or) (imd)₂ (H₂O)₂ on MCF-7 (Breast Cancer) Cell Line

Conc (ug/ml)	OD of Tamoxifen at 450 nm	% Cell Survival	% Cell Inhibition	OD of Extract at 450 nm	% Cell Survival	% Cell Inhibition
12.5	0.468	89.3	10.7	0.616	98.1	1.9
25	0.366	66	34	0.523	82.3	17.7
50	0.201	33.6	66.4	0.294	43.3	56.7
100	0.126	17.9	82.1	0.282	41.2	58.8
200	0.110	14.6	85.4	0.227	31.9	68.1

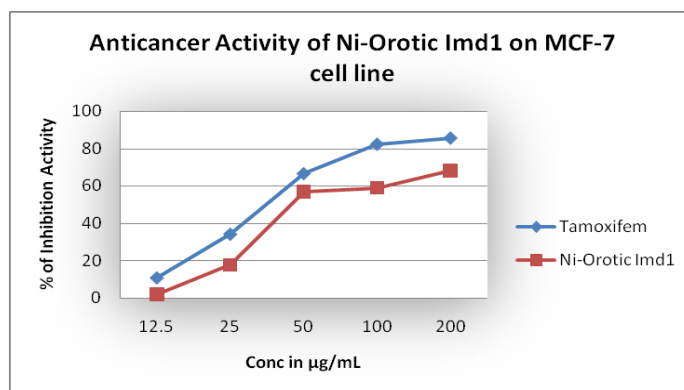


Figure 8

Comparison for Standard Drug and the Complex

IC ₅₀ Standard	39.671 µg/mL	IC ₅₀	108.353 µg/mL
---------------------------	--------------	------------------	---------------

Slope - 0.30336559

Correlation coefficient - 0.79696766

Intercept - 17.1291667

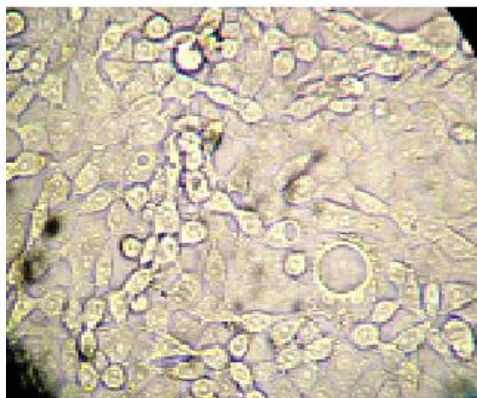


Figure 9: Untreated MCF-7 Cells

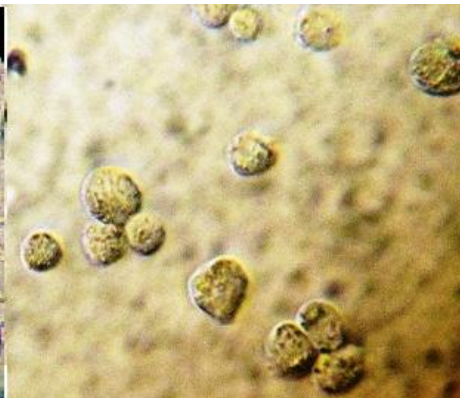


Figure 10: Treated MCF-7 Cells

CONCLUSIONS

The IR and raman spectrum reveals the existence of functional groups. UV spectrum confirms the complexation of metal and ligand. The particular absorbance values represents d-d transition of the metal complex. From the P-XRD spectrum, the crystalline size has been found, and SEM gave idea about the surface morphology and the particle size of the ligand as well as the metal complex. The complex of $\text{Ni}(\text{H}_2\text{O})_2(\text{imd})_2(\text{H}_2\text{O})_2$ was tested for cytotoxic activity (breast cancer). The bioactivity of this synthesized compound is a complex phenomenon related to different factors and the metal complexes are more active than the free ligands. These active compounds may serve as a starting point for further studies on metal complexes acting as drugs.

ACKNOWLEDGEMENTS

Dr BKB acknowledges grants from the Ref No: 42-354/2013 UGC (INDIA), New Delhi .We are grateful for the technical assistance provided by the Department of Engineering Chemistry at the andhra University, visakhapatnam (INDIA) and We are thankful to M. Ravichandra and S.V. Tammy for providing SEM and Spectral data.

REFERENCES

1. Sakurai, H.; Kojima, Y.; Yoshikawa, Y.; Kawabe, K.; Yasui, H.; (2002). *Antidiabetic vanadium(IV) and zinc(II) complexes Coord Chem Rev* 226 ,187-198.
2. Sadler, P.J.; Li, H.; Sun, H.; (1999) *Coordination chemistry of metals in medicine: target sites for bismuth. Coord Chem Rev* 185-186 ,689-709.
3. Ali, H.; van Lier, J.E.; (1999). *Metal complexes as photo- and radiosensitizers. Chem Rev* 99 ,2379-2450.
4. Louie, A.Y.; Meade, T.J.; (1999) *Metal complexes as enzyme inhibitors. Chem Rev* 99 ,2711-2734.
5. Volkert W.A.; Hoffman T.J.; (1999) *Therapeutic radiopharmaceuticals. Chem Rev* 99:2269-2292.
6. Sarkar, B.; (1999)*Treatment of Wilson and Menkes diseases. Chem Rev* 99 ,2535- 2544.
7. Liu, Z.D.; Hider, R.C.; (2002) *Design of iron chelators with therapeutic application. Coord Chem Rev* 232 ,151-171.

8. Whittaker, M.; Floyd, C.D.; Brown, P.; Gearing, A.J.H.; (1999) *Design and therapeutic application of matrix metalloproteinase inhibitors. Chem Rev* 99 ,2735-2776.
9. Padmarao, Ch. V.; Praveen, K.; Kishore Babu, B.; Mohana Rao. K.; Yellamandarao, T.; (2013) *International Journal of Applied and Natural Sciences*, Vol. 2, Issue 4, 43-48.
10. Fasman, G.D.; *Handbook of Biochemistry and Molecular Biology, Nucleic acids, I*, 65-215, CRC Pres.
11. Helios, K.; Wysokin´ ski, R.; Zierkiewicz, W.; Proniewicz, L.M.; Michalska, D.; (2009) *J. Phys. Chem. B* ,113, 8158.
12. Baranwal, B.P.; Fatma, T.; Varma, A.; Singh, A.K.; (2010) *Spectrochim. Acta A*, 75, 1177.
13. Baranwal, B.P.; Fatma, T.; Varma, A.; (2009) *J. Mol. Struct.*, 920, 472.
14. Mosmann T. Rapid colorimetric assay for cellular growth and survival: application to proliferation and cytotoxicity assays.(1983) *J. Immunol. Methods* , 65, 55.

NEW DIMETHYLGLYOXIME PSEUDOHALIDE COMPLEXES

K. PRAVEEN¹, CH.V. PADMARAO², B. KISHORE BABU³, B. SWARNALATHA⁴ & V.VEERIAIAH⁵

^{1,2,3}Department of Engineering Chemistry, AUCE(A), Andhra University, Visakhapatnam, Andhra Pradesh, India

^{4,5}Department of Physics, Andhra University, Visakhapatnam, Andhra Pradesh, India

ABSTRACT

In this study, Three new metal psuedohalide complexes, $[\text{Co}(\text{dmg})_2(\text{N}_3)_2]$ (1), $[\text{Cu}(\text{dmg})(\text{Lys})(\text{N}_3)_2]$ (2) $[\text{Ni}(\text{dmg})_2(\text{N}_3)_2]$ (3) have been synthesized from dimethylglyoxime and lysine. The structures of these metal complexes were proposed based upon IR spectroscopy. These mixed psuedohalide complexes are showing trans-coordination with short bridging ligand(N_3). Three complexes were reported in this paper and proposed their chemical structures with the help of chem draw. These structures are in good agreement with IR frequencies.

KEYWORDS: Dimethylglyoxime (DMG), Coordination Chemistry, Cu(II), Co(II), Complex, Ni(II), Aminoacid

INTRODUCTION

In general, oxime and dioxime derivatives are very important compounds in the chemical industry and in medicine. Copper(II)-containing vicdioximes currently are used as cerebral and myocardial perfusion imaging agents¹. Recently, B.Kishore Babu. Et al published Fe(II), Cd(II) and Pb(II) dimethylglyoxime pseudohalide complexes in the International journal². Recent studies focused on the transition-metal complexes of aminoacids and its isomers. structural, thermodynamic, spectral, and kinetic methods have been widely applied to characterize their physicochemical properties³⁻⁹. In general, aminoacids bond to metal centers by the amino N atom, carboxylate O atoms, and phenolate O atom. The carboxylate groups can coordinate to a metal ion in a monodendate⁵, chelate⁶ or bridging fashion, depending on their physicochemical properties³⁻⁹. Amino acid complexes are used in conventional livestock production to protect trace minerals during digestion^{10, 11}. The metal lysine complexes of this invention are formed with iron, copper, zinc, manganese, and cobalt, all of which play important roles in metabolic processes. Metal complexes have been synthesized, extending our previous work and the objective was to add new complexes to the literature of coordination chemistry.

EXPERIMENTAL

Reagents

All chemicals were purchased from Ranbaxy chemicals and used without further purification.

SYNTHESIS

Synthesis of $[\text{Co}(\text{dmg})_2(\text{N}_3)_2]$ (1)

An aqueous (5 ml) solution of Cobalt nitrate (0.291g, 1.0 mmol) was added to an methanolic solution (5ml) of dmg (0.232g, 2.0 mmol) under stirring conditions and the solution turned to wine red colour and then aqueous solution of sodium azide (0.065g, 1.0 mmol) was added which turned to dark red solution and on addition of tyrosine (tyr) (0.181g, 1.0 mmol) dissolved in 10 ml of sodium hydroxide solution resulted into reddish brown solution. After constant stirring at room temperature for 30 minutes, The solution was filtered off, brown precipitate was formed and the light brown colour solution was left for slow evaporation in the beaker and black crystals were obtained in 3 days. The expected complex is

[Co(dmg)(tyr)(N₃)₂], But the obtained complex is [Co(dmg)₂(N₃)₂]. The absence of peaks in the range of 1578-1593 cm⁻¹ confirms the non coordination of amino acid.

Molecular Formula: C₈H₁₆CoN₁₀O₄; Mol. Wt.: 375.21

IR Data: 3350, 2964, 2037, 1442, 1143, 1087, 740, 513.

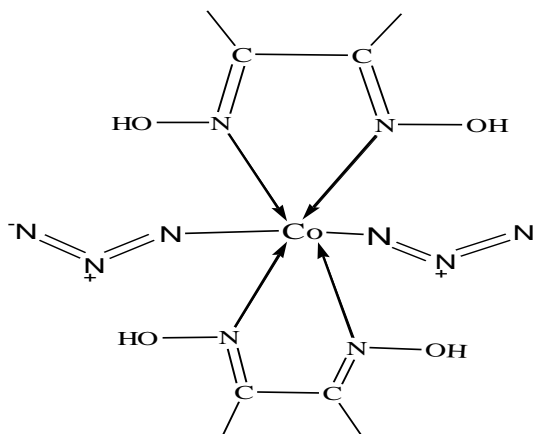


Figure 1: Proposed Structure of [Co(dmg)₂(N₃)₂]

Synthesis of [Cu(dmg)(Lys)(N₃)₂] (2)

An aqueous (5 ml) solution of Lysine (0.164g, 1.0 mmol) was added to a methanolic solution (5ml) of dmg (0.232g, 2.0 mmol) under stirring conditions and the solution remained colourless and then aqueous solution of sodium azide (0.065g, 1.0 mmol) was added which remained as same solution and on stirring white precipitate formed and on addition of aqueous solution of copper acetate (0.199g, 1.0 mmol), thick brown solution formed. After constant stirring at room temperature for 30 minutes, The brown solution was filtered off, brown precipitate was formed and the light brown colour solution is left for slow evaporation in the beaker and brown crystalline precipitate was formed on the next day.

Molecular Formula: C₁₀H₂₀CuN₁₀O₄; Mol. Wt.: 407.88

IR Data: 3414, 3074, 2856, 2075, 1599, 1471, 1157, 1024, 758, 412.

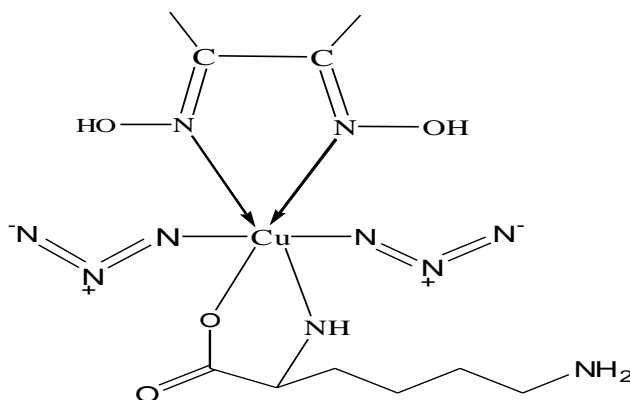


Figure 2: Proposed Structure of [Cu(dmg)(Lys)(N₃)₂]

Synthesis of [Ni(dmg)₂(N₃)₂] (3)

A methanolic (5 ml) solution of 1,10 phenanthroline (0.198g, 1.0 mmol) was added to an aqueous solution (5ml) of Nickel chloride (0.237g, 1.0 mmol) under stirring conditions and the solution turned violet, but on the addition of dmg

(0.116g, 1.0 mmol) Orange red precipitate was formed. Then aqueous solution of sodium azide (0.065g, 1.0 mmol) was added which remained as same solution. After constant stirring at room temperature for 30 minutes, The solution was filtered off, Orange red precipitate was formed and the colourless solution is left for slow evaporation in the beaker and brown crystals were formed within 4 days. The expected complex is $[\text{Ni}(\text{dmg})(\text{Phen})(\text{N}_3)_2]$. But the obtained complex is $[\text{Ni}(\text{dmg})_2(\text{N}_3)_2]$. In this preparation the 1,10 phenanthroline did not coordinate to the metal, this was confirmed by the absence of peaks at 1520 and 1427 in IR spectrum.

Molecular Formula: $\text{C}_8\text{H}_{16}\text{N}_{10}\text{NiO}_4$: Mol. Wt: 374.97

IR Data: 3375, 2031, 1585, 1421, 1138, 1091, 736.

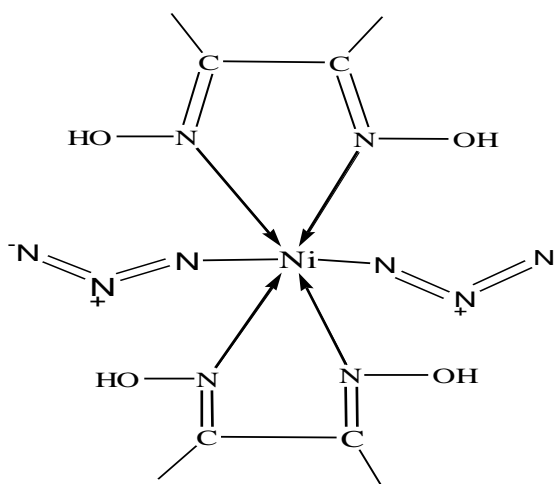


Figure 3: Proposed Structure of $[\text{Ni}(\text{dmg})_2(\text{N}_3)_2]$

RESULTS AND DISCUSSIONS

Physical Properties

Table 1: Color, Yield, Melting Point and Solubility Data for the Complexes

COMPOUND	COLOR	YIELD	M.P.	SOLUBILITY
L	White	-	240 ⁰ C	Methanol
$[\text{Co}(\text{L})_2(\text{N}_3)_2]$	Black	51.5%	Above 300 ⁰ C	Methanol
$[\text{Cu}(\text{L})(\text{Lys})(\text{N}_3)_2]$	Brown	61.8%	Above 300 ⁰ C	Methanol
$[\text{Ni}(\text{L})_2(\text{N}_3)_2]$	Brown	70.8%	Above 300 ⁰ C	Methanol

L = Dimethyl glyoxime(dmg)

Lys = Lysine

N_3 = Azide

IR SPECTRA

The assignment of some of the most characteristic FT-IR band of the complexes are shown in Table (2) together with that of dmg recorded for comparative purposes and facilitate the spectral analysis. Absorption bands in the 2050-2070 cm^{-1} region are considered to be due to metal-nitrogen(of pseudohalide) vibrations^{12,13} while those occurring around 1143 cm^{-1} are thought to arise from nitrogen-oxygen vibration in coordinated $\text{dmg}^{14,15}$. $\nu(\text{C}=\text{N})$ band appearing at 1447 cm^{-1} in dimethylglyoxime is slightly shifted to 1444 cm^{-1} . This suggests that dmg is coordinated to the metal ion through the nitrogen atom of oxime. In the IR spectra of the complex 1 there is a strong and sharp absorption around 513 cm^{-1} which is assigned to the $\nu(\text{Co}-\text{N})$ vibration, these bands are not found in the spectrum of the ligand. The sharp and weak band

occurring around 1020 cm^{-1} and 1145 cm^{-1} in all the complexes is assigned to the N - O stretching vibration of the oxime moieties¹⁶. The spectra of aminoacids exhibit $\nu(\text{NH}_3^+)$ bands in the $3030\text{--}3130\text{ cm}^{-1}$ range. In the complexes, the $\nu(\text{NH}_3^+)$ band is shifted to higher wavenumbers. The peak at 3074 in complex 2 confirms the complexation of aminoacid¹⁶. The bands of medium intensity appearing at $1578\text{--}1593\text{ cm}^{-1}$ are due to the asymmetric stretching vibration of the COO moiety^{17,18}.

Table 2: Selected Characteristics IR Bands (4000 – 400 CM^{-1})

Complex	$\nu(\text{OH})$	$\nu(\text{NH})_y$	$\nu(\text{C}=\text{N})$	$\nu(\text{N}-\text{O})$	$\nu(\text{C}=\text{N}-\text{O})$	$\nu(\text{M}-\text{N}_x)$	$\nu(\text{COO})_v$	
							asym	sym
dmg	3400	-	1570	1141	756	-	-	-
1	3350	-	1442	1143	740	2037	-	-
2	3414	3074	1450	1157	758	2075	1599	1471
3	3375	-	1421	1138	736	2031	-	-

Complex 1 = $[\text{Co}(\text{L})_2(\text{N}_3)_2]$

Complex 2 = $[\text{Cu}(\text{L})(\text{Lys})(\text{N}_3)_2]$

Complex 3 = $[\text{Ni}(\text{L})_2(\text{N}_3)_2]$

L = Dimethyl glyoxime; Lys = Lysine; N_3 = Azide

X = Pseudohalide

Y = Aminoacid

CONCLUSIONS

Our research group presented the results of the synthesis and characterization studies of a series of mixed-ligand complexes involving dimethylglyoxime, Lysine and pseudohalide short bridging ligands. The IR spectra reveals the existence of functional groups and coordinated pseudohalide ions, confirms the complexation of metal and ligand.

ACKNOWLEDGMENTS

BKB acknowledges grants from the Ref No: 42-354/2013 UGC (INDIA), New Delhi. We are grateful for the technical assistance provided by the Department of Engineering Chemistry at the andhra University, visakhapatnam (INDIA) and the University of Hyderabad for providing the spectral data.

REFERENCES

1. Prushan, M.J.; Addison, A.W.; Butcher, R.J. Pentadentate thioetheroxime macrocyclic and quasi-macrocyclic complexes of copper(II) and nickel(II). *Inorg. Chim. Acta* 2000, 300, 992–1003.
2. Praveen. K., Padma Rao. Ch. V., Kishorebabu. B., Naga Sirisha. J., Swarna Latha. B.,
3. Suseelabai. G., Venketeswara Rao. B., Raghu Babu. K. and Padma. M. *Der Pharma Chemica*, 2013, 5(2):149-153.
4. Hamalainen, R.; Lajunen, K.; Valkonen, J. *Finn. Chem. Lett.* 1977, 4-5, 108–112.
5. Kiss, T.; Gergely, A. *J. Chem. Soc., Dalton Trans.* 1984, 1951–1957.
6. Molchanov, A. S.; Ledenkov, S. F. *Russ. J. Phys. Chem. A* 2009, 28, 2028–2031.
7. Pettit, L. D. *Pure Appl. Chem.* 1984, 56, 247–292.

8. Mosset, A.; Bonnet, J. J. *Acta Crystallogr.* 1977, B33, 2807–2812.
 - Yamauchi, O.; Odani, A.; Kohzuma, T.; Masuda, H.; Toriumi, K.; Sato, K. *Inorg. Chem.* 1989, 28, 4066–4068.
 - Yamauchi, O.; Odani, A.; Masuda, H. *Inorg. Chim. Acta* 1992, 198, 749–761.
 - Ramakrishna, S.; Rajendiran, V.; Palaniandavar, M.; Periasamy, V. S; Sring, B. S.; Krishnamurthy, H.; Akbarsha, M. A. *Inorg. Chem.* 2009, 48, 1309–1322.
9. Liu, W.; Song, Y.; Li, Y.; Zou, Y.; Dang, D.; Ni, Ch.; Meng, Q. *Chem. Commun.* 2004, 20, 2348–2349.
 - Wojciechowska, A.; Daszkiewicz, M.; Bienko, A. *Polyhedron* 2009, 28, 1481–1489.
 - Zhang, S.; Hu, N.- H. *Acta Crystallogr.* 2009, C65, m7–m9.
 - Weng, J.; Hong, M.; Shi, Q.; Cao, R; Chan, A. S. C. *Eur. Inorg. Chem.* 2002, 2553–2556.
 - Apfelbaum-Tibika, F.; Bino, A. *Inorg. Chem.* 1984, 23, 2902–2905.
 - Ye, Q.; Li, Y.-H.; Wu, Q.; Song, Y.-M.; Wang, J.-X.; Zhao, H.; Xiong, R.-G.; Xue, Z. *Chem.—Eur. J.* 2005, 11, 988–994.
 - Facchin, G.; Torre, M. H. T.; Kremer, E.; Piro, O. E.; Castellano, E. E.; Baran, E. J. J. *Inorg. Biochem.* 2002, 89, 174–180.
 - Wang, R.; Zheng, Z.; Jin, T.; Staples, R. J. *Angew. Chem., Int. Ed.* 1999, 38, 1813–1815.
 - Li, D. Q.; Zhou, J.; Liu, X. *Acta Crystallogr.* 2007, C63, m371–373.
10. G.A. Apgar, E.T. Komegay, *J. Anim. Sci.* 72 (1994) 273.
11. G.R. Lenz, A.E. Martell, *Biochemistry* 3 (1964) 745.
12. Nakamoto, K. J. Wiley and sons., *Infrared spectra of Inorganic and coordination compounds* 4 th edn New york, **1996** .
13. Klienstien, A; I. Gabe, *An.St.Univ, Lasi XIV*, **1968**, 139. .
14. During, J.D.; D.W. Wertz, *Appl. Spectrosc* , **1963**, 22, 636 .
15. Buckingham, D.A.; D. Jones, *Inorg, chem.* **1965**, 4, 1387 .
16. Adkhis, A.; Benali- Baiitich, O.; Khan, M.A.; G. Bouet *Synth.React.Inorg.Met-Org.Chem.*,30(10),1849-1858(2000).
17. Bellamy. L.J. "The Infrared Spectra of Complexes Molecules". 3rd Edn. Wiley, New York, p. 226 (1975).
18. Nakamoto. K. "Infrared and and Raman Spectra of Inorganic and Coordination Compounds". 3rd Edn.. Wiley, New York, p. 273 (I 972).



Scholars Research Library

Der Pharma Chemica, 2013, 5(2):149-153
(<http://derpharmachemica.com/archive.html>)



ISSN 0975-413X
CODEN (USA): PCHHAX

Synthesis and characterization of the pseudohalide metal complexes

Praveen. K, Padma Rao. Ch. V., Kishorebabu. B.*, Naga Sirisha. J., Swarna Latha. B.,
Suseelabai. G., Venketeswara Rao. B., Raghu Babu. K. and Padma. M.

Department of Engineering Chemistry, AUCE(A), Andhra University, Visakhapatnam, Andhra Pradesh, India

ABSTRACT

This paper presents the synthesis and study of some new complexes containing DMG and NCS with some metals. The resulting products were found to be solid crystalline complexes which have been characterized by using (FT-IR, UV-Vis) spectra, melting point, elemental analysis (C.H.N). The proposed structure of the complexes using program, CS chem office 3D(2000).

The general formula have been given for the prepared complexes :

$[M(A)_2(B)_2]$

M(II): Pb(II), Fe(II), Cd(II).

A = DMG(dimethyl glyoxime) = $C_4H_8N_2O_2$

B = NCS(thiocyanate) for first 2 complexes (oac)₂(acetate) for third complex

Key words: DMG, Coordination chemistry, Pb(II), Fe(II), complex, Cd(II), spectra

INTRODUCTION

It is well known that the oximatogroup(=N-O⁻) can act as a bridge to find two metal ions through the imino nitrogen atoms and the deprotonated oxygen atoms, which can co-ordinate with metal ions in versatile ways. H₂dmg is a potential tetradentate ligand as well as a mono, bi and tridentate ligand. Framework molecular model shows that it is more likely to act as a bridge between two metal ions than as a terminal ligand[1-4] With the aim of investigating versatility of oximes in coordination chemistry and for further research on the supramolecular polymer chemistry, designed and synthesised some polymeric chain like complexes successfully with oximato groups as bridges[5-9]. In order to add other kinds of anion on complex, we synthesized short bridging ligand complexes, proposed structures and spectroscopic properties of the afore mentioned complexes were discussed.

MATERIALS AND METHODS

A: Reagents and instruments : DMG and NCS were purchased from BDH .

All solutions and metal chloride were purchased from merck and. Elemental analysis was obtained using a FLASH EA 1112 SERIES CHNS analyzer. Melting point were recorded by using stuart melting point apparatus . IR spectra were obtained with a Shimadzu FT-IR 8000 spectrometer .The proposed molecular structure of the complexes were determined by using chem office 2000, 3DX prog .

*B: General synthesis :**Synthesis of $Cd(dmgl)_2(NCS)_2$*

An methanolic (10 ml) solution of dimethylglyoxime (0.116g, 1.0 mmol) was added to an aqueous solution(10ml) of cadmium acetate (0.268g, 1.0 mmol) under stirring conditions and then aqueous solution of NCS (0.097 g, 1.0 mmol) was added which resulted into colourless solution with some turbidity. After constant stirring at room temperature for 30 minutes,The product was precipitated,filtered off and washed with methanol. The product is also obtained from the solution left for evaporation in the beaker in the form of crystalline precipitate. The compounds are soluble in methanol. Yield 0.185 g

Synthesis of $[Fe(dmgl)_2(NCS)_2]$

An methanolic (10 ml) solution of dimethylglyoxime (0.116g, 1.0 mmol) was added to an aqueous solution(10ml) of ferrous sulphate (0.260g, 1.0 mmol) under stirring conditions and then aqueous solution of NCS(0.097 g, 1.0 mmol) was added which resulted into colourless solution with some turbidity. After constant stirring at room temperature for 30 minutes,The product was precipitated,filtered off and washed with methanol. The product is also obtained from the solution left for evaporation in the beaker in the form of crystalline precipitate. The compounds are soluble in methanol. Yield 0.153 g

Synthesis of $[Pb(dmgl)_2(oac)_2]$

An methanolic (10 ml) solution of dimethylglyoxime (0.116g, 1.0 mmol) was added to an aqueous solution(10ml) of lead acetate (0.379g, 1 mmol) under stirring conditions and then aqueous solution of NCS(0.097 g, 1.0 mmol) was added which resulted into colourless solution with some turbidity. After constant stirring at room temperature for 30 minutes,The product was precipitated,filtered off and washed with methanol. The product is also obtained from the solution left for evaporation in the beaker in the form of crystalline precipitate. The compounds are soluble in methanol. Yield 0.240 g

RESULTS AND DISCUSSION

Physical properties and elemental analysis are presented in Table (1) . Formula $M(A)_2 (B)_2$ giving good agreement between the observed and the calculated values by elemental analysis . All complexes are dissolved in Methanol solvent .

The electronic spectra :

The electronic spectra of all complexes are listed inTable (2) . In the $[Pb(dmgl)_2(oac)_2]$ complexes the two bands at 233 and 223.50nm are characteristic. In the $[Fe(dmgl)_2(NCS)_2]$ complex the two bands at 236.50 and 227.50 nm are characteristic of this complex. In $[Cd(dmgl)_2(NCS)_2]$ two bands at 237 and 227.50 nm are characteristic of this complex.

Fourier-transform infrared spectra :

The assignment of some of the most characteristic FT-IR band of the complexes are shown in Table (3) together with that of dmgl recorded for comparative purposes and facilitate the spectral analysis .Absorption bands in the $2050-2070\text{ cm}^{-1}$ region are considered to be due to metal-nitrogen(of pseudohalide) vibrations [10,11] whilst those occurring around 1143 cm^{-1} are thought to arise from nitrogen-oxygen vibration in coordinated dmgl [12,13] the sharp bands at $(3325-3300)\text{ cm}^{-1}$ are attributed to the N-H stretching[14] .

Nomenclature of prepared complexes :

Complexes	Nomenclature
$Cd(dmgl)_2(NCS)_2$	Didimethylglyoximatodithiocyanato N-Cadmium(II)
$Fe(dmgl)_2(NCS)_2$	Didimethylglyoximatodithiocyanato N-Ferrate(II)
$Pb(dmgl)_2(oac)_2$	Didimethylglyoximatodiacetato Lead(II)

Proposed molecular structure :

Studying complexes on bases of the above analysis , the existence of tetracoordinated $[M(A)_2(B)_2]$, $M(II) = Cd , Fe , Pb$

A proposed models of the speciese were built with chem 3D (15) shows in Fig (1)(2)(3) .

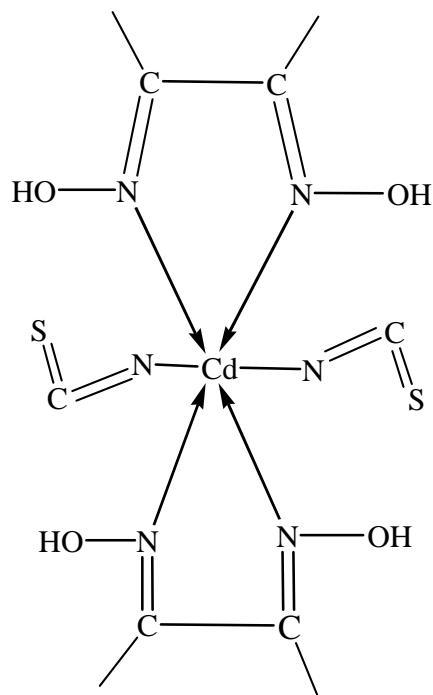
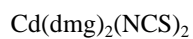


Fig (1) : The proposed structure of the complex 1

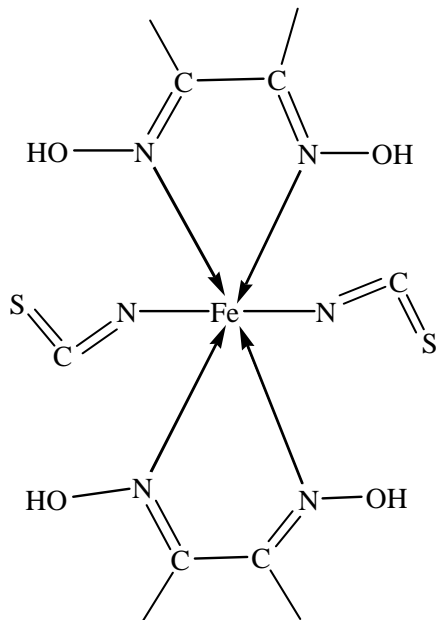
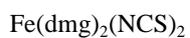


Fig (2) : The proposed structure of the complex 2

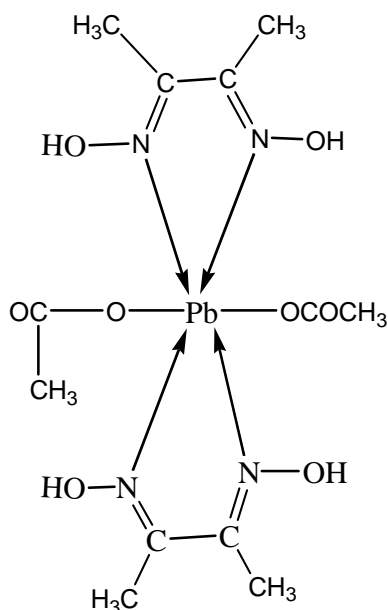
Pb(dm_g)₂(oac)₂

Fig (3) : The proposed structure of the complex 3

Table 1: The physical properties of the complexes Elemental Analysis

Compound	Colour	M.P. ^o c	%C		%H		%N	
			Calc	Found	Calc	Found	Calc	Found
DMG	White	240-241	-	-	-	-	-	-
NCS	White	173.2	-	-	-	-	-	-
Cd(dm _g) ₂ (NCS) ₂	White	Above 300	26.06	25.86	3.50	4.02	18.24	18.86
Fe(dm _g) ₂ (NCS) ₂	Grey	Above 300	29.71	29.02	3.99	4.32	20.79	21.44
Pb(dm _g) ₂ (oac) ₂	White	Above 300	25.85	24.98	3.98	4.19	10.05	10.76

M.P = Melting point

Table 2 :Electronic spectra of the studied complexes and two ligands

Compounds	Wavelength (nm)		Wavenumber (cm ⁻¹)	
DMG	229.99		43480	
NCS	266		37593.98	
Cd(dm _g) ₂ (NCS) ₂	246	237	40650.40	42194.09
	230	227.50	43478.26	43956.04
Fe(dm _g) ₂ (NCS) ₂	236.50		42283.29	
	227.50		43956.04	
Pb(dm _g) ₂ (oac) ₂	233		49218.45	
	223.50		44742.72	

Table 3 : FT-IR Spectrl Data of the Ligands and its Complexes

complex	v(OH)	v(NH)	v(C-H)	v(C=C)	v(N-O)	v(C=N-O)	v(M-N)	v(COO)
dmg	3205	2928	2850	1490	1143	760	-	-
1	3410	-	2926	1431	1143	761	2067	-
2	-	3246	2924	1437	1143	758	2056	-
3	3312	3236	2924	1440	1143	752	-	1363

Complex 1 = Cd(dm_g)₂(NCS)₂Complex 2 = Fe(dm_g)₂(NCS)₂Complex 3 = Pb(dm_g)₂(oac)₂

CONCLUSION

Metal complexes were synthesized by self-assembly method. All the proposed structures are showing Octahedral geometry and agreed with electronic data. The obtained results were characterized by using spectroscopy and physical methods.

Acknowledgments

KP and CHP is grateful to UGC (INDIA) for providing the fellowship grants. BKB acknowledges grants from the UGC (INDIA) .. We are grateful for the technical assistance provided by the Department of Engineering Chemistry at the andhra University ,visakhapatnam (INDIA) and the University of Hyderabad for providing the spectral data.

REFERENCES

- [1] J. m. Lehn , supramolecular chemistry-concepts and perspectives, Vch, Weinheim.,**1995**.
- [2] M. Ohkita, J.M. Lehn, G. Baum, et al, *J.chem.Eur.*, **1999**, 5(12) , 3471-3481.
- [3] A.N. Khlobystov, A.J. Blake, N.R. Champness, et al., *J.Coord.Chem.Rev.*, **2001**, 222, 155-192.
- [4] G.R. Desiraju, *J.Angew.Chem.Int.Edit .*, **1995**, 34(21), 2311-2327.
- [5] P. Chaudhuri, *Coord.Chem. Rev.*, **2003**, 243(1-2), 143-190.
- [6] F. Birkelbach, U. Florke, H.J. Haupt, et al., *Inorg.chem.*, **1998**, 37(8), 2000-2008.
- [7] R. Ruiz, M. Julve, J. Faus, et al., *Inorg. Chem.*, **1997**, 36(16), 3434-3439.
- [8] F. Birkelbach, M. Winter, U. Florke, et al.; *Inorg.Chem.*,**1994**, 33(18), 3990-4001.
- [9] D. Burdinski, F. Birkelbach, T. Weyhermuller, et al., *Inorg.chem.*,**1998**, 37(5), 1009-1020.
- [10] K. Nakamoto, J. Wiley and sons., *Infrared spectra of Inorganic and coordination compounds*, *4ED th. ; .*; New york, **1996** .
- [11] A. Klienstien, I. Gabe, *An.St.Univ, Lasi XIV*, **1968**, 139. .
- [12] J.D. Doring, D.W. Wertz, *Appl. Spectrosc* , **1963**, 22, 636 .
- [13] D.A. Buckingham, D. Jones, *Inorg, chem.* **1965**, 4, 1387 .
- [14] A. Klierstien, G.A. Webb, *J.Inorg. Nucl, chem*, **1971**, 33, 405 .
- [15] Chem 3D pro (Ver 3.5.2) Cambridge soft corporation , Cambridge , Massachutes **1997** .



Scholars Research Library

Der Pharma Chemica, 2013, 5(5):280-284
(<http://derpharmachemica.com/archive.html>)



ISSN 0975-413X
CODEN (USA): PCHHAX

Zinc dimethylglyoxime complexes

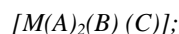
Padma Rao. Ch. V.¹, Praveen K.¹, Kishorebabu B.*¹, Padma M.¹, Anna Sudheer K.¹,
Sandhya Rani K.¹, Koteswarao K.¹, Suseelabai G.¹, Venkateswara Rao B.¹, Mohana Rao K.
and Swarna Latha B.²

¹Department of Engineering Chemistry, AUCE(A), Andhra University, Visakhapatnam, Andhra Pradesh, India
²V. K. R. College, Buddhavaram, Dept of Physics, Andhra Pradesh, India

ABSTRACT

Metal-ligand complexes of the general formula $[M(A)_2(B)(C)]$ where A=dimethylglyoxime B= N_3, NCS, NCO and $M= Zn(II)$ were prepared. Each complex was characterized by elemental analysis and infrared spectra. The IR spectra, which have indicate that the dimethylglyoxime was coordinated with the metal ions through the N and O atoms of the oxime group, pseudohalides and acetate were coordinated with metal ions through the N atom and terminal carboxyl oxygen atom. The proposed structure of the complexes were drawn using program, CS chem office 3D(2000).

The general formula have been given for the prepared complexes :



M(II): Zn(II).

A = DMG(dimethyl glyoxime) = $C_4H_8N_2O_2$

B = N_3, NCS and NCO .

C = Acetate ion(CH_3COO^-)

Key words: DMG, Pseudohalides, Zn(II),spectra, Dimethylglyoxime complexes.

INTRODUCTION

The oxime group ($>C=N-OH$), which may be considered to be derived from oxy-imine, is amphoteric with slightly basic nitrogen and mildly acidic hydroxyl groups [1]. Vic-dioxime ligands react with many transition metals in the Periodic Table and form highly stable complexes [2]. Formation and structural analysis of such complexes have been reviewed by Chakravorty [3] and Schrauzer [4]. The dimethylglyoxime derivatives have received considerable attention from both of the chemical and biological scientists. It is stimulated the reactions of vitamin B12 and vitamin- B12 Preparation and Spectral Properties of Mixed-Ligand Complexes S581 model chemistry[5-7]. Moreover, the dioximes are capable of coordinating through N, N or N, O sites of the oxime groups. Thus, some of the dioximes derivatives exhibited significant anti carcinogenic activity and antitumor agents[5]. In order to add other kinds of anion on complex, we synthesized short bridging ligand complexes, proposed structures and spectroscopic properties of the afore mentioned complexes were discussed. Synthesis and characterization of the pseudo halide metal complexes with Fe, Cd and Pb were published by Dr. B. Kishore Babu et al [8].

MATERIALS AND METHODS

A: Reagents and instruments : DMG and Pseudohalide ligands were purchased from SRL .

Metal salts were purchased from merck and Elemental analysis was obtained using a FLASH EA 1112 SERIES CHNS analyzer. Melting point were recorded by using stuart melting point apparatus . IR spectra were obtained with a Shimadzu FT-IR 8000 spectrometer. The proposed molecular structure of the complexes were determined by using chem office 2000, 3DX prog .

B: General synthesis :

Synthesis of $Zn(dmgl)_2(N_3)(oac)$

An methanolic (5 ml) solution of dimethylglyoxime (0.116g, 1.0 mmol) was added to an aqueous solution(5 ml) of Zinc acetate dihydrate (0.219g, 1.0 mmol), white precipitate was formed and then aqueous solution(5 ml) of NaN_3 (0.065 g, 1.0 mmol) was added which remained same. After constant stirring at 60⁰c temperature for 30 minutes,The product was filtered off and washed with methanol. Yield 46%

Synthesis of $[Zn(dmgl)_2(NCS)(oac)]$

An methanolic (5 ml) solution of dimethylglyoxime (0.116g, 1.0 mmol) was added to an aqueous solution(5 ml) of Zinc acetate dihydrate (0.219g, 1.0 mmol), white precipitate was formed and then aqueous solution(5 ml) of KNCS (0.097 g, 1.0 mmol) was added which turned pale. After constant stirring at 60⁰c temperature for 30 minutes,The product was filtered off and washed with methanol. Yield 45%

Synthesis of $[Zn(dmgl)_2(NCO)(oac)]$

An methanolic (5 ml) solution of dimethylglyoxime (0.116g, 1.0 mmol) was added to an aqueous solution(5 ml) of Zinc acetate dihydrate (0.219g, 1.0 mmol), white precipitate was formed and then aqueous solution (5 ml) of NaOCN (0.081 g, 1.0 mmol) was added which remained same. After constant stirring at 60⁰c temperature for 30 minutes, The product was filtered off and washed with methanol. Yield 45%

RESULTS AND DISCUSSION

Physical properties and elemental analysis are presented in Table (1). Formula $M(A)_2 (B) (C)$ giving good agreement between the observed and the calculated values by elemental analysis .

Fourier-transform infrared spectra :

The assignment of some of the most characteristic FT-IR band of the complexes are shown in Table (2) together with that of dmg recorded for comparative purposes and facilitate the spectral analysis. Absorption bands in the 2050-2295 cm^{-1} region are considered to be due to metal-nitrogen(of pseudohalide) vibrations [9,10] whilst those occurring around 1143 cm^{-1} are thought to arise from nitrogen-oxygen vibration in coordinated dmg [11,12].

Nomenclature of prepared complexes :

Complexes	Nomenclature
$Zn(dmgl)_2(N_3)_2$	Didimethylglyoximatodiaido N-Zinc(II)
$Zn(dmgl)_2(NCS)_2$	Didimethylglyoximatodithiocyanato N-zinc(II)
$Zn(dmgl)_2(NCO)_2$	Didimethylglyoximatodiocyanato N- Zinc(II)

Proposed molecular structure :

Studying complexes on bases of the above analysis , the existence of tetra coordinated

$[M(A)_2(B) (C)]$,

$M(II) = Zn(II)$

A proposed models of the species were built with chem 3D [13] shows in Fig (1)(2)(3) .

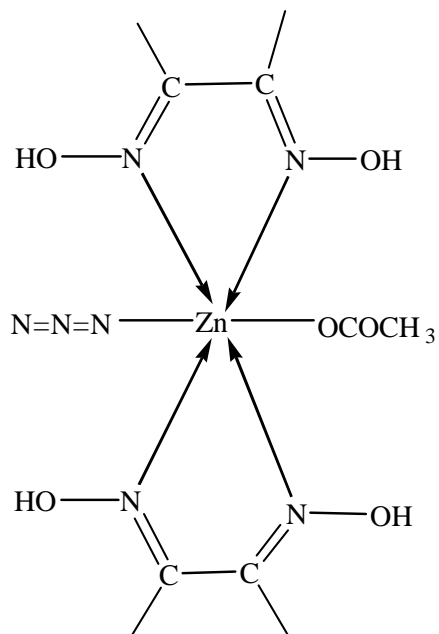
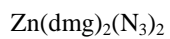


Fig (1) : The proposed structure of the complex 1

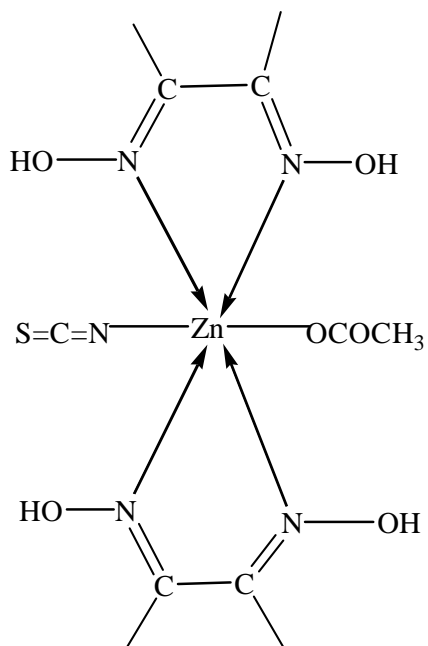
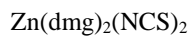


Fig (2) : The proposed structure of the complex 2

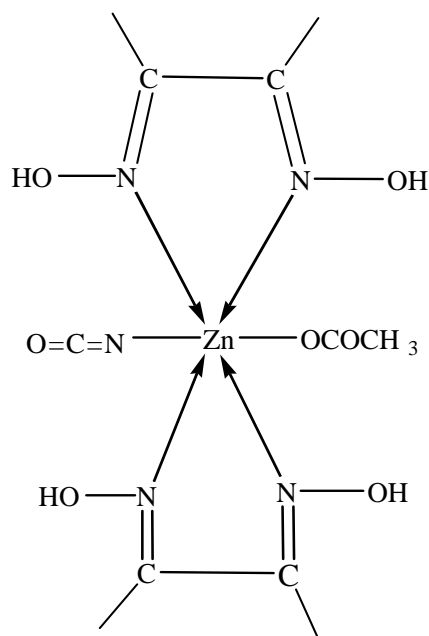
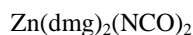


Fig (3) : The proposed structure of the complex 3

Table 1: The physical properties of the complexes

Elemental Analysis								
Compound	Colour	M.P. ^o c	%C		%H		%N	
			Calc	Found	Calc	Found	Calc	Found
DMG	White	240-241	-	-	-	-	-	-
Zn(dmga) ₂ (N ₃) ₂	White	Above 300	37.25	37.12	6.56	5.98	14.43	14.21
Zn(dmga) ₂ (NCS) ₂	White	Above 300	37.27	37.18	6.52	6.12	14.49	14.36
Zn(dmga) ₂ (NCO) ₂	White	Above 300	35.54	35.22	5.97	5.78	15.07	14.98

M.P = Melting point

Table 2 : FT-IR Spectrl Data of the Ligands and its Complexes

complex	v(OH)	v(C=C)	v(N-O)	v(C=N-O)	v(M-N) _x	V(COO)
dmg	3205	1490	1143	760	-	-
1	3210	1446	1139	745	2190	1364
2	3205	1435	1139	745	2194	1364
3	3210	1441	1139	750	2295	1364

X= Pseudohalide (N₃, NCS, NCO)

Complex 1 = Zn(dmga)₂(N₃)₂

Complex 2 = Zn(dmga)₂(NCS)₂

Complex 3 = Zn(dmga)₂(NCO)₂

CONCLUSION

Metal complexes were synthesized by self-assembly method. The obtained results were characterized by using spectroscopy and physical methods.

Acknowledgments

KP, CHP and BKB is grateful to UGC (INDIA) for providing the fellowship grants. We are grateful for the technical assistance provided by the Department of Engineering Chemistry at the Andhra University, Visakhapatnam (INDIA) and the University of Hyderabad for providing the spectral data.

REFERENCES

- [1] D.C. Bradley, R.C. Mehrotra, I.P. Rothwell and A. Sing, Alkoxo and Aryloxo Derivatives of Metals, Academic Press, London, **2001**.
- [2] S. Serin, *Transition Met. Chem.*, **2001**, 26, 300.
- [3] A. Chakravorty, *Coord. Chem. Rev.*, **1974**, 13, 1.
- [4] G.N. Schrauzer, *Angew. Chem. Int. Ed. Eng.*, **1976**, 15, 47.
- [5] M. Emel, A. Vefa, *J Chem Research (S)*, **1999**, 142-143.
- [6] S.C. Nayak, P.K. Das, K.K. Sahoo, *Chem Pap.*, **2003**, 57(2), 91-96.
- [7] S.C. Nayak, P.K. Das, K.K. Sahoo, *J Anal Appl Pyrolysis*, **2003** b, 70(2), 699-709.
- [8] Praveen. K, Padma Rao. Ch. V., Kishorebabu. B, etal. *Der Pharma Chemica*, **2013**, 5(2), 149-153.
- [9] K. Nakamoto, J. Wiley and sons., Infrared spectra of Inorganic and coordination compounds "4ED th. ; ; New york, **1996** .
- [10] A. Klienstien, I. Gabe, *An.St.Univ, Lasi XIV*, **1968**, 139. .
- [11] J.D. Doring, D.W. Wertz, *Appl. Spectrosc* , **1963**, 22, 636 .
- [12] D.A. Buckingham, D. Jones, *Inorg, chem.* **1965**, 4, 1387 .
- [13] Chem 3D pro (Ver 3.5.2) Cambridge soft corporation , Cambridge , Massachutes **1997** .

ANDHRA UNIVERSITY

Tel. No 0091-891-2844042
Fax No 0091-891-2525611 / 2755324
deanacademic.au@gmail.com



All official letters, packages, etc.,
should be addressed to the Dean by
designation and not by the name

NOTIFICATION

AWARD OF RESEARCH DEGREE
in
CHEMISTRY

It is hereby notified that the Vice-Chancellor on the recommendation of the Board of Examiners is pleased to order that **Sri MOHANA RAO KOTA** be declared qualified for the **Degree of Doctor of Philosophy (Ph.D.)** in **CHEMISTRY** on the thesis entitled "**NOVEL CRYSTALLINE METAL-ORGANIC FRAMEWORKS : ANTI-PATHOGENIC AND ANTI-CANCER STUDIES**"

(BY ORDER)

Central Administrative Office
Visakhapatnam
Dt: 15-12-2018


(T. V. SATYAVATHI DEVI)
DEPUTY REGISTRAR (ACADEMIC)

Endt No. T(2)/8491/2018/P.T.

Dt: 15-12-2018

Forwarded to the Director of Stationery and Printing Andhra Pradesh Central Press, Hyderabad (AP) for favour of publication in the next issue of the Andhra Pradesh Gazette and supply to this office with six spare copies of notification.


(T. V. SATYAVATHI DEVI)
DEPUTY REGISTRAR (ACADEMIC)

25 copies to the Coordinator, Media Cell, Andhra University, Visakhapatnam for arranging Publication in all News papers as news item in their dailies at free of charge.
Copies to the Manager of (1) U.N.I., and (2) P.T.I.
Copy to the Warden, Research Scholars Hostel, A.U., Visakhapatnam
Copies to SII., A.V., A VI., U.G.C. and SC & ST Cell Sections

ANDHRA UNIVERSITY

Tel. No 0091-891-2844042
Fax No. 0091-891-2525611 / 2755324
deanacademic.au@gmail.com



All official letters, packages, etc.,
should be addressed to the Dean by
designation and not by the name

Endt. No. T(2)/8491/2018/P.T.

Dt: 15-12-2018

NOTIFICATION
AWARD OF RESEARCH DEGREE
in
CHEMISTRY

It is hereby notified that the Vice-Chancellor considered the reports of the following examiners appointed to adjudicate and report on the thesis entitled "**NOVEL CRYSTALLINE METAL-ORGANIC FRAMEWORKS : ANTI-PATHOGENIC AND ANTI-CANCER STUDIES**".

01. **PROF. DR. AHMED ABDOU ALI EL-SHERIF, DEPARTMENT OF CHEMISTRY, FACULTY OF SCIENCE, CAIRO UNIVERSITY, GIZA, EGYPT**
02. **DR. K. VENKATESWARA RAO, PROFESSOR OF NANOTECHNOLOGY & HEAD, CENTER FOR NANO SCIENCE & TECHNOLOGY (CNST), INSTITUTE OF SCIENCE & TECHNOLOGY (IST), JAWAHARLAL NEHRU TECHNOLOGICAL UNIVERSITY, HYDERABAD (J.N.T.U.H.), KUKATPALLY, HYDERABAD - 500085, TELANGANA.**
03. **DR. KATHI SUDARSHAN, SCIENTIFIC OFFICER - F, RADIOCHEMISTRY DIVISION, BHABHA ATOMIC RESEARCH CENTRE, MUMBAI - 400085**

On the recommendation of the following examiners who have conducted the Viva-Voce examination, the Vice-Chancellor is pleased to order that **Sri MOHANA RAO KOTA** be declared qualified for the **Degree of Doctor of Philosophy (Ph.D.) in CHEMISTRY**

- | | | | |
|-----|------------------------------------|---|--|
| 01. | PROF. CH. PANDU RANGA REDDY | - | D.C. MEMBER |
| 02. | PROF. P. VASUDEVA REDDY | - | D.C. MEMBER |
| 03. | PROF. B. VENKATESWARA RAO | - | D.R.C. MEMBER |
| 04. | PROF. G. SUSHEELA BAI | - | D.R.C. MEMBER |
| 05. | DR. S. PAUL DOUGLAS | - | D.R.C. MEMBER &
HEAD OF THE DEPARTMENT |
| 06. | PROF. V. V. BASAVA KUMAR | - | CHAIRMAN, P.G. BOARD OF STUDIES |
| 07. | PROF. V. VEERAI AH | - | JOINT RESEARCH DIRECTOR |
| 08. | DR. B. KISHORE BABU | - | RESEARCH DIRECTOR &
CONVENER OF VIVA-VOCE |

Date of submission of thesis: **24-04-2018**

(BY ORDER)

Central Administrative Office,
Visakhapatnam
Dt: **15-12-2018**


(T. V. SATYAVATHI DEVI)
DEPUTY REGISTRAR (ACADEMIC)

Endt. No. T(2)/8491/2018/P.T.

Dt: 15-12-2018

Forwarded to the candidate **Sri MOHANA RAO KOTA, PERAIAH, PONNAVALLI POST, CHANDARLAPADU (M.D.), KRISHNA DISTRICT - 521183, ANDHRA PRADESH** with the information that out of the three copies of the thesis submitted by him/her one copy is retained for reference in the University Library and the remaining two copies will be given to him/her if the adjudicators returned them.


(T. V. SATYAVATHI DEVI)
DEPUTY REGISTRAR (ACADEMIC)

Copy to the Examiners.

Copy to the Research Director: **DR. B. KISHORE BABU**

Copy to the Joint Research Director: **PROF. V. VEERAIHAH**, Department of Physics, Andhra University

Copy to the above members of Viva-Voce Committee

Copy to the C-I Section, to Report the same to the Executive Council

Copy to the Librarian, Dr.V.S.K.Library, Andhra University

Copy to the Convener, Board of Research Studies, Andhra University

Copy to the Principal, College of **SCIENCE & TECHNOLOGY**, Andhra University, Visakhapatnam

Copy to the Head of the Department of **CHEMISTRY**, Andhra University, Visakhapatnam

Copy to the Principal, College of **ENGINEERING**, Andhra University, Visakhapatnam

Copy to the Head of the Department of **ENGINEERING CHEMISTRY**, Andhra University, Visakhapatnam

Copy to the Librarian, Association of Indian Universities, Rouse Avenue, New Delhi.

Copy to the Secretary General, Association of Indian Universities, A.I.U. House, 16
Comrade Indrajit Gupta Marge (Kotla Marg), New Delhi - 110 002

Copy to the Director, Information & Library Network Centre, Gujarat University Campus,

Post Box No: 4116, Navrangpura, Ahmedabad - 380009.

Copy to the Secretary to the Vice-Chancellor, Andhra University, Visakhapatnam

Copy to the P.A. to the Registrar, Andhra University

Copy to the Dean of Academic Affairs, Andhra University

Copy to the Coordinator, Department of Journalism, Andhra University

Copies to SII., A.V., A VI., U.G.C. and SC & ST Cell Sections & OOF.

* * *

Final Report Assessment / Evaluation Certificate
(Two Members Expert Committee Not Belonging to the Institute of Principal Investigator)
(to be submitted with the final report)

It is certified that the final report of Major Research Project entitled "SYNTHESIS, STRUCTURE AND PROPERTIES OF NANOPARTICULATE METAL COMPLEXES AND THEIR BIOLOGICAL ACTIVITY "File No: 42/354//2013/(SR) From 01-04-2013 to 31-03-2017" by Dr. B.Kishore Babu, Dept. of Engineering Chemistry has been assessed by the committee consisting the following members for final submission of the report to the UGC, New Delhi under the scheme of Major Research Project.

Comments/Suggestions of the Expert Committee:-

The above mentioned project has been successfully completed. Five publications were published in 2 impact factor journals. Three more papers were already accepted. The above project has been successfully completed with good publications. Several papers are accepted or published in high impact factor Journals.

Name & Signatures of Experts with Date:-

Prof. G.V.R. SHARMA, GVR Sharma
Prof. A.V.L. KRISHNA HARIMARAN - A.H.
HEAD
Department of Chemistry
GITAM Institute of Science
GITAM Institute of Technology and Management
GITAM Institute of Technology to be University
Dr. A.V.L. KRISHNA HARIMARAN
PROFESSOR IN CHEMISTRY
GITAM UNIVERSITY
VISAKHAPATNAM

Name of Expert University/College name Signature with Date

1. GITAM deemed to be University, Visakhapatnam - TS. - A.H.
- 2.

It is certified that the final report has been uploaded on UGC-MRP portal on

It is also certified that final report, Executive summary of the report, Research documents, monograph academic papers provided under Major Research Project have been posted on the website of the University/College.

Principal

Registrar

Seal